

# Obstructing Lagrangian concordance for closures of 3-braids

*Angela Wu*

A dissertation submitted in partial fulfillment  
of the requirements for the degree of  
**Doctor of Philosophy**  
of  
**University College London.**

Department of Mathematics  
University College London

June 14, 2021

I, Angela Wu, confirm that the work presented in this thesis is my own, except for the contents of Chapter 6 which is in collaboration with Bahar Acu, Orsola Capovilla-Searle, Agnes Gadbled, Aleksandra Marinković, Emmy Murphy, and Laura Starkston. Where information has been derived from other sources, I confirm that this has been indicated in the work.

# Abstract

The study of knot concordance for smooth knots is a classical and essential problem in knot theory, an important field in topology since the mid 1800s. Two knots are said to be concordant if they jointly form the boundary of a cylinder in four-dimensional Euclidean space. This project studies the variant most relevant to symplectic geometry, called Lagrangian concordance, in which we ask for the knots to be Legendrian and for them to bound a Lagrangian surface. We ask which knots are Lagrangian concordant to and from the standard Legendrian unknot and find obstructions coming from the cyclic  $p$ -fold branched covers of these knots. We restrict large classes of closures of 3-braids from candidacy using a variety of techniques from smooth, symplectic, and contact topology. For the remaining family of braids, we draw Weinstein diagrams of symplectic fillings of their double covers. We use the Chekanov-Eliashberg differential graded algebra of the links in these diagrams to compute the symplectic homology of these fillings in order to obstruct the last of these 3-braids.

# Acknowledgements

Thank you to my supervisor Steven Sivek whose guidance, insights, support, and patience have been invaluable to me. This thesis exists because of him. I am so grateful to be his student.

Thank you to Roger Casals, Orsola Capovilla-Searle, Jonathan Evans, Yankı Lekili, and Laura Starkston for the things they've taught me. Echoes of our conversations have wound their way directly and indirectly into this text.

Thank you to my kind examiners Andy Wand and Ed Segal for taking the time to read this thesis and for their helpful comments and corrections.

Thank you to the LSGNT, Nicky Townsend, and my cohort who have been on this journey with me over the last four years.

Thank you to my team from the Women in Symplectic and Contact Geometry and Topology workshop, Bahar Acu, Orsola Capovilla-Searle, Agnes Gadbled, Aleksandra Marinković, Emmy Murphy, and Laura Starkston. Working with these amazing women over the last two years has shown me that I have something to contribute to mathematics, something I wasn't convinced of before.

Thank you to the hard working educators and mentors who led me to math, and to geometry: my middle school teacher Sarah Garrett who worked with me after school on math problems for hours of her free time, the myriad of friends and mentors from summer camp who exposed me to a mathematical community I never knew existed, and Rina Rotman for teaching me about topology and geometry, giving me my first research project, helping me with applications, and commiserating with me when I felt down about it all. Thank

you to Alfonso Gracia-Saz who taught me how to learn and how to teach, I will miss you.

Thank you to Wendy and Ira for your amazing work and for occasionally showing up at my backdoor with a dog in hand. Thanks to Chip, Gloria, Alfie, Elsie, Ed, Badger, Blaze, Phoebe, Nellie, Teddy, Ricardo, Max, Finn, Frankie, Rex, Lottie, Murphy, Rosie, Honey, and Baxter for sharing your joy with me and making these last two years brighter.

Thank you to my family who have supported me my whole life and throughout this degree (not mutually exclusive). I love you and I miss you, and I'll be home soon! And of course, thank you Todd for so many things, for making me laugh, lifting me up, and being there for me, always.

# Impact Statement

The research in this thesis impacts various fields of mathematics. Mainly, we answer questions about symplectic and contact topology. Our main result is the symplectic version of a long standing problem in smooth topology. It is proved using both classical tools from smooth topology and new technology from symplectic and contact geometry including the Chekanov-Eliashberg DGA, open book decompositions, Lefschetz fibrations, and symplectic homology. We contribute to the understanding of Lagrangian cobordisms, which are of great interest to modern symplectic geometers as they form the building blocks of many currently studied mathematical structures including symplectic field theory, Legendrian contact homology, and the wrapped Fukaya category. Our results also give insight to the topology of contact manifolds.

# Contents

<b>1</b>	<b>Introduction</b>	<b>13</b>
1.1	Structure of the thesis . . . . .	23
<b>2</b>	<b>Background</b>	<b>25</b>
2.1	Symplectic fillings . . . . .	25
2.2	Knots in contact manifolds . . . . .	26
2.2.1	Legendrian knots . . . . .	26
2.2.2	Transverse knots . . . . .	31
2.3	Weinstein Manifolds . . . . .	32
2.3.1	Smooth Handlebodies . . . . .	32
2.3.2	Handle Moves . . . . .	34
2.3.3	Weinstein handle decomposition . . . . .	34
2.3.4	Contact surgery diagrams . . . . .	40
<b>3</b>	<b>Obstructing families of Murasugi braids</b>	<b>43</b>
3.1	Initial obstructions from fillings . . . . .	43
3.2	Obstructing Murasugi type 2 and 3 braids . . . . .	46
3.3	Using Gompf's 3-dimensional 2-plane field invariant . . . . .	51
<b>4</b>	<b>From open book decompositions to Weinstein diagrams</b>	<b>58</b>
4.1	Open Book Decompositions and Lefschetz Fibrations . . . . .	58
4.2	Obtaining Weinstein Lefschetz fibrations . . . . .	61
4.3	Drawing Weinstein diagrams . . . . .	68

<b>5</b>	<b>Nonvanishing symplectic homology</b>	<b>78</b>
5.1	The Chekanov-Eliashberg Differential Graded Algebra . . . . .	78
5.1.1	The DGA for Knots . . . . .	78
5.1.2	With 1-handles . . . . .	81
5.1.3	Cyclically composable Reeb chords . . . . .	84
5.2	Computing the Chekanov-Eliashberg DGA from $\mathcal{D}(\Lambda)$ . . . . .	84
5.3	Nonvanishing symplectic homology . . . . .	88
5.4	The Main Theorem . . . . .	94
<b>6</b>	<b>Weinstein Complements of Smoothed Toric Divisors</b>	<b>100</b>
6.1	Existence of a Weinstein structure . . . . .	100
6.2	The Centeredness Condition . . . . .	103
6.3	Drawing handlebody diagrams . . . . .	105
<b>Appendices</b>		<b>108</b>
<b>A Handle moves on parallel strands</b>		<b>109</b>
<b>B The Chekanov-Eliashberg DGA for another example</b>		<b>113</b>
<b>Bibliography</b>		<b>115</b>



# List of Figures

1.1	The standard contact structure on $\mathbb{R}^3$ [Msr09]. . . . .	15
1.2	A Legendrian knot which is concordant from but not to the standard $tb = -1$ unknot $U$ . . . . .	16
1.3	A Lagrangian concordance $C_1$ from $U$ to $\Lambda$ glued to a Lagrangian concordance $C_2$ from $\Lambda$ to $U$ . . . . .	17
1.4	A braid and its closure. . . . .	18
1.5	A positive Markov move and its inverse. . . . .	19
1.6	A Weinstein filling of $\Sigma_2(\Lambda')$ . . . . .	22
2.1	Front projections of a Legendrian unknot, trefoil, and figure 8 knot. . . . .	28
2.2	Legendrian Reidemeister moves in the front projection. . . . .	28
2.3	Lagrangian projections of a Legendrian unknot, trefoil and figure 8 knot. . . . .	29
2.4	Legendrian Reidemeister moves in the Lagrangian projection. . . . .	29
2.5	Resolving to a Lagrangian projection. . . . .	30
2.6	Positive and negative stabilizations in the front projection. . . . .	31
2.7	A 2 dimensional 1-handle. . . . .	33
2.8	A Kirby diagram containing two 0-framed 2-handles and two 1-handles. . . . .	34
2.9	A 2 dimensional 1-handle slide of $h_1$ over $h_2$ . . . . .	35
2.10	A 2-dimensional 1-handle $h_1$ cancelled with a 2-dimensional 2-handle $h_2$ . . . . .	35

2.11	A cancelling pair consisting of a 1-handle and a 2-handle in a Kirby diagram. . . . .	35
2.12	The standard Weinstein $k$ -handle in $\mathbb{R}^{2n}$ . . . . .	38
2.13	Gompf moves. . . . .	39
2.14	Handle slides in surgery diagrams. . . . .	41
2.15	From 1-handles to (+1) surgery. . . . .	41
3.1	$\Sigma_p(C') \cup B^4$ , a filling of $\Sigma_p(U')$ . . . . .	44
3.2	$V \cup X$ , a filling of $\Sigma_p(U')$ . . . . .	45
3.3	Murasugi type 2 braids. . . . .	47
3.4	A smooth isotopy of the closure of the braid $(\sigma_1\sigma_2)^3\sigma_1^{-3}\sigma_2^{-1}$ . . . . .	50
4.1	A right handed and left handed Dehn twist. . . . .	59
4.2	Curves on the torus. . . . .	62
4.3	The double cover of a planar page branched over 3 points . . . . .	63
4.4	A Weinstein filling of $\Sigma_2(\Lambda')$ . . . . .	69
4.5	The Murasugi sum of two annuli paged open books. . . . .	70
4.6	Surgeries corresponding to Dehn twists. . . . .	71
4.7	The Legendrian lift of $\tau_\beta^{-1}(\alpha)$ . . . . .	72
4.8	Drawing $\tau_\beta^{-n_1}(\alpha)$ . . . . .	73
4.9	Drawing $\tau_\alpha\tau_\beta^{-n_1}(\alpha)$ . . . . .	74
4.10	Drawing $\tau_\alpha^{n_2}\tau_\beta^{-n_1}(\alpha)$ . . . . .	75
4.11	Effect of applying $\tau_\alpha^{n_j}$ and $\tau_\beta^{-n_i}$ . . . . .	76
4.12	Simplifying the Weinstein diagram. . . . .	76
4.13	A filling of the double cover of the transverse $m(8_{20})$ knot. . . . .	77
5.1	Reeb and orientation signs at crossings. . . . .	80
5.2	Counting disks in the DGA of the trefoil. . . . .	81
5.3	A half twist for the Lagrangian resolution. . . . .	82
5.4	A negative corner at a 1-handle. . . . .	83
5.5	$\mathcal{D}(\Lambda)$ labelled for a DGA computation. . . . .	85
5.6	The Lagrangian resolution for $\mathcal{D}(m(8_{20}))$ . . . . .	87

5.7  $\mathcal{D}(m(8_20))$  labelled for a DGA computation. . . . . 87

5.8 Diagrams of  $X_{\Lambda'_k}$  and  $\Sigma_2(\Lambda'_k)$  . . . . . 98

6.1 A Delzant polytope and smoothing a toric divisor. . . . . 101

6.2 Centeredness in Delzant polytopes. . . . . 102

6.3 Weinstein diagrams of cotangent bundles of surfaces . . . . . 105

6.4 The Weinstein diagram of the complement of any toric divisor  
smoothed in adjacent nodes of a blow up. . . . . 107

6.5 The Weinstein handlebody diagram of the complement of the  
toric divisor of  $\mathbb{C}\mathbb{P}^1 \times \mathbb{C}\mathbb{P}^1$  smoothed in two opposite nodes. . . 108

6.6 The Weinstein diagram of the complement the smooth cubic in  
 $\mathbb{C}\mathbb{P}^2$ . . . . . 108

A.1 Sliding parallel strands over a (+1) curve. . . . . 109

A.2 Performing Gompf move 5 with parallel strands. . . . . 110

A.3 Performing Reidemeister 3 with parallel strands. . . . . 110

A.4 Performing Reidemeister 2 with parallel strands. . . . . 111

A.5 Performing Reidemeister 1 with parallel strands. . . . . 112

B.1 A front diagram of  $\mathcal{D}(\Lambda)$  where  $\Lambda$  is the knot  $10_{155}$ . . . . . 113

B.2 The labelled Lagrangian resolution of  $\mathcal{D}(\Lambda)$  where  $\Lambda$  is the knot  
 $10_{155}$ . . . . . 114

# List of Tables

4.1 Effect of a Dehn twist about  $\alpha$  or  $\beta$  on  $(p, q)$  in the torus with one boundary component. . . . . 65

# Chapter 1

## Introduction

Knot concordance was first defined by Fox and Milnor in [FM66] as a way to endow topological knots with a group structure. Since then, the study of knot concordance for smooth knots has become a classical and essential problem in low dimensional topology where many easily asked questions regarding knot concordance have not still not been answered. Two knots are said to be smoothly concordant if they jointly form the boundary of a smooth cylinder in four-dimensional Euclidean space. We study a variant of the problem of concordance defined in the symplectic setting by Chantraine [Cha10] called *Lagrangian concordance*. By bringing concordance to this setting, we can tackle questions by combining the geometric properties of symplectic manifolds with classical obstructions to smooth concordance. Lagrangian concordance asks for the boundary knots to be Legendrian in a contact manifold, and for the cylinder to be Lagrangian in a symplectic manifold. If the Lagrangian surface between the two boundary Legendrians has higher genus, this is a Lagrangian cobordism.

Beyond its applications in smooth topology, Lagrangian cobordisms between Legendrian submanifolds have been studied in symplectic and contact topology due to their key role in symplectic field theory [EY00]. Indeed, Lagrangian cobordisms were first defined to construct a category whose objects are Legendrian submanifolds and whose morphisms are given by the exact Lagrangian cobordisms. This led to the development of a new invariant by

Chekanov and Eliashberg [Che02, Eli98], a differential graded algebra that was used to distinguish between two knots that were not distinguishable by classical invariants. The homology of this differential graded algebra, called *Legendrian contact homology* gives a functor from the category of Legendrians to the category of these differential graded algebras. The study of Lagrangian cobordisms has also led to the development of the wrapped Fukaya category [FSS08].

With this motivation, a lot of recent work aims to understand the structure and behaviour of the Lagrangian cobordism relation. The basic question we ask is the following:

**Question 1.0.1.** Let  $\Lambda_-$  and  $\Lambda_+$  be Legendrian knots. When does there exist a Lagrangian cobordism from  $\Lambda_-$  to  $\Lambda_+$ ?

To make the problem tractable, we may study specific kinds of Lagrangian cobordisms. For example we can consider *decomposable* Lagrangian cobordisms, which are built out of some elementary moves [BLL<sup>+</sup>20]. In our case, we limit the cobordism by its genus and ask:

**Question 1.0.2.** Let  $\Lambda_-$  and  $\Lambda_+$  be Legendrian knots. When does there exist a Lagrangian concordance from  $\Lambda_-$  to  $\Lambda_+$ ?

Studying this question in the symplectic setting has produced results in smooth topology. For instance in [Cha10], Chantraine deduces a criterion to compute the slice genus of some knots.

To formally define Lagrangian concordance, we begin with some basic definitions to describe the symplectic setting:

**Definition 1.0.3.** A *symplectic manifold*  $(X, \omega)$  is a smooth  $2n$ -dimensional manifold  $X$  equipped with a closed nondegenerate 2-form  $\omega$ .

Let  $(X_1, \omega_1)$  and  $(X_2, \omega_2)$  be symplectic manifolds of equal dimension. A *symplectomorphism*  $\varphi : X_1 \rightarrow X_2$  is a diffeomorphism such that  $\varphi_*\omega_2 = \omega_1$ .

**Definition 1.0.4.** A *Lagrangian submanifold* of a  $2n$ -dimensional symplectic manifold  $(X, \omega)$  is an  $n$ -dimensional submanifold  $L$  of  $X$  such that  $\omega|_L = 0$ .

**Definition 1.0.5.** A *3-dimensional contact manifold* is an oriented 3-manifold  $M$  along with a *contact structure* which is a completely nonintegrable plane field  $\xi \subset TM$ . This means that for each  $x \in M$ , we associate a 2-dimensional subspace  $\xi_x \subset T_xM$ ,  $\xi_x = \ker(\alpha_x)$  where  $\alpha$  is a 1-form and  $\alpha \wedge d\alpha > 0$ .

For example, consider  $\mathbb{R}^3$  with the *standard contact structure*:

$$\xi_{std} = \ker(dz - ydx) = \text{span} \left\{ \frac{\partial}{\partial y}, \frac{\partial}{\partial x} + y \frac{\partial}{\partial z} \right\}.$$

The contact planes for this contact structure are pictured in Figure 1.1. By Darboux's Theorem, all contact structures look locally like  $(\mathbb{R}^3, \xi_{std})$ .

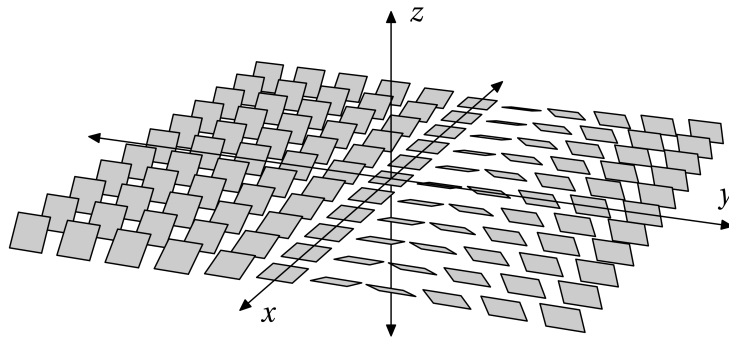


**Figure 1.1:** The standard contact structure on  $\mathbb{R}^3$  [Msr09].

Next we define the knots found in contact manifolds which are compatible with the ambient contact structure.

**Definition 1.0.6.** Let  $(M^3, \xi)$  be a contact manifold. A *Legendrian knot*  $\Lambda$  is an embedded  $S^1$  tangent to  $\xi$ , ie.  $T_x\Lambda = \xi_x$  for all  $x \in \Lambda$ .

For Lagrangian concordance, we restrict the setting to Legendrian knots in  $\mathbb{R}^3$  with the standard contact structure  $\ker \alpha$ ,  $\alpha = dz - ydx$ . Let  $\mathbb{R}^4$  be the symplectization of  $\mathbb{R}^3$ ,  $\mathbb{R}_t \times \mathbb{R}^3$  with the symplectic form  $\omega = d(e^t\alpha)$ .

**Definition 1.0.7.** [Cha10] Let  $\Lambda_+, \Lambda_- \subset \mathbb{R}^3$  be Legendrian knots where  $\mathbb{R}^3$  is equipped with the standard contact structure  $\xi = \ker(\alpha)$ . A *Lagrangian cobordism from  $\Lambda_-$  to  $\Lambda_+$*  is a Lagrangian  $L$  embedded in  $\mathbb{R}^4$  such that

$$((-\infty, -T) \times \mathbb{R}^3) \cap L = (-\infty, -T) \times \Lambda_-$$

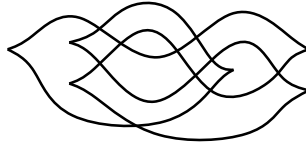


**Figure 1.2:** A Legendrian knot which is concordant from but not to the standard  $tb = -1$  unknot  $U$ .

and

$$((T, \infty) \times \mathbb{R}^3) \cap L = (T, \infty) \times \Lambda_+$$

for some  $T \geq 0$ .

**Definition 1.0.8.** If a Lagrangian cobordism has zero genus, then we call it a *Lagrangian concordance*. If there is a Lagrangian concordance from  $\Lambda_-$  to  $\Lambda_+$ , we write  $\Lambda_- \prec \Lambda_+$  and say that  $\Lambda_-$  is *Lagrangian concordant to*  $\Lambda_+$ .

In [Cha10], Chantraine showed that Legendrian isotopic Legendrian knots are Lagrangian concordant, and that Lagrangian concordance can be obstructed by classical Legendrian knot invariants: the rotation number and the Thurston-Bennequin number. Lagrangian concordance is both reflexive and transitive, suggesting that as a relation, it is potentially a partial order on Legendrian knots. In [Cha13], it is proved that Lagrangian concordance is not symmetric. This is by an explicit construction of a Lagrangian concordance from the maximum Thurston Bennequin number ( $tb = -1$ ) unknot  $U$  to the knot  $\Lambda$  in Figure 1.2 and a proof via augmentations of the Chekanov-Eliashberg DGA that no concordance from  $\Lambda$  to  $U$  exists.

It is not known if Lagrangian concordance is antisymmetric, ie. if  $\Lambda_1 \prec \Lambda_2 \prec \Lambda_1$ , then  $\Lambda_1$  is Legendrian isotopic to  $\Lambda_2$ . As a first step to understanding the potential antisymmetry of this relation, we pose the following question about the simplest case:

**Question 1.0.9.** Which Legendrian knots  $\Lambda$  satisfy  $U \prec \Lambda \prec U$  (as in Figure 1.3)?

The answer to this question is not known. Even simpler, it is not known whether any knot is Lagrangian concordant to the standard  $tb = -1$  unknot



$U$ , other than  $U$  itself. We know that if a Legendrian knot  $\Lambda$  satisfies  $U \prec \Lambda$ , then  $U$  can be filled at the negative end by a Lagrangian disk. The result is a Lagrangian filling of  $\Lambda$  with genus zero. Boileau and Orevkov showed that any such  $\Lambda$  must be *quasipositive* [BO01], meaning it is the closure of a braid consisting of conjugates of positive generators. Furthermore,  $\Lambda$  must be *smoothly slice*, meaning it bounds a smooth disk in  $B^4$ . Thus, to obstruct concordance from the unknot, we can use smooth obstructions to sliceness.

Cornwell, Ng, and Sivek [CNS16] answer Question 1.0.9 in a special case. They show that no nontrivial  $\Lambda$  can have a *decomposable* Lagrangian concordance to  $U$ . They also provide many obstructions to and examples of Lagrangian concordance. For example, if  $\Lambda$  has at least two normal rulings, then  $\Lambda \not\prec U$ .

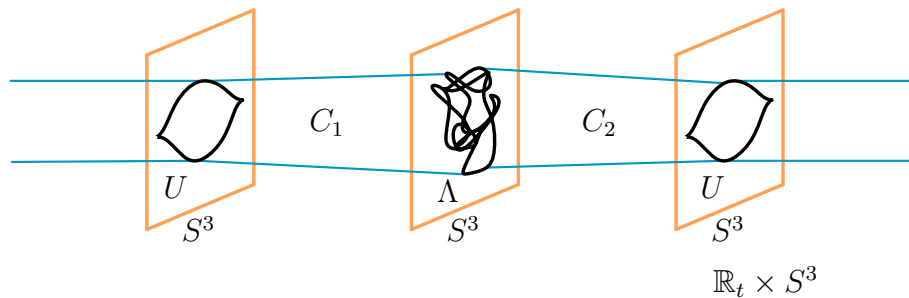


**Figure 1.3:** A Lagrangian concordance  $C_1$  from  $U$  to  $\Lambda$  glued to a Lagrangian concordance  $C_2$  from  $\Lambda$  to  $U$ .

The main result of this thesis gets us closer to an answer to Question 1.0.9. We provide a new obstruction to the double concordance  $U \prec \Lambda \prec U$  on the topological knot type of  $\Lambda$ :

**Theorem 5.4.3.** Let  $U$  be the standard  $tb = -1$  unknot. Let  $\Lambda$  be a Legendrian knot satisfying  $U \prec \Lambda \prec U$ , and  $\Lambda \neq U$ . Then  $\Lambda$  cannot be smoothly the closure of a 3-braid.

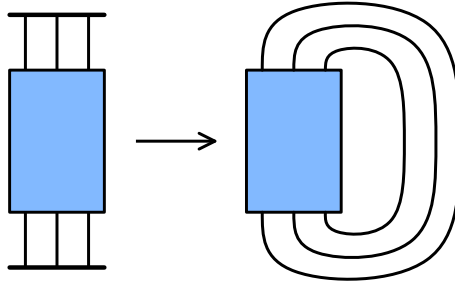


**Figure 1.4:** A braid (with crossings in the blue box) and its closure.

Braids are a tractable way to think about knots. The  $n$ -stranded braids physically consist of  $n$  strings which weave over and under each other with fixed ends. Their properties are captured by the Artin braid group  $\mathcal{B}_n$  given by the presentation:

$$\langle \sigma_1 \dots \sigma_{n-1} \mid \sigma_i \sigma_{i+1} \sigma_i = \sigma_{i+1} \sigma_i \sigma_{i+1} \text{ for } 1 \leq i < n, \sigma_i \sigma_j = \sigma_j \sigma_i \text{ for } |i - j| \geq 2 \rangle.$$

Individual braids can be represented by braid words consisting of these  $\sigma_i$ 's which indicate a positive crossing of the  $i + 1$ th string over the  $i$ th string. From an  $n$ -stranded braid, we can easily obtain its closure: the knot or link we get by identifying or “closing up” the fixed ends of the strings, see Figure 1.4. Likewise, every link in  $S^3$  is the closure of some  $n$ -braid [Ale23]. Braids which are conjugate have isotopic closures.

The 3-stranded braids are particularly tangible because we can write them down explicitly. In [Mur74], Murasugi found representatives for all conjugacy classes of 3-braids, allowing us to list all such links as the closures of one of the three following braid words:

1.  $(\sigma_1 \sigma_2)^{3d} \sigma_1 \sigma_2^{-a_1} \dots \sigma_1 \sigma_2^{-a_k}$  for  $a_1, \dots, a_k \geq 0$ ,
2.  $(\sigma_1 \sigma_2)^{3d} \sigma_2^m$  for  $m \in \mathbb{Z}$ ,
3.  $(\sigma_1 \sigma_2)^{3d} \sigma_1^k \sigma_2^{-1}$  for  $k = -1, -2, -3$ .

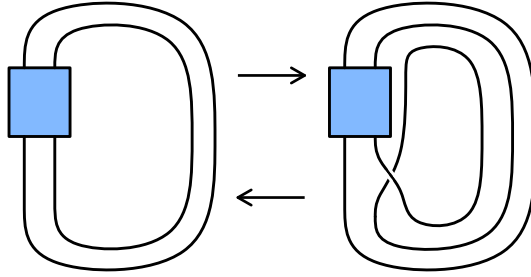


**Figure 1.5:** Going from left to right, a positive Markov move (or stabilization) and from right to left its inverse (or de-stabilization).

for  $d \in \mathbb{Z}$ .

Bennequin [Ben83] showed that any conjugacy class of braids can be closed in a natural way to produce a transverse knot in  $(S^3, \xi_{std})$ , and that every transverse knot is transversely isotopic to a closed braid. In [OS03, Wri02], the Markov Theorem for transverse knots is proved, showing that two transverse closed braids that are isotopic as transverse knots are also isotopic as transverse braids. More precisely:

**Theorem 1.0.10.** [OS03, Wri02] Two braids represent transversally isotopic links if and only if one can pass from one braid to another by conjugations in braid groups, positive Markov moves, and their inverses.

*Markov moves*, also called *positive or negative stabilizations*, are an operation on braids that increases the number of strands but preserves the topological knot type of the braids. These moves take a braid  $B$  in  $\mathcal{B}_n$  to a braid  $B'$  in  $\mathcal{B}_{n+1}$  by  $B' = B\sigma_n^{\pm 1}$ , see Figure 1.5. They are called positive when the added crossing is positive ( $\sigma_n$ ), and negative when the added crossing is negative ( $\sigma_n^{-1}$ ).

Using conjugations and positive Markov moves (and their inverses), Hayden proves the following:

**Theorem 1.0.11.** [Hay18] Every quasipositive link has a quasipositive representative of minimal braid index.

**Remark 1.0.12.** Thus every transverse representative given by a quasipositive link type is transversely isotopic to a transverse quasipositive braid of minimal braid index. In our case, if a quasipositive knot has braid index 3, then any quasipositive transverse representative of that smooth knot type is transversely isotopic to a transverse 3-braid. For a candidate  $\Lambda$  satisfying  $U \prec \Lambda \prec U$ , we obtain a transverse knot  $\Lambda'$  which is a positive push off of  $\Lambda$ . If  $\Lambda$  is smoothly the closure of a 3-braid, then so is  $\Lambda'$ . We will obstruct the transverse braid  $\Lambda'$  in order to obstruct  $\Lambda$ .

We first eliminate Murasugi braids of type 2 and 3 by using obstructions to smooth concordance. We will then reframe the problem of Lagrangian concordance as one of fillings of  $\Sigma_p(\Lambda')$ , the  $p$ -fold cyclic cover of  $S^3$  branched over  $\Lambda'$ . This construction is used to obtain the following obstructions:

**Theorem 3.1.5.** If  $\Lambda$  is a Legendrian knot which satisfies  $U \prec \Lambda \prec U$ , then any  $p$ -fold cyclic branched cover  $\Sigma_p(\Lambda')$  of  $S^3$  branched over the transverse push-off  $\Lambda'$  of  $\Lambda$  embeds as a contact type hypersurface in  $(B^4, \xi_{std})$ . Moreover,  $\Sigma_p(\Lambda')$  is Stein fillable and has a Stein filling which embeds in  $(B^4, \xi_{std})$ .

**Theorem 3.1.6.** If  $\Lambda$  is a Legendrian knot which satisfies  $U \prec \Lambda \prec U$ , then any filling of the  $p$ -fold cyclic branched cover  $\Sigma_p(\Lambda')$  of  $S^3$  branched over the transverse push-off  $\Lambda'$  must embed in a blow up of  $B^4$  and must have negative definite intersection form.

We restrict to the double cover to obtain further obstructions. For instance the following:

**Theorem 3.3.2.** If  $\Lambda$  is a Legendrian knot which satisfies  $U \prec \Lambda \prec U$ , then the contact cyclic branched double cover  $(\Sigma_2(\Lambda'), \xi)$  of  $S^3$  branched over the transverse push-off  $\Lambda'$  of  $\Lambda$  has

$$d_3(\xi) = -\frac{1}{2}.$$

Here,  $d_3$  is Gompf's 3-dimensional invariant on 2-plane fields. It was defined and proved to be an invariant in [Gom98]. Theorem 1.2 of [Pla06]

states that for  $\Lambda'$  a transverse knot and  $(\Sigma_2(\Lambda'), \xi)$  the double cover of  $S^3$  branched over  $\Lambda'$ ,  $d_3(\xi)$  is completely determined by the topological link type of  $\Lambda'$  and its self-linking number  $\text{sl}(\Lambda')$ . Indeed, Plamenevskaya's work [Pla06] gives an algorithm to produce the contact surgery diagram of  $\Sigma_2(\Lambda')$ . From there we can use work of Ding, Geiges, and Stipsicz (Corollary 3.6 of [DGS04]) to explicitly compute  $d_3$  from the Legendrian link in the surgery diagram. For our obstruction, we compute  $d_3$  using Theorem 3.1.5 and formulas from Ito [Ito17].

We are able to obstruct Murasugi type 2 and 3 braids using smooth obstructions to sliceness. In particular we show that the closure of these braids is either not quasipositive (and thus not Lagrangian fillable) or that they are strongly quasipositive, which as observed by Rudolph [Rud93], implies they are not slice by a result of Kronheimer and Mrowka [KM93].

Using Theorem 3.3.2, we can restrict the family of Murasugi type 1 braids to a small family. We produce the following obstruction on the remaining braids of Murasugi type 1:

**Corollary 3.3.7.** If  $\Lambda$  is a Legendrian knot which satisfies  $U \prec \Lambda \prec U$ , and  $\Lambda'$ , the transverse pushoff of  $\Lambda$ , is the closure of a 3-braid  $\beta$ , then the algebraic length of  $\beta$  is 2.

We study particular fillings of  $\Sigma_2(\Lambda')$  by drawing their Weinstein handlebody diagrams [Wei91]. Weinstein diagrams are the symplectic analogue to Kirby diagrams. They are used to illustrate a symplectic version of handle decomposition. In 4-dimensions, we depict 1-handles as pairs of balls or walls (ie. as a pair of line segments), and 2-handles as Legendrian knots. Surgery diagrams and Weinstein diagrams are related by replacing 1-handles with (+1)-surgery components. As stated previously, one way to obtain these surgery diagrams for  $\Sigma_2(\Lambda')$  is through the algorithm laid out in [Pla06, HKP08] by Harvey, Kawamuro, and Plamenevskaya. To avoid linked positive surgery components, which cannot be easily transformed to 1-handles, we obtain Weinstein diagrams in an alternative way by adapting the recipe laid out by Casals

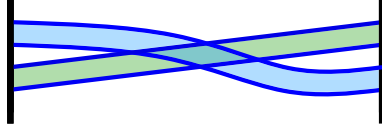


**Figure 1.6:** A Weinstein filling of  $\Sigma_2(\Lambda')$ . The shaded blue and shaded green represent parallel strands of a single Legendrian link in  $S^1 \times S^2$ .

and Murphy in [CM19]. We prove the following theorem:

**Theorem 4.3.2.** Let  $\Lambda$  be a Legendrian knot which is the closure of a quasi-positive 3-braid of algebraic length 2. Let  $\Lambda'$  be a positive transverse push off of  $\Lambda$ . Then there is a filling of  $\Sigma_2(\Lambda')$ , the double cover of  $S^3$  branched over  $\Lambda'$ , given by the handle decomposition consisting of a single 1-handle and a single 2-handle pictured in Figure 1.6.

We use these Weinstein diagrams to compute the *symplectic homology* of the filling, via the *Chekanov-Eliashberg differential graded algebra* of the Legendrian attaching sphere depicted in the diagram. The homology of the Chekanov-Eliashberg differential graded algebra, called the *Legendrian contact homology* was introduced by Chekanov and Eliashberg [Che02, Eli98], and was the first non-classical Legendrian link invariant. The differential graded algebra is generated by Reeb chords in a Legendrian link in  $\mathbb{R}^3$ , and the differential counts holomorphic disks in  $\mathbb{R} \times \mathbb{R}^3$ . A  $\mathbb{Z}$ -graded version of the Chekanov-Eliashberg differential graded algebra was defined by Etnyre, Ng, and Sabloff [ENS<sup>+</sup>02], and a version of this differential graded algebra was defined for links in  $\#^m(S^1 \times S^2)$  by Ekholm and Ng [EN15], counting an infinite family of generators coming from Reeb chords in the 1-handles. The differential graded algebra was then simplified by Etgü and Lekili [EL19] who showed that the internal DGA of a given 1-handle is generated by a subalgebra consisting of finitely many generators. The Chekanov-Eliashberg DGA can be used to compute invariants of the Weinstein manifolds which correspond to handle attachments along these links. In particular, we will use the DGA to compute the *symplectic homology* of the filling of  $\Sigma_2(\Lambda')$  following work of [BEE12] and show:

**Theorem 5.3.4.** Let  $\Lambda \neq U$  be a Legendrian knot which is the closure of a quasipositive 3-braid of algebraic length 2. Let  $\Lambda'$  be a positive transverse push off of  $\Lambda$ . Then there is a filling of  $\Sigma_2(\Lambda')$ , the double cover of  $S^3$  branched over  $\Lambda'$ , which has nonvanishing symplectic homology.

The main result of the thesis (Theorem 5.4.3) will follow from an argument showing that a filling of  $\Sigma_2(\Lambda')$  cannot embed in  $B^4$ . A corollary of this result may be of separate interest. In [MT20], Mark and Tosun pose the following question: *which smooth, oriented manifolds can be realized, up to diffeomorphism, as contact type hypersurfaces in  $\mathbb{R}^{2n}$  with the standard symplectic structure?* In their paper, they rule out a large class of 3-dimensional homology spheres from arising as contact type hypersurfaces in  $\mathbb{R}^4$ , specifically the Brieskorn spheres. The following result provides another infinite family of contact manifolds which are rational homology spheres but do not embed in  $\mathbb{R}^4$ .

**Corollary 5.4.5.** Let  $\Sigma_2(\Lambda')$  be the double cover of  $S^3$  branched over a quasipositive transverse knot which is the closure of a 3-braid of algebraic length 2. Suppose  $\Lambda'$  is not the unknot. Then  $\Sigma_2(\Lambda')$  does not embed as a contact type hypersurface in  $\mathbb{R}^4$ .

## 1.1 Structure of the thesis

Chapter 2 introduces some basic concepts regarding Symplectic fillings, Legendrian and transverse knots, as well as background on Weinstein manifolds and their handlebody diagrams. In Chapter 3, we build some basic obstructions from fillings using the concordance  $U \prec \Lambda \prec U$ . We then use both smooth and contact/symplectic properties to eliminate large families of 3-braids from concordance, reducing the problem to studying the family of quasipositive 3-braids with algebraic length 2. In Chapter 4, we produce open book decompositions of the double covers of the knots in this remaining family of 3-braids from which we produce Weinstein Lefschetz fibrations of a filling of these double covers. We then draw the Weinstein handlebody diagrams for these fillings.

In Chapter 5, we compute the Chekanov-Eliashberg differential graded algebra of the Legendrian attaching spheres of these Weinstein handlebody diagrams. We use this to prove that these fillings have non-zero symplectic homology, and we use this fact to prove the main theorem. In Chapter 6, we summarize some results from [ACSG<sup>+</sup>20a, ACSG<sup>+</sup>20b] written in collaboration with Bahar Acu, Orsola Capovilla-Searle, Agnes Gadbled, Aleksandra Marinković, Emmy Murphy, and Laura Starkston. This work develops a technique for drawing Weinstein handlebody diagrams for a certain class of symplectic manifolds.



## Chapter 2

# Background

This section begins with some background material on symplectic and contact geometry and the tools which we will apply to the Lagrangian concordance problem.

### 2.1 Symplectic fillings

We begin with some background on symplectic fillings.

**Definition 2.1.1.** Let  $(X, \omega)$  be a compact connected symplectic manifold with boundary  $M$ . A *Liouville vector field*  $V$  on  $(X, \omega)$  is a vector field which points transversely outwards at  $\partial X = M$  satisfying  $\mathcal{L}_V \omega = \omega$ . A *Liouville form*  $\lambda$  is a 1-form such that  $d\lambda = \omega$ . A Liouville vector field  $V$  induces a Liouville contact form  $\lambda$  on  $M$ , where  $\lambda = \iota_V \omega|_M$ . If the Liouville vector field exists globally on  $(X, \omega)$ , then we call  $(X, \omega)$  a *Liouville domain* or an *exact symplectic filling* of  $(M, \xi)$ , where  $\xi = \ker(\lambda)$ .

Note that the flow of a Liouville vector field dilates the symplectic form. When a vector field points transversally outwards at a boundary, we call this boundary *convex*, and when it points inwards, we call this *concave*. When we have a convex or concave boundary component, it naturally inherits a contact structure, and this contact structure determines the symplectic form in a collar neighborhood of the boundary. We now formally define the different kinds of symplectic fillings.

**Definition 2.1.2.** Let  $(M, \xi)$  be a contact manifold.

1. We say  $(X, \omega)$  is a *weak filling* of  $(M, \xi)$  if  $\omega|_{\xi} > 0$ .
2. We say  $(X, \omega)$  is a *strong filling* of  $(M, \xi)$  if there is a Liouville vector field  $V$  defined near  $\partial X$ .
3. We say  $(X, \omega)$  is a *exact filling* if  $V$  extends globally over  $X$ , in which case  $\iota_V \omega$  defines a global primitive of  $\omega$ .
4. We say  $(X, \omega)$  is a *Stein filling* if it comes with an integrable complex structure  $J$ , and admits a plurisubharmonic function  $\phi : X \rightarrow [0, \infty)$  for which  $\partial X$  is a regular level set, and  $V$  is the gradient  $\nabla \phi$ , and  $\omega = -dd^c \phi$ .

We can think of the filling of a contact manifold  $(M, \xi)$  as a sort of symplectic cobordism from the empty manifold to  $(M, \xi)$ . Similarly, a symplectic cobordism from  $(M, \xi)$  to the empty manifold is called a *symplectic cap*.

**Definition 2.1.3.** We say that a contact manifold  $(M^3, \xi)$  is *overtwisted* if there is a contact embedding of an overtwisted disk (a disk whose boundary is tangent to  $\xi$ , and whose interior is transverse to  $\xi$  everywhere except at one point) into  $(M, \xi)$ .

A contact manifold that is not overtwisted is called *tight*.

Overtwisted manifolds are not fillable. Any fillable contact manifold is tight, though not every tight contact manifold is fillable [EH02]. In fact, we have the following hierarchy of fillability criteria:

Stein fillable  $\subsetneq$  exactly fillable  $\subsetneq$  strongly fillable  $\subsetneq$  weakly fillable  $\subsetneq$  tight.

## 2.2 Knots in contact manifolds

### 2.2.1 Legendrian knots

We defined Legendrian knots in the introduction; we now go into some detail. For a more thorough treatment, see [Etn03]. As stated in the introduction,

locally, every contact manifold looks like  $(\mathbb{R}^3, \xi_{std})$ . Hence for visualization and intuition, it is convenient to consider a Legendrian  $L$  in  $(\mathbb{R}^3, \xi_{std})$ . We parametrize  $L$  by the smooth immersion  $\phi : S^1 \rightarrow \mathbb{R}^3 : \theta \mapsto (x(\theta), y(\theta), z(\theta))$ , and since  $L$  is tangent to  $\xi = \ker(dz - ydx)$ ,

$$z'(\theta) - y(\theta)x'(\theta) = 0. \quad (2.1)$$

**Definition 2.2.1.** We say two knots  $L$  and  $L'$  are *Legendrian isotopic* if there is a continuous family  $L_t$ ,  $t \in [0, 1]$  of Legendrian knots such that  $L_0 = L$  and  $L_1 = L'$ .

Equivalently,  $L$  and  $L'$  are *Legendrian isotopic* if there is a one parameter family  $\phi_t : M \rightarrow M$ ,  $t \in [0, 1]$ , of contactomorphisms of  $M$  such that  $\phi_0$  is the identity map and  $\phi_1(L) = L'$ .

To visualize Legendrian knots diagrammatically, we consider the *front projection* of the knot  $L$ , which is its image under the map

$$\pi : \mathbb{R}^3 \rightarrow \mathbb{R}^2 : (x, y, z) \mapsto (x, z).$$

Then  $\pi(L)$  is parametrized by  $\phi_\pi : S^1 \rightarrow \mathbb{R}^2 : \theta \mapsto (x(\theta), z(\theta))$ . Note that  $\pi(L)$  cannot have any vertical tangencies since the equation (2.1) implies that if  $x'(\theta) = 0$ , then  $z'(\theta) = 0$ . Note also that because of equation (2.1), we can recover the  $y$  coordinate of  $L$  by taking the slope

$$y(\theta) = \frac{z'(\theta)}{x'(\theta)}$$

when  $x'(\theta) \neq 0$ , and

$$y(\theta) = \lim_{\sigma \rightarrow \theta} \frac{z'(\sigma)}{x'(\sigma)}$$

otherwise. Given a front projection, this also means that at each crossing, the order of the strands can be determined by their slopes with the more negatively sloped strand in front.

As in the case of topological knots, Legendrian knots in the front pro-

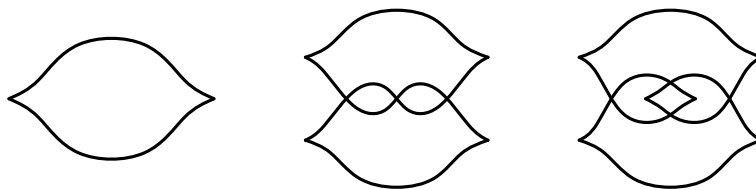


**Figure 2.1:** Front projections of a Legendrian unknot, trefoil, and figure 8 knot.

jection are related by a series of Reidemeister moves.

**Theorem 2.2.2.** Two front diagrams are Legendrian isotopic if and only if they are related by regular homotopy and a sequence of Legendrian Reidemeister moves (See Figure 2.2).

We call the moves in Figure 2.2 *Reidemeister 1*, *Reidemeister 2*, and *Reidemeister 3*, respectively.

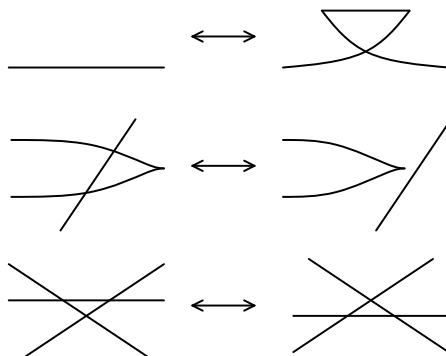


**Figure 2.2:** Legendrian Reidemeister moves in the front projection (along with rotations of these diagrams 180° about each axis).

Another important projection to consider is the *Lagrangian projection*

$$\pi : \mathbb{R}^3 \rightarrow \mathbb{R}^2 : (x, y, z) \mapsto (x, y).$$

Parametrizing a Legendrian knot  $L$  by  $\phi$  as above gives a parametrization of  $\pi(L)$  by  $\phi(\theta) = (x(\theta), y(\theta))$ . By equation (2.1) the  $z$  coordinate can be recovered by integration in the other two coordinates up to overall translation in the  $z$ -direction. Choosing some  $z_0 = z(0)$ , we get:

$$z(\theta) = z_0 + \int_0^\theta y(t)x'(t)d(t).$$

Note that since the  $z$  coordinate must go back to itself along the knot, Green's theorem implies that the Lagrangian projection bounds a signed area of zero. A diagram of an unknot without a crossing cannot be a Lagrangian projection. The Lagrangian projection is particularly useful when computing the Chekanov-Eliashberg DGA and the Legendrian Contact Homology of a Legendrian link [BEE12, Ekh19, EL17, EN15]. We will describe this computation in Chapter 5.

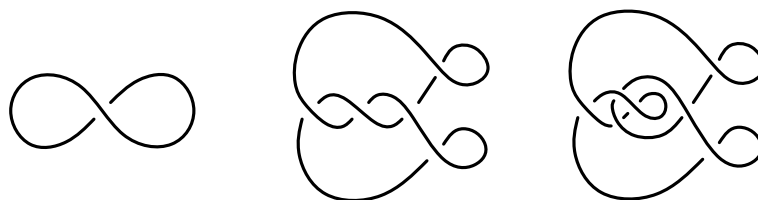


**Figure 2.3:** Lagrangian projections of a Legendrian unknot, trefoil and figure 8 knot.

We also have Reidemeister moves in the Lagrangian projection, which yield a weaker result.

**Theorem 2.2.3.** Two Lagrangian diagrams are Legendrian isotopic only if they are related by regular homotopy and a sequence of Legendrian Reidemeister moves as illustrated in Figure 2.4.

Note that unlike the case of the front projection, these moves are not sufficient to guarantee Legendrian isotopy.

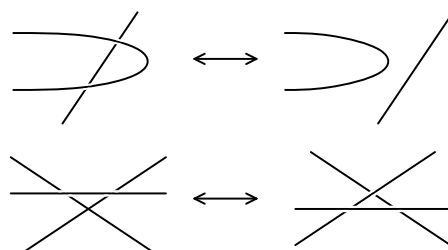


**Figure 2.4:** Legendrian Reidemeister moves in the Lagrangian projection (along with rotations of these diagrams  $180^\circ$  about each axis).

Additionally, there is a method of diagrammatically translating between the front and Lagrangian projections of a Legendrian knot.

**Theorem 2.2.4.** [Ng03] Given a front projection of a Legendrian knot  $L$ , we can obtain a diagram isotopic to the Lagrangian projection by altering cusps in the front diagram as in Figure 2.5.

These moves will become an important part of computing the Chekanov-Eliashberg DGA for certain Legendrian links.

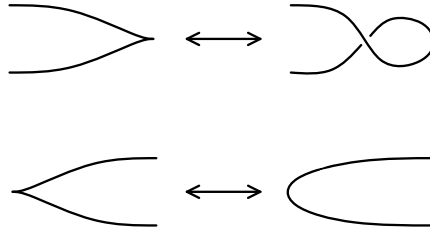


**Figure 2.5:** Left cusps become loops and right cusps are smoothed out to translate between the front and Lagrangian projections of the same knot.

As with smooth knots, we can attempt to understand Legendrian knots by looking at their invariants. In fact the first invariant of a Legendrian knot to note is the smooth type of the knot. The second is comes from the “twisting” of the ambient contact structure about the knot.

**Definition 2.2.5.** For any contact manifold equipped with a contact 1-form  $\alpha$ , there is a vector field  $V$  called *the Reeb vector field*, determined by  $i_V(d\alpha) = 0$  and  $\alpha(V) = 1$ . On the standard contact  $\mathbb{R}^3$ , this is the vector field  $\frac{\partial}{\partial z}$ . Let  $L$  be a Legendrian link. We define a *Reeb chord* of  $L$  to be an integral curve for the Reeb vector field with both endpoints on  $L$ .

**Definition 2.2.6.** Let  $L$  be a Legendrian knot in  $(M, \xi)$ . Let  $V$  be the Reeb vector field. Then  $V$  is a vector field transverse to  $\xi$  along  $L$ . The *Thurston-Bennequin number*  $tb(L)$  is the linking number of  $L$  with a pushoff of  $L$  in the  $z$ -direction. Given a front diagram, this is easily computed as

$$tb(L) = \text{writhe}(L) - \frac{1}{2}(\text{the number of cusps in } L).$$

In the Lagrangian projection,  $tb(L) = \text{writhe}(L)$ .

Given a Legendrian knot  $L$ , we can obtain another Legendrian knot of the same topological knot type via a process called *stabilization*. Let  $L \subset \mathbb{R}^3$  and view it in the front projection. A stabilization of  $L$  is removing a strand and replacing it with a zigzag as in Figure 2.6. If the zigzag is pointing down (where down cusps are added) then the stabilization  $S_+(L)$  is called *positive*, and if the zigzag is pointing up (where up cusps are added) then the stabilization  $S_-(L)$  is called *negative*.

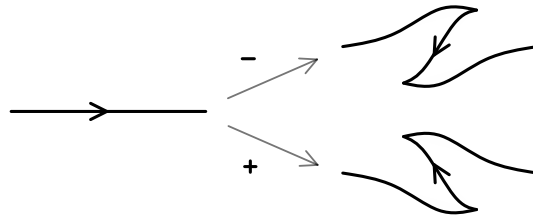


**Figure 2.6:** Positive and negative stabilizations in the front projection.

The Thurston-Bennequin number of a stabilized knot is  $tb(S_{\pm}(L)) = tb(L) - 1$ . Eliashberg showed in [Eli92] that this number is bounded above by proving the *Bennequin-Eliashberg inequality* which says: if  $(M, \xi)$  is a tight contact 3-manifold, let  $L$  be a Legendrian knot in  $M$  with Seifert surface  $\Sigma(L)$ . Then

$$tb(L) + |\text{rot}(L)| \leq \chi(\Sigma(L)),$$

where  $\text{rot}(L)$  denotes the *rotation number* of the knot, an invariant given by the “winding number” of  $L$  in  $\mathbb{R}^2$ . In the front diagram,  $\text{rot}(L)$  is easily computed as:

$$\text{rot}(L) = \frac{1}{2}(D - U)$$

where  $D$  denotes the number of down cusps and  $U$  the number of up cusps. Thus the maximum Thurston-Bennequin number is a knot invariant for smooth knots.

### 2.2.2 Transverse knots

Closely related to Legendrian knots are knots which are not tangent but transverse to a contact structure.

**Definition 2.2.7.** A *transverse knot*  $T \subset (M^3, \xi)$  is an embedded  $S^1$  always transverse to  $\xi$ .

Two transverse knots  $T$  and  $T'$  are *transverse isotopic* if they are homotopic through a family of transverse knots.

Usefully, transverse knots can be classified using braid words:

**Theorem 2.2.8.** [Ben83] Any transverse knot in  $(\mathbb{R}^3, \xi_{std})$  is transversely isotopic to the closure of a braid.

Furthermore, given a Legendrian knot, we can deform it to a transverse knot of the same smooth type by taking a transverse pushoff:

**Definition 2.2.9.** Given  $L$  a Legendrian in  $(M, \xi)$ , let  $A = S^1 \times [-\epsilon, \epsilon]$  be an annulus such that  $S^1 \times \{0\} = L$ , and  $TA|_L = \xi|_L$ . For sufficiently small  $\epsilon > 0$ , let  $L_+ = S^1 \times \{\frac{\epsilon}{2}\}$  and  $L_- = S^1 \times \{-\frac{\epsilon}{2}\}$ . Then  $L_{\pm}$  are the *positive and negative transverse pushoffs* of  $L$ .

## 2.3 Weinstein Manifolds

Weinstein manifolds are symplectic manifolds which are compatible with a symplectic handle decomposition.

### 2.3.1 Smooth Handlebodies

In smooth manifolds, smooth knots can be used to depict handle attachment. We will briefly discuss how to use this data to study smooth manifolds, before moving into the symplectic setting. For a full treatment, see [GSI<sup>+</sup>99].

**Definition 2.3.1.** For  $0 \leq k \leq n$ , an *n-dimensional k-handle* is a copy of  $D^k \times D^{n-k}$  attached to the boundary of an  $n$ -manifold  $X$  along  $\partial D^k \times D^{n-k}$  by an embedding  $\phi : \partial D^k \times D^{n-k} \rightarrow \partial X$  which we call the *attaching map*. We call  $k$  the *index* of the handle.

Given an  $n$ -dimensional  $k$ -handle  $h \cong D^k \times D^{n-k}$ , we call

1.  $D^k \times 0$  the *core*,



2.  $0 \times D^{n-k}$  the *co-core*,
3.  $\partial D^k \times D^{n-k}$  and  $\phi(\partial D^k \times D^{n-k})$  the attaching regions,
4.  $\partial D^k \times 0$  the *attaching sphere*,
5. and  $0 \times \partial D^{n-k}$  the *belt sphere*, see Figure 2.7.

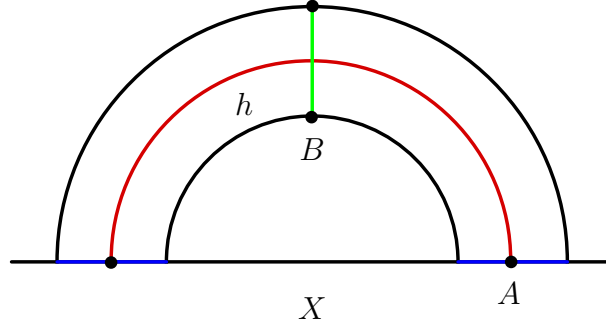


**Figure 2.7:** The 2 dimensional 1-handle  $h$  attached to the the boundary of  $X$ , with a red core, green co-core, blue attaching regions, attaching sphere  $A \cong S^0$ , and belt sphere  $B \cong S^0$ .

When considering the diffeomorphism type of  $X \cup_{\phi} h$ , it is sufficient to specify  $\phi$  up to isotopy. We can construct  $\phi : \partial D^k \times D^{n-k} \rightarrow \partial X$  from an embedding  $\phi_0 : \partial D^k \times 0 \rightarrow \partial X$  together with a *framing*: an identification  $f$  of the normal bundle of  $\text{Im}\phi_0$  with  $\partial D^k \times \mathbb{R}^{n-k}$ , and these two pieces of data specify  $\phi$  up to isotopy. In other words, handles are specified by a knotted sphere  $\phi_0 : S^{k-1} \rightarrow \partial X$  along with a framing  $f$  of that sphere.

**Definition 2.3.2.** Let  $X^n$  be a compact manifold with  $\partial X = \partial_+ X \sqcup \partial_- X$  where  $\partial_+ X$  and  $\partial_- X$  are two compact submanifolds, either of which may be empty. A *handle decomposition* of  $X$  is an identification of  $X$  with a manifold obtained from  $I \times \partial_- X$  by attaching handles such that  $\partial_- X$  corresponds to  $\{0\} \times \partial_- X$ . If  $\partial_- X = \emptyset$ , then we call  $X$  a *handlebody*.

**Definition 2.3.3.** A *Kirby diagram* of a manifold  $X^4$  is a description of a 4-dimensional handle decomposition by a diagram in  $\mathbb{R}^3$  consisting of pairs of identified spheres (denoting the attaching spheres of 1-handles), links which

may pass through the 1-handles (denoting the attaching spheres of 2-handles), and framing data for each link.

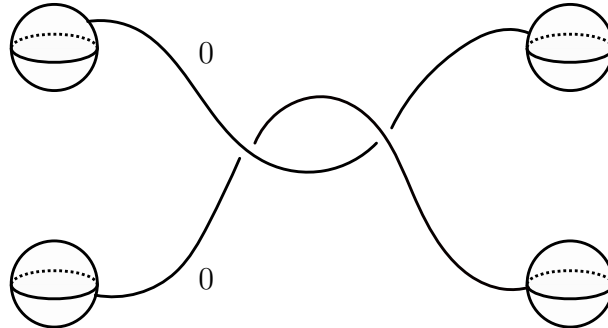


**Figure 2.8:** A Kirby diagram containing two 0-framed 2-handles and two 1-handles.

### 2.3.2 Handle Moves

**Definition 2.3.4.** Given two  $k$ -handles,  $h_1$  and  $h_2$  attached to  $\partial X$ , a *handle slide* of  $h_1$  over  $h_2$  is given by isotoping the attaching sphere of  $h_1$ , and pushing it through the belt sphere of  $h_2$ , see Figure 2.9.

**Definition 2.3.5.** A  $(k-1)$ -handle  $h_{k-1}$  and a  $k$ -handle  $h_k$ ,  $1 \leq k \leq n$  can be cancelled, provided that the attaching sphere of  $h_k$  intersects the belt sphere of  $h_{k-1}$  transversely in a single point. We call this a *handle cancellation*, see Figure 2.10.

Any two Kirby diagrams of the same manifold  $X$  are related by a finite sequence of link isotopies, handle slides, and the creation and cancellation of handle pairs.

### 2.3.3 Weinstein handle decomposition

We now bring handle decomposition to the symplectic setting. Weinstein handles were first described in [Wei91]. For more details, see [CE12].

**Definition 2.3.6.** For a Morse function  $f$  on a manifold  $X$ , a *gradient-like vector field*  $V$  for  $f$  satisfies the following:

1.  $V(f) > 0$  away from critical points, and

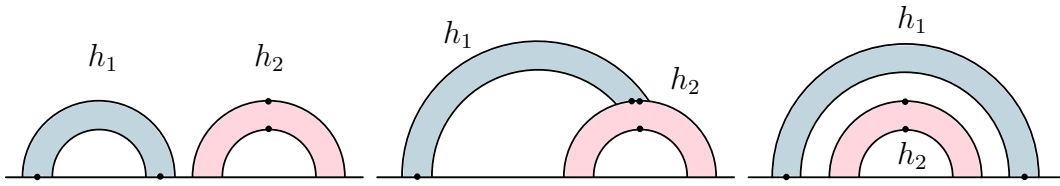


**Figure 2.9:** A 2 dimensional 1-handle slide of  $h_1$  over  $h_2$ .

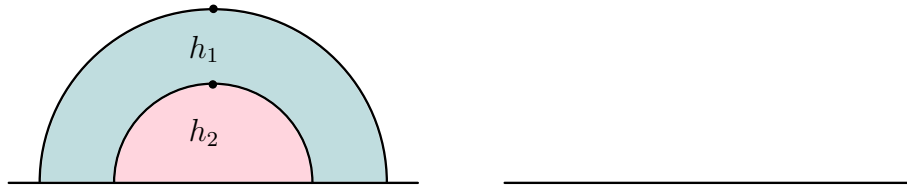


**Figure 2.10:** A 2-dimensional 1-handle  $h_1$  cancelled with a 2-dimensional 2-handle  $h_2$ .

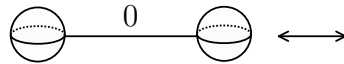


**Figure 2.11:** A cancelling pair consisting of a 1-handle and a 2-handle in a Kirby diagram.

2. for  $p \in \text{Crit}(X)$ , there is a coordinate neighbourhood of  $p$  such that  $V$  is the gradient of  $f$ , ie.  $V = -2x_1 \frac{\partial}{\partial x_1} - \dots - 2x_\lambda \frac{\partial}{\partial x_\lambda} + 2x_{\lambda+1} \frac{\partial}{\partial x_{\lambda+1}} + \dots + 2x_m \frac{\partial}{\partial x_m}$ .

**Definition 2.3.7.** A *Weinstein structure* on a smooth manifold  $X$  is encoded by:

1. a symplectic structure  $\omega$  on  $X$ ,
2. a Liouville vector field  $V$  for  $\omega$  on  $X$ ,
3. a Morse function  $\phi$  such that  $V$  is gradient like for  $\phi$ .

A *Weinstein domain*  $(X, \omega, V, \phi)$  is a symplectic manifold with *contact type boundary*, meaning  $V$  is defined near  $\partial X$  and is everywhere pointing transversely outwards along  $\partial X$ , and a Weinstein structure. A *Weinstein manifold* is a Weinstein domain extended by a cylindrical end to make  $V$  complete.

For example,  $\mathbb{C}^n$  carries the canonical Weinstein structure:

$$\begin{aligned}\omega_{std} &= \sum_{j=1}^n dx_j \wedge dy_j, \\ V_{std} &= \frac{1}{2} \sum_{j=1}^n \left( x_j \frac{\partial}{\partial x_j} + y_j \frac{\partial}{\partial y_j} \right), \text{ and} \\ \phi_{std} &= \frac{1}{4} \sum_{j=1}^n (x_j^2 + y_j^2).\end{aligned}$$

Different Weinstein structures can exist on the same symplectic manifold. For example, consider  $\mathbb{C}^n$  with the standard symplectic structure as the cotangent bundle of  $\mathbb{R}^n$ . This gives us the Weinstein structure with

$$\omega = \sum_{i=1}^n x_i dy_i, \quad V = \sum_{i=1}^n x_i \frac{\partial}{\partial x_i}, \quad \text{and} \quad \phi = \frac{1}{2} \sum_{i=1}^n |x_i|^2.$$

This  $\phi$  is not Morse, so we may perturb slightly by a Morse function  $f$  to obtain  $V' = V + V_F$  where  $V_F$  is the Hamiltonian vector field of  $F(x, y) = \langle x, \nabla f(y) \rangle$  and  $\phi' = \phi + f$ .

Given a Weinstein manifold  $(X, \omega, V, \phi)$ , any regular level set  $\Sigma_c := \phi^{-1}(c)$  carries a canonical contact structure  $\xi$  defined by the contact form  $\alpha = (\iota_V \omega)|_{\Sigma}$ .

**Definition 2.3.8.** A smooth family  $(X, \omega_s, V_s)$ ,  $s \in [0, 1]$  of Liouville manifolds is a *simple Liouville homotopy* if there exists a smooth family of exhaustions  $X = \bigcup_{k=1}^{\infty} X_s^k$  by compact domains  $X_s^k \subset V$  with smooth boundaries along which  $V_s$  is outward pointing.

A smooth family  $(X, \omega_s, V_s)$ ,  $s \in [0, 1]$  of Liouville manifolds is a *Liouville homotopy* if it is a finite composition of simple Liouville homotopies.

A *Weinstein homotopy* is a smooth family of Weinstein structures  $(\omega_t, V_t, \phi_t)$ ,  $t \in [0, 1]$  where we allow birth-death type degenerations, such that the associated Liouville structures  $(\omega_t, V_t)$  form a Liouville homotopy.

**Theorem 2.3.9.** If two Weinstein manifolds are Weinstein homotopic, then they are symplectomorphic.

Weinstein manifolds are manifestly topological as they can be specified up to Weinstein homotopy by some handle attachment data. An exhaustion of a Weinstein manifold  $(X, \omega, V, \phi)$  by regular sublevel sets  $\Sigma_c$ ,  $c \leq d_k$ , such that each interval  $(d_{k-1}, d_k)$  contains at most one critical value provides a handlebody decomposition of  $V$  whose core discs are symplectically isotropic and whose attaching spheres are contactly isotropic.

**Theorem 2.3.10.** [Wei91] Weinstein handle attachment is completely specified (up to Weinstein homotopy) by the attaching data of the Liouville vector fields along the isotropic attaching spheres, ie. given a Weinstein manifold  $(X^{2n}, \omega, V, \phi)$ , let  $S^{k-1}$  be an embedded isotropic sphere with trivial conformal symplectic normal bundle in  $\Sigma = \Sigma_{d_k}$ . Then the elementary cobordism from  $\Sigma$  to  $\Sigma'$  obtained by attaching a standard Weinstein  $k$ -handle to  $\Sigma \times I$  along a neighbourhood of  $S^{k-1}$  carries a symplectic structure and a Liouville vector field transverse to  $\Sigma$  and  $\Sigma'$ .

We can also think of these handle attachments in terms of contact surgery on  $\Sigma$  along  $S^{k-1}$ . The contact structure induced on  $\Sigma$  is the given one, and the contact structure on  $\Sigma'$  differs only from  $\Sigma$  on the spheres where the surgery took place.

**Definition 2.3.11.** [Wei91] The *standard Weinstein  $k$ -handle* is constructed as a submanifold of

$$(\mathbb{R}^{2n}, \omega, V_k, f_k),$$

where

$$\begin{aligned} \omega &= \sum_{j=1}^n dx_j \wedge dy_j, \\ V_k &= \nabla f_k, \\ f_k &= \frac{1}{4} \sum_{j=1}^{n-k} (x_j^2 + y_j^2) + \sum_{j=n-k+1}^n (x_j^2 - \frac{1}{2}y_j^2). \end{aligned}$$

Consider the closed unit  $k$ -disc in  $\{x_1 = \cdots = x_n = y_1 = \cdots = y_{n-k} = 0\}$ ,

isotropic with respect to  $\omega$ . For some  $\epsilon > 0$ , take the tubular neighbourhood

$$h_k^\epsilon = \left\{ \sum_{j=1}^n x_j^2 + \sum_{j=1}^{n-k} y_j^2 \leq \epsilon \right\} \cap \left\{ \sum_{j=n-k+1}^n y_j^2 \leq 1 \right\}$$

with the induced Weinstein structure. Notice that  $X_k$  is transverse to  $\partial h_k^\epsilon$ , flowing in one boundary component and out the other, see Figure 2.12.

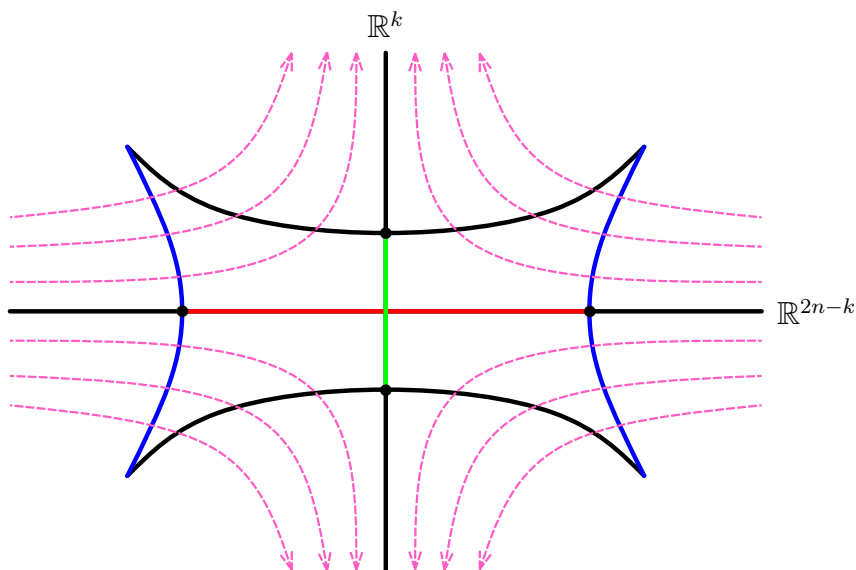


**Figure 2.12:** The standard Weinstein  $k$ -handle in  $\mathbb{R}^{2n}$ . The Liouville vector field  $X_k$  (in pink) flows in one of the boundary components and out the other.

We saw that smooth handle decomposition is depicted by smooth knots, we now look at Weinstein handle decomposition depicted via Legendrian knots.

**Definition 2.3.12.** [Gom98] A *Legendrian link diagram* in *Gompf standard form* with  $n \geq 0$  1-handles is given by the following data:

1. A rectangular box parallel to the axes in  $\mathbb{R}^2$ ,
2. A collection of  $n$  distinguished segments of each vertical side of the box, aligned horizontally in pairs and denoted by balls or walls and
3. A front projection of a Legendrian tangle (a disjoint union of Legendrian

knots and arcs) contained in the box, with endpoints lying in the distinguished segments and aligned horizontally in pairs.

Note that while framing data was required to define a smooth Kirby diagram, in the case of Legendrian link diagrams, the framing is given by the Thurston-Bennequin number minus 1. Gompf showed that given such a diagram, the boundary of a 1-handlebody  $H$  can be identified with a contact manifold obtained from the standard contact structure on  $S^3$  by removing smooth balls and gluing in the resulting boundaries as in a given Legendrian link diagram in standard form. Two Legendrian links in standard form are contact isotopic in  $\partial H$  if and only if they are related by a finite sequence of the six moves shown in Figures 2.2 and 2.13, and Legendrian isotopies of the box that fix the outside boundary of the balls and introduce no vertical tangencies. We call the moves in Figure 2.13 *Gompf 4*, *Gompf 5*, and *Gompf 6*, respectively.

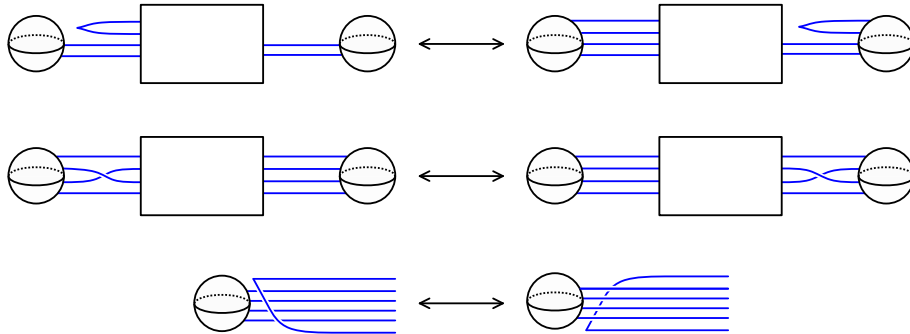


**Figure 2.13:** Gompf's three additional isotopic moves, up to 180 degree rotation about each axis.

Thus, if two Weinstein diagrams are related by a finite sequence of isotopies consisting of the six Gompf moves, handle slides, and the creation and cancellation of handle pairs, then they are two different Weinstein diagrams of the same Weinstein domain. These moves also relate the contact manifold which is the boundary of such a Weinstein domain.

### 2.3.4 Contact surgery diagrams

As stated in the previous section, a Weinstein diagram depicts not only a 4-dimensional manifold but also the 3-dimensional contact manifold at its boundary. An equivalent treatment of these link diagrams is given by contact surgery.

**Definition 2.3.13.** Let  $L \subset S^3$  be a Legendrian knot. Let  $N(L)$  denote a small neighbourhood of  $L$  with meridian and longitude  $\mu$  and  $\lambda$  respectively along  $\partial N(L)$  such that  $\lambda$  lies on a Thurston-Bennequin number framed push-off of  $L$ . An  $(\frac{a}{b})$ -Legendrian surgery is a Dehn surgery along  $L$  with a slope  $\frac{a}{b} \neq 0$  with respect to the Thurston-Bennequin framing: we construct a new manifold  $M = (S^1 \times D^2) \cup_f S^3 \setminus N(L)$  where  $S^1 \times D^2$  is glued in via the map  $f : S^1 \times \partial D^2 \rightarrow \partial N(L)$  which sends  $\{\star\} \times \partial D^2$  to  $a\mu + b\lambda$ .

When  $\frac{a}{b} = -1$ , we call this a *Legendrian surgery*.

Note that if  $\frac{a}{b} \neq \frac{1}{n}$ , then the contact structure on the surgered manifold is not unique.

A contact surgery diagram thus consists of a link in  $S^3$  along with framing coefficients  $\frac{a}{b}$  for each component of the link.

**Theorem 2.3.14.** [DG09] Let  $L \subset (M, \xi)$  be a Legendrian knot. Let  $L'$  be a Legendrian push-off of  $L$ . Then the manifold  $(M', \xi')$  given by a Legendrian-surgery along  $L$  and a contact  $(+1)$ -surgery along  $L'$  is contact isotopic to  $(M, \xi)$ .

Thus in a contact surgery diagram, a cancelling pair of surgeries consists of a  $(+1)$ -surgery and a  $(-1)$ -surgery along a pair of parallel Legendrian knots. Additionally we can use the three Reidemeister moves and three Gompf moves to manipulate surgery diagrams because of the following theorem:

**Theorem 2.3.15.** Let  $(X, \omega)$  be a Weinstein domain whose handle decomposition is given by a Weinstein diagram. Attaching a 2-handle to  $(X, \omega)$  along a Legendrian knot  $L$  in its boundary  $M$  gives a symplectic manifold  $(X', \omega')$  whose boundary  $M'$  is the result of a Legendrian surgery on  $L \subset M$ .



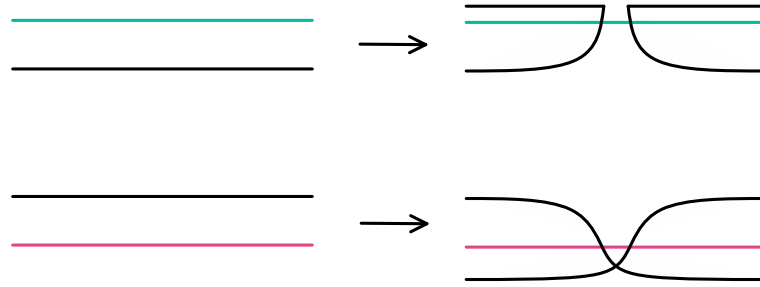


**Figure 2.14:** Top: handle sliding over a  $(-1)$ -surgery Legendrian (turquoise). Bottom: handle sliding over a  $(+1)$ -surgery Legendrian (pink) resulting in a cusp and a cone respectively. The crossing may appear on either the top or bottom of the pink strand by a single application of Reidemeister 3.

In [DG09], Ding and Geiges establish handle slides for surgery diagrams as band sums between the sliding knot and a Legendrian push-off of the knot that was slid over. This is realized diagrammatically as a spherical cusp–edge for a Legendrian handle slide over a  $(-1)$ -surgery Legendrian knot, and as a cone singularity for a Legendrian handle slide over a  $(+1)$ -surgery Legendrian knot. This is also shown (and generalized to higher dimensional Legendrians) in Proposition 2.14 of [CM19]. This allows us to manipulate surgery diagrams by handle slides as shown in Figure 2.14.

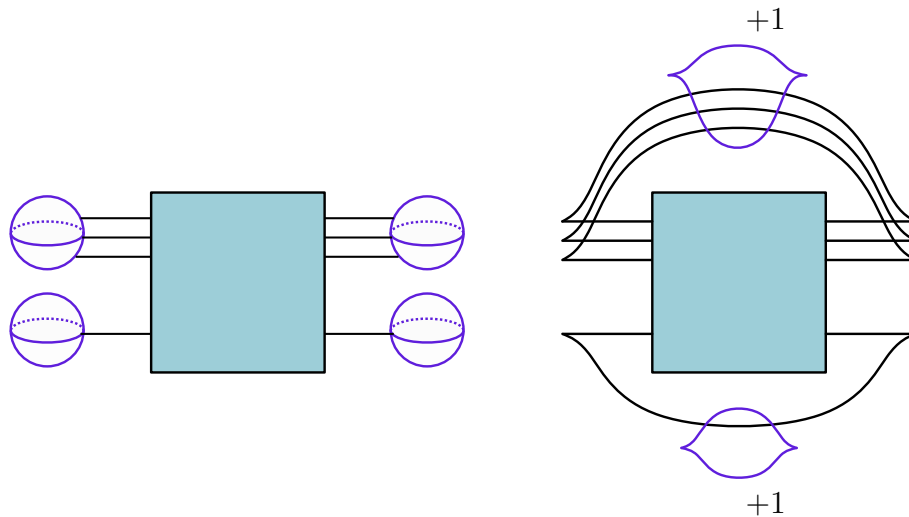


**Figure 2.15:** Diagrams depicting the same contact 3-manifold, we swap the 1-handles in the diagram on the left for the  $(+1)$  contact surgeries on the right. The blue box denotes some arbitrary Legendrian tangle.

Ding and Geiges also show that there is a standard way to replace 1-handles by contact  $(+1)$ -surgeries along trivial Legendrian unknots. This process is illustrated in Figure 2.15.

Thus once we obtain a Legendrian link diagram depicting a contact 3-manifold we can manipulate it as a contact surgery diagram as well as using the calculus developed by Kirby and Gompf for Weinstein diagrams, with the link diagram representing the contact boundary of a Weinstein domain.

## Chapter 3

# Obstructing families of Murasugi braids

### 3.1 Initial obstructions from fillings

In this section, we prove some new obstructions to Lagrangian concordance to and from the unknot which come from restrictions on the fillings of cyclic branched covers of knots. We use these theorems to obstruct some families of Murasugi braids. To begin, we will need Lemma 4.1 of [CGHS13] which gives a way of approximating a Lagrangian filling with a symplectic one:

**Lemma 3.1.1.** [CGHS13] Let  $(X, \omega)$  be a strong filling of  $(Y, \xi)$  with an oriented Lagrangian  $L \subset X$  whose boundary is a Legendrian  $\Lambda \subset Y$ . Then, the Lagrangian surface  $L$  may be  $C^\infty$  approximated by a symplectic surface  $L'$  that satisfies:

1.  $\omega|_{L'} > 0$  and
2.  $\partial L'$  is a positive transverse link smoothly isotopic to  $\Lambda$ .

This result follows from Lemma 2.3.A proved by Eliashberg [Eli95]:

**Lemma 3.1.2.** [Eli95] Let  $F$  be a connected surface with boundary in a 4-dimensional symplectic manifold  $(X, \omega)$ . Suppose that  $\omega|_F$  is positive near  $\partial F$  and non-negative elsewhere. Then  $F$  can be  $C^\infty$ -approximated by a surface  $F'$  which coincides with  $F$  near  $\partial F = \partial F'$  and such that  $\omega|_{F'} > 0$ .

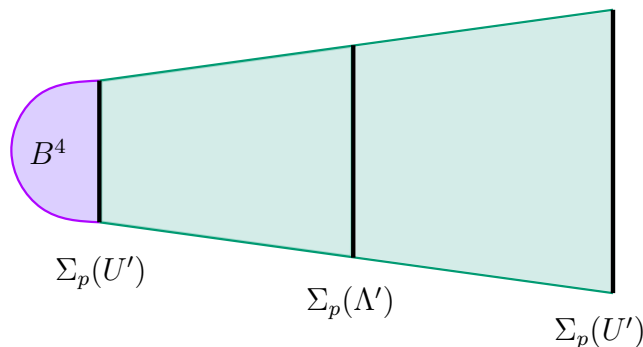


**Figure 3.1:**  $\Sigma_p(L') \cup B^4$ , a filling of  $\Sigma_p(U')$ . Here,  $\Sigma_p(C')$  is represented by the green area.

Additionally, we will use Theorem 1.2 of [Cha10]:

**Theorem 3.1.3.** [Cha10] Consider the standard contact  $S^3$  and let  $U$  be the standard Legendrian unknot with  $tb(U) = -1$ . Let  $C$  be an oriented Lagrangian cobordism from  $U$  to itself, then there is a compactly supported symplectomorphism  $\phi$  of  $\mathbb{R} \times S^3$  such that  $\phi(C) = \mathbb{R} \times U$ .

This theorem follows from an important result of Eliashberg and Polterovich, Theorem 1.1.A of [EP96]:

**Theorem 3.1.4.** [EP96] Any flat at infinity Lagrangian embedding of  $\mathbb{R}^2$  into the standard symplectic  $\mathbb{R}^4$  is isotopic to the flat embedding via an ambient compactly supported Hamiltonian isotopy of  $\mathbb{R}^4$ .

**Theorem 3.1.5.** If  $\Lambda$  is a Legendrian knot which satisfies  $U \prec \Lambda \prec U$ , then any  $p$ -fold cyclic branched cover  $\Sigma_p(\Lambda')$  of  $S^3$  branched over the transverse push-off  $\Lambda'$  of  $\Lambda$  embeds as a contact type hypersurface in  $(B^4, \xi_{std})$ . Moreover,  $\Sigma_p(\Lambda')$  is Stein fillable and has a Stein filling which embeds in  $(B^4, \xi_{std})$ .

Note that since  $\Lambda$  must be quasipositive, fillability of  $\Sigma_p(\Lambda')$  also follows from a result of [Pla06].

*Proof of Theorem 3.1.5.* Suppose we have some Legendrian knot  $\Lambda$  in  $S^3$  such that  $U \prec \Lambda \prec U$  in  $\mathbb{R}_t \times S^3$  (which is symplectomorphic to  $\mathbb{R}^4 \setminus B^4$ ). Suppose  $\Lambda \in \{0\} \times S^3$ . Let  $C_1$  be the Lagrangian cylinder from  $U$  to  $\Lambda$  and  $C_2$  be the

Lagrangian cylinder from  $\Lambda$  to  $U$ , see Figure 1.3. By Theorem 3.1.3,  $C_1 \cup C_2$  is Hamiltonian isotopic to the product cylinder  $\mathbb{R} \times U$ .

Fill in  $C_1$  at the negative end by a Lagrangian disk in  $B^4$ . Then  $C := D^2 \cup C_1 \cup C_2$  is a Lagrangian filling of the unknot  $U$  by a standardly embedded disk. By Lemma 3.1.1, there is a symplectic approximation of  $C$ , call it  $\phi(C) = C'$  with transverse boundary  $\partial C' = U'$  where  $U'$  is the transverse unknot with self linking number  $-1$ . The  $p$ -fold cyclic branched cover of  $S^3$  branched over  $U'$  is the standard  $S^3$  (see Lemma 2.4 of [CE19]).

The  $p$ -fold cyclic branched cover of  $\mathbb{R}_t \times S^3$  branched over  $C'$ , which we will call  $\Sigma_p(C')$  is the standard four ball,  $(B^4, \xi_{std})$ .

For  $\phi$  a small enough perturbation, there is some  $t$  in a neighbourhood of 0 such that  $C'$  is transverse to  $\{t\} \times S^3$ , and  $\Lambda' = C' \cap (\{t\} \times S^3)$  is a transverse push-off of  $\Lambda$  in  $\{t\} \times S^3$ . Then  $\Sigma_p(\Lambda')$ , the  $p$ -fold cyclic branched cover of  $S^3$ , branched over  $\Lambda'$  is a contact type hypersurface in  $(B^4, \xi_{std})$ . We illustrate this in Figure 3.1.

Taking the negative end of  $\Sigma_p(C')$  bounded by  $\Sigma_p(\Lambda')$  gives a Stein filling  $X$  of  $\Sigma_p(\Lambda')$  which embeds in  $(B^4, \xi_{std})$ .  $\square$

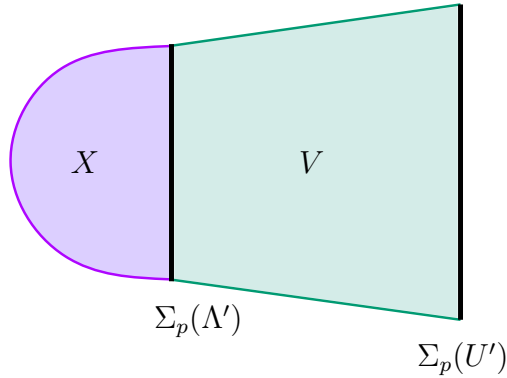


**Figure 3.2:**  $V \cup X$ , a filling of  $\Sigma_p(U')$ , where  $X$  is a filling of  $\Sigma_p(\Lambda')$ .

**Theorem 3.1.6.** If  $\Lambda$  is a Legendrian knot which satisfies  $U \prec \Lambda \prec U$ , then any filling of the  $p$ -fold cyclic branched cover  $\Sigma_p(\Lambda')$  of  $S^3$  branched over the transverse push-off  $\Lambda'$  must embed in a blow up of  $B^4$  and must have negative definite intersection form.

*Proof.* Suppose we have a Legendrian knot  $\Lambda$  in  $S^3$  such that  $\Lambda \prec U$  in  $\mathbb{R}_t \times S^3$ . Recall the construction from Theorem 3.1.5, of the branched cover  $\Sigma_p(C')$ . Recall also the 4-manifold  $X$  which is a filling of the 3-manifold  $\Sigma_p(\Lambda')$ , and which embeds in  $\Sigma_p(C')$ . Let

$$V := \Sigma_p(C') \setminus X.$$

Let  $X_0$  be any filling of  $\Sigma_p(\Lambda')$  and let  $W = X_0 \cup V$  be obtained by gluing  $X_0$  to  $V$  along  $\Sigma_p(\Lambda')$ . The boundary  $\partial(W) = \Sigma_p(U') = S^3$ . By a theorem of McDuff (Theorem 1.7 of [McD90]) or of Gromov (p 311 of [Gro85]),  $W$  is necessarily a blowup of  $B^4$  with the standard symplectic structure, as  $S^3$  has a unique minimal filling,  $B^4$ .

Finally, since any surface embedded in  $X$  is embedded in  $B^4 \# n \overline{\mathbb{C}\mathbb{P}^2}$  for some  $n \geq 0$ ,  $X$  must be negative definite.  $\square$

## 3.2 Obstructing Murasugi type 2 and 3 braids

In this section, we will begin obstructing families of 3 braids using Murasugi's classification. Recall that Murasugi [Mur74] found representatives for all conjugacy classes of 3-braids, allowing us to list all such links as the closures of one of the three following types of braid words:

1.  $(\sigma_1 \sigma_2)^{3d} \sigma_1 \sigma_2^{-a_1} \dots \sigma_1 \sigma_2^{-a_k}$  for  $a_1, \dots, a_k \geq 0$ ,
2.  $(\sigma_1 \sigma_2)^{3d} \sigma_2^m$  for  $m \in \mathbb{Z}$ ,
3.  $(\sigma_1 \sigma_2)^{3d} \sigma_1^k \sigma_2^{-1}$  for  $k = -1, -2, -3$ ,

for some  $d \in \mathbb{Z}$ . We will call these Murasugi type 1, 2, or 3 braids respectively.

First, we will show that if the Legendrian knot  $\Lambda$  satisfies  $U \prec \Lambda \prec U$ , then  $\Lambda'$ , the transverse push off of  $\Lambda$  cannot be the closure of a 3-braid of

Murasugi type 2 or type 3 unless it is the unknot. We will eliminate these braids by showing their closures are links which are not slice. First let us consider braids of Murasugi type 2.

**Lemma 3.2.1.** If the Legendrian knot  $\Lambda$  satisfies  $U \prec \Lambda \prec U$ , then  $\Lambda'$ , the transverse push off of  $\Lambda$ , cannot be the closure of a 3-braid of Murasugi type 2, ie. be of the form:

$$(\sigma_1\sigma_2)^{3d}\sigma_2^m, m \in \mathbb{Z}.$$

*Proof.* Suppose  $\hat{\beta}$  is the closure of the braid

$$\beta = (\sigma_1\sigma_2)^{3d}\sigma_2^m, m \in \mathbb{Z}.$$

We note that both a full twist  $(\sigma_1\sigma_2)^3$  and its inverse,  $(\sigma_2^{-1}\sigma_1^{-1})^3$  do not change the relative positions of the strands in the braid. Thus when we take the closure of  $\beta$ , we connect the first strand to itself and  $\hat{\beta}$  is a multiple component link and, thus cannot be concordant to the unknot, see Figure 3.3.  $\square$

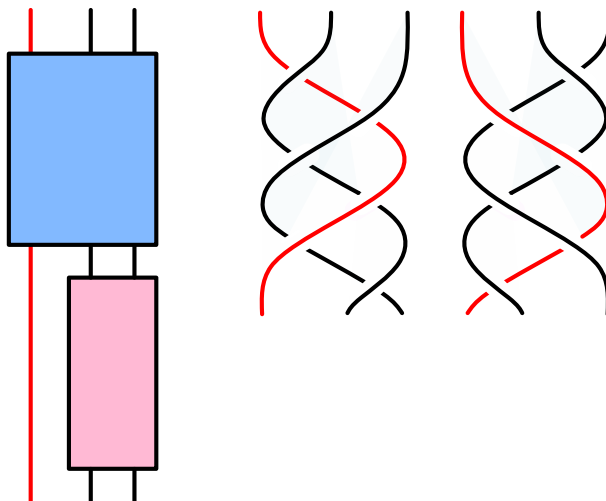


**Figure 3.3:** The red strand in a Murasugi type 2 braid forms a single component. The blue box contains some number of positive or negative full twists, which are shown to the right. The pink box contains some number of full twists of the two strands it contains.

Eliminating the Murasugi type 3 braids depends on the fact that if  $\hat{\beta}$  is the closure of a braid  $\beta$ , then  $\beta$  must be quasipositive but not strongly

quasipositive (and therefore not positive). Recall that a braid is called *positive* if it can be represented as the product of positive generators of the braid group.

A braid is *strongly quasipositive* if it is the product of positive bands

$$\sigma_{i,j} = (\sigma_j \dots \sigma_{i-2})\sigma_{i-1}(\sigma_j \dots \sigma_{i-2})^{-1}$$

where  $j < i$ . Thus any positive braid is strongly quasipositive. A braid is *quasipositive* if it is the product of conjugates of positive generators of the braid group. We know that strongly quasipositive braids are quasipositive. A knot is called *(strongly) quasipositive* if it is the closure of a (strongly) quasipositive braid. It follows from [BO01] that Lagrangian fillable Legendrian knots are quasipositive and it follows from [KM93] that slice knots are not strongly quasipositive. Thus if  $\Lambda$  satisfies  $U \prec \Lambda \prec U$ ,  $\Lambda$  must be quasipositive, but not strongly quasipositive. We will eliminate all braid words of Murasugi type 3 by showing they are either positive or negative by demonstrating a word of an equivalent braid up to conjugation with either all positive or all negative generators, except the case of the word  $(\sigma_1\sigma_2)^3\sigma_1^{-3}\sigma_2^{-1}$  as this is the unknot, see Figure 3.4.

**Lemma 3.2.2.** If the Legendrian knot  $\Lambda$  satisfies  $U \prec \Lambda \prec U$ , then  $\Lambda'$ , the transverse push off of  $\Lambda$ , cannot be the closure of a 3-braid of Murasugi type 3, ie. be of the form:

$$(\sigma_1\sigma_2)^{3d}\sigma_1^{-m}\sigma_2^{-1}, m \in \{1, 2, 3\}$$

unless it is the unknot (the closure of the braid  $(\sigma_1\sigma_2)^3\sigma_1^{-3}\sigma_2^{-1}$ ).

*Proof.* Let  $\hat{\beta}$  be the closure of the braid

$$\beta = (\sigma_1\sigma_2)^{3d}\sigma_1^{-m}\sigma_2^{-1}, m \in \{1, 2, 3\}.$$

If  $d \leq 0$ ,  $\beta$  is the product of negative generators. It is not quasipositive and thus fails to be Lagrangian slice. In fact, the mirror of  $\beta$  is a positive braid,



hence  $m(\hat{\beta})$  cannot be smoothly slice, so neither can  $\hat{\beta}$ . Thus we consider the case that  $d > 0$ . In this case we perform the following manipulations using the braid relation  $\sigma_1\sigma_2\sigma_1 = \sigma_2\sigma_1\sigma_2$  when  $m = 1$ :

$$\begin{aligned}
& (\sigma_1\sigma_2)^{3d}\sigma_1^{-1}\sigma_2^{-1} \\
&= (\sigma_1\sigma_2)^{3(d-1)}\sigma_1\sigma_2\sigma_1(\sigma_2\sigma_1\sigma_2)\sigma_1^{-1}\sigma_2^{-1} \\
&= (\sigma_1\sigma_2)^{3(d-1)}\sigma_1\sigma_2\sigma_1(\sigma_1\sigma_2\sigma_1)\sigma_1^{-1}\sigma_2^{-1} \\
&= (\sigma_1\sigma_2)^{3(d-1)}\sigma_1\sigma_2\sigma_1\sigma_1.
\end{aligned}$$

Similarly, for  $m = 2$ , since  $\sigma_1\sigma_2 = \sigma_2^{-1}\sigma_1\sigma_2\sigma_1$ :

$$\begin{aligned}
& (\sigma_1\sigma_2)^{3d}\sigma_1^{-2}\sigma_2^{-1} \\
&= (\sigma_1\sigma_2)^{3(d-1)}\sigma_1\sigma_2\sigma_1\underline{\sigma_2\sigma_1\sigma_2}\sigma_1^{-2}\sigma_2^{-1} \\
&= (\sigma_1\sigma_2)^{3(d-1)}\sigma_1\sigma_2\sigma_1\underline{\sigma_1\sigma_2}\sigma_1^{-1}\sigma_2^{-1} \\
&= (\sigma_1\sigma_2)^{3(d-1)}\sigma_1\sigma_2\sigma_1\underline{\sigma_2^{-1}\sigma_1\sigma_2\sigma_1}\sigma_1^{-1}\sigma_2^{-1} \\
&= (\sigma_1\sigma_2)^{3(d-1)}\underline{\sigma_1\sigma_2\sigma_1}\sigma_2^{-1}\sigma_1 \\
&= (\sigma_1\sigma_2)^{3(d-1)}\underline{\sigma_2\sigma_1\sigma_2}\sigma_2^{-1}\sigma_1 \\
&= (\sigma_1\sigma_2)^{3(d-1)}\sigma_2\sigma_1\sigma_1.
\end{aligned}$$

Note that these braids can also be eliminated for being 2-component links. For  $m = 3$  if  $d > 1$ , since  $\sigma_2\sigma_1 = \sigma_1^{-1}\sigma_2\sigma_1\sigma_2$ :

$$\begin{aligned}
& (\sigma_1\sigma_2)^{3d}\sigma_1^{-3}\sigma_2^{-1} \\
&= (\sigma_1\sigma_2)^{3(d-1)}\sigma_1\sigma_2\sigma_1\underline{\sigma_2\sigma_1\sigma_2}\sigma_1^{-3}\sigma_2^{-1} \\
&= (\sigma_1\sigma_2)^{3(d-1)}\sigma_1\sigma_2\sigma_1\underline{\sigma_1\sigma_2}\sigma_1^{-2}\sigma_2^{-1} \\
&= (\sigma_1\sigma_2)^{3(d-1)}\sigma_1\sigma_2\sigma_1\underline{\sigma_2^{-1}\sigma_1\sigma_2\sigma_1}\sigma_1^{-2}\sigma_2^{-1} \\
&= (\sigma_1\sigma_2)^{3(d-1)}\sigma_1\sigma_2\sigma_1\underline{\sigma_2^{-1}\sigma_1\sigma_2}\sigma_1^{-1}\sigma_2^{-1} \\
&= (\sigma_1\sigma_2)^{3(d-1)}\underline{\sigma_1\sigma_2\sigma_1}\sigma_2^{-1}\sigma_2^{-1}\sigma_1\sigma_2\sigma_1\sigma_1^{-1}\sigma_2^{-1} \\
&= (\sigma_1\sigma_2)^{3(d-1)}\underline{\sigma_2\sigma_1\sigma_2}\sigma_2^{-2}\sigma_1
\end{aligned}$$

$$\begin{aligned}
&= (\sigma_1 \sigma_2)^{3(d-1)} \sigma_2 \sigma_1 \sigma_2^{-1} \sigma_1 \\
&= (\sigma_1 \sigma_2)^{3(d-2)} \sigma_1 \sigma_2 \sigma_1 \sigma_2 \sigma_1 \sigma_2 \sigma_1 \sigma_2^{-1} \sigma_1 \\
&= (\sigma_1 \sigma_2)^{3(d-2)} \sigma_1 \sigma_2 \sigma_1 \sigma_2 \sigma_1 \sigma_2 \sigma_1^{-1} \sigma_2 \sigma_1 \sigma_2 \sigma_2^{-1} \sigma_1 \\
&= (\sigma_1 \sigma_2)^{3(d-2)} \sigma_1 \sigma_2 \sigma_1 \sigma_1 \sigma_2 \sigma_1 \sigma_1^{-1} \sigma_2 \sigma_1 \sigma_1 \\
&= (\sigma_1 \sigma_2)^{3(d-2)} \sigma_1 \sigma_2 \sigma_1 \sigma_1 \sigma_2 \sigma_2 \sigma_1 \sigma_1.
\end{aligned}$$

In all these cases  $\beta$  can be written as a product of positive generators. Thus  $\beta$  is strongly quasipositive, and hence, not smoothly slice. The only case that remains is when  $d = 1$  and  $m = 3$ . In this case,  $\hat{\beta}$  is the unknot, as illustrated by the isotopy pictured Figure 3.4.  $\square$

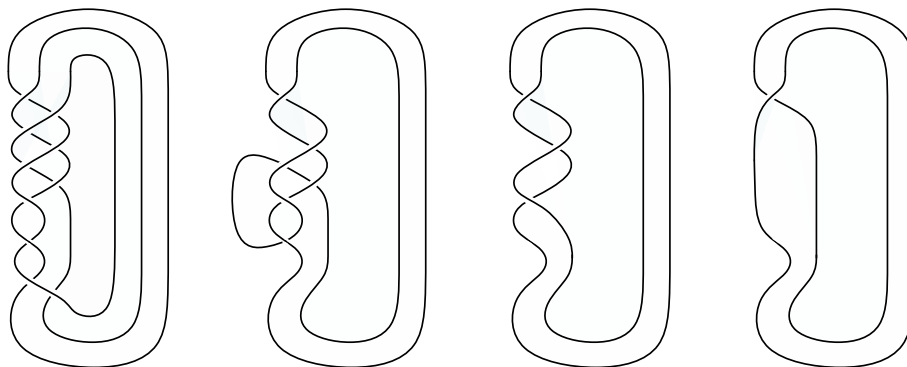


**Figure 3.4:** A smooth isotopy of the closure of the braid  $(\sigma_1 \sigma_2)^3 \sigma_1^{-3} \sigma_2^{-1}$ .

**Remark 3.2.3.** Chantraine's restriction on the Thurston-Bennequin number [Cha10] states that if  $\Lambda_-$  is cobordant to  $\Lambda_+$ , then

$$tb(\Lambda_-) - tb(\Lambda_+) = -\chi(L)$$

where  $L$  is the Lagrangian cobordism.

In the case that  $\Lambda$  is the unstabilized unknot, since for concordance  $\chi(L) = 0$ , and we know that  $tb(\Lambda) = -1$ , we can eliminate all stabilized Legendrian unknots with  $tb < -1$  from concordance both to and from  $\Lambda$ . In other words, the only Legendrian unknot concordant to  $U$  is  $U$ .

Thus, if, the Legendrian knot  $\Lambda \neq U$  satisfies  $U \prec \Lambda \prec U$ , and  $\Lambda$  is a 3-braid, then it must be of Murasugi type 1.

### 3.3 Using Gompf's 3-dimensional 2-plane field invariant

Next, we will prove an obstruction to the concordance  $U \prec \Lambda \prec U$  coming from the  $d_3$  invariant of  $\Sigma_2(\Lambda')$ , proved in Theorem 4.16 of [Gom98], and apply it to the case where  $\Lambda'$  is a transverse knot which is the closure of a 3-braid of Murasugi type 1, that is of the form

$$(\sigma_1\sigma_2)^{3d}\sigma_1\sigma_2^{-a_1} \dots \sigma_1\sigma_2^{-a_n}$$

for  $d \in \mathbb{Z}$ ,  $a_1, \dots, a_n \geq 0$ , and some  $a_i > 0$ .

For a given contact 3-manifold  $(M, \xi)$ , we can define the  $d_3$  invariant on the homotopy type of the 2-plane field:

**Theorem 3.3.1.** [Gom98] Suppose we have a contact 3-manifold  $(M, \xi)$ , and suppose we have an almost complex 4-manifold  $(X, J)$  such that  $\partial X = M$ , with  $\xi$  induced by the complex tangencies:  $\xi = (TM) \cap J(TM)$ . Let  $\sigma(X)$  denote the signature of  $X$ , and let  $\chi(X)$  denote the Euler characteristic of  $X$ . For  $c_1(\xi)$  a torsion class, the rational number

$$d_3(\xi) = \frac{c_1^2(X, J) - 3\sigma(X) - 2\chi(X)}{4}$$

is an invariant of the homotopy type of the 2-plane field  $\xi$ .

Using Theorem 3.1.5, we prove a restriction to  $d_3(\xi)$  for such  $(\Sigma_2(\Lambda'), \xi)$ :

**Theorem 3.3.2.** If  $\Lambda$  is a Legendrian knot which satisfies  $U \prec \Lambda \prec U$ , then the contact 2-fold cyclic branched cover  $(\Sigma_2(\Lambda'), \xi)$  of  $S^3$  branched over the positive transverse push-off  $\Lambda'$  of  $\Lambda$  has

$$d_3(\xi) = -\frac{1}{2}.$$

*Proof.* Suppose we have a Legendrian knot  $\Lambda$  satisfying  $U \prec \Lambda \prec U$ . Consider a transverse push-off  $\Lambda'$  in  $S^3$  of  $\Lambda$  and  $\Sigma_2(\Lambda')$ , the cyclic double cover of  $S^3$  branched over  $\Lambda'$ . By Theorem 3.1.5, there is a filling  $(X, \omega)$  of  $\Sigma_2(\Lambda')$  which embeds in  $\mathbb{R}^4$ .

Now we will compute  $d_3(\xi)$  using  $X$ . We begin with  $\sigma(X)$ , which is the signature of the intersection form  $Q_X$ . Let  $S$  be any surface in  $X$  and take the class  $[S] \in H_2(X)$ . Then since  $S$  embeds in  $X$  and  $X$  embeds in  $\mathbb{R}^4$ ,  $S$  embeds in  $\mathbb{R}^4$  and has self-intersection 0. Thus  $Q_X \equiv 0$ , and  $\sigma(X) = 0$ .

Next we want to find  $c_1^2(X, J)$ . We know  $c_1(X, J) \in H^2(X, \mathbb{Z})$  and by Poincaré duality,  $H^2(X) \cong H_2(X, \partial X)$ . Thus, let us consider a properly embedded surface  $F \subset X$  such that

$$[F] = PD(c_1(X, J)) \in H_2(X, \partial X).$$

Consider the exact sequence

$$0 \rightarrow H_2(X) \rightarrow H_2(X, \partial X) \rightarrow H_1(\partial X).$$

Note that for  $\Sigma_2(K)$ , the branched double cover of a knot  $K$ ,  $|H_1(\Sigma_2(K))| = \det(K)$  where the determinant of a knot is the Alexander polynomial evaluated at  $-1$ . Thus  $H_1(\partial X)$  is finite and  $[\partial F] \in H_1(\partial X)$ , thus

$$\partial(d[F]) = 0$$

for some  $d > 0$ , for instance  $d = \det(K)$ , in  $H_1(\partial X)$ . So  $d[F] = [S]$  for some closed surface  $S \subset X$ , and

$$[F]^2 = [F] \cdot \frac{1}{d}[S] = \frac{Q_X(F, S)}{d} \in \frac{1}{d}\mathbb{Z}.$$

Since  $Q_X = 0$ , we have  $c_1(X, J)^2 = [F]^2 = 0$ .

Finally, we compute the Euler characteristic of  $X$ . Note that  $X$  is the branched double cover of a properly embedded disk  $D$  in  $B^4$ ,  $X = \Sigma_2(D)$ .

Thus if we let  $\nu(D)$  denote a neighbourhood of  $D$  in  $X$ , we compute:

$$\chi(X) = 2\chi(B^4 \setminus \nu(D)) + \chi(\nu(D)) - \chi(B)$$

where  $B$  is a circle bundle over  $D$ . Thus,

$$\chi(X) = 2 \cdot 0 + 1 - 0 = 1.$$

Thus,

$$\begin{aligned} d_3(\xi) &= \frac{c_1^2(X, J) - 3\sigma(X) - 2\chi(X)}{4} \\ &= \frac{0 - 3(0) - 2(1)}{4} \\ &= -\frac{1}{2}. \quad \square \end{aligned}$$

Next, we will use this result to restrict our braid candidates. We do this using Theorem 1.1 of the work of Ito [Ito17]:

**Theorem 3.3.3.** [Ito17] If a contact 3-manifold  $(M, \xi)$  is a  $p$ -fold cyclic contact branched covering of  $(S_3, \xi_{std})$  branched along a transverse link  $K$ , then

$$d_3(\xi) = -\frac{3}{4} \sum_{\omega: \omega^p=1} \sigma_\omega(K) - \frac{p-1}{2} sl(K) - \frac{1}{2}p$$

where  $\sigma_\omega(K)$  is the Tristram-Levine signature of  $K$ , given by  $(1 - \omega)A + (1 - \bar{\omega})A^T$  where  $A$  is the Seifert matrix of  $K$ , and  $sl(K)$  is the self-linking number of  $K$ .

To compute the classic or Murasugi signature of the closure of a braid, we will use the following lemma of Erle [Erl99]:

**Lemma 3.3.4.** [Erl99] Let  $\hat{\beta}$  denote the closure of the 3-braid

$$\beta = (\sigma_1\sigma_2)^{3d}\sigma_1^{-a_1}\sigma_2^{b_1}\dots\sigma_1^{-a_m}\sigma_2^{b_m}$$

where  $d \in \mathbb{Z}$ ,  $m \geq 1$ , and  $a_i, b_i \geq 1$ . Then the signature of  $\hat{\beta}$  is

$$\sigma(\hat{\beta}) = -4d + \sum_{i=1}^m (a_i - b_i).$$

The Murasugi signature of a knot agrees with the Tristram-Levine signature for  $\omega = -1$  by definition, see [Con19]. Thus Erle's formula can be applied to Ito's formula for double covers. Doing so results in the following obstruction to Lagrangian concordance:

**Theorem 3.3.5.** If  $\Lambda \neq U$  is a Legendrian knot which satisfies  $U \prec \Lambda \prec U$ , and  $\Lambda'$ , the transverse pushoff of  $\Lambda$ , is the closure of a 3-braid  $\beta$ , then, up to conjugation,

$$\beta = (\sigma_1 \sigma_2)^{3d} \sigma_1 \sigma_2^{-a_1} \dots \sigma_1 \sigma_2^{-a_n}$$

for some  $d \in \mathbb{Z}$ ,  $a_1, \dots, a_n \geq 0$ , and some  $a_i > 0$ , and  $\sum a_i = n + 4$ .

*Proof.* Let  $\Lambda$  be a Legendrian knot which satisfies  $U \prec \Lambda \prec U$ , and  $\Lambda'$  be a transverse pushoff of  $\Lambda$ . Suppose  $\Lambda'$  is the closure of a 3-braid. Let  $(\Sigma_2(\Lambda'), \xi)$  be a cyclic double cover of  $S^3$  branched over  $\Lambda'$ . Then from 3.3.3 and 3.3.2, we get that

$$-\frac{1}{2} = d_3(\xi) = -\frac{3}{4} \sum_{\omega: \omega^2=1} \sigma_\omega(K) - \frac{2-1}{2} sl(K) - \frac{1}{2}.$$

By Lemmas 3.2.1 and 3.2.2, the braid  $\beta$  whose closure is  $\Lambda$  is a Murasugi type 1 braid, that is

$$\beta = (\sigma_1 \sigma_2)^{3d} \sigma_1 \sigma_2^{-a_1} \dots \sigma_1 \sigma_2^{-a_n}$$

for some  $d \in \mathbb{Z}$ ,  $a_1, \dots, a_n \geq 0$ , and some  $a_i > 0$ . Then we can compute the algebraic length of  $\beta$ . Recall that the algebraic length of a braid is given by  $n_+ - n_-$  where  $n_+$  is the sum of the positive exponents in the braid word, and  $n_-$  is the sum of the negative exponents in the braid word. Thus we have  $\text{len}(\beta) = 6d + n - \sum_{i=1}^n a_i$ .

The self-linking number of  $\Lambda'$  can be computed from this algebraic length and is given by:

$$sl(\Lambda') = \text{len}(\beta) - (\text{number of strands of } \beta) = 6d + n - \sum_{i=1}^n a_i - 3.$$

To apply Erle's formula (Lemma 3.3.4) for signature to  $\Lambda$ , we first convert  $\beta$  to the form

$$(\sigma_1\sigma_2)^{3d}\sigma_1^{-a_1}\sigma_2^{b_1}\dots\sigma_1^{-a_m}\sigma_2^{b_m}.$$

This can be done with a series of braid manipulations.

We know  $\sigma_1 = \sigma_2^{-1}\sigma_1^{-1}\sigma_2\sigma_1\sigma_2$ , thus we get:

$$\begin{aligned}\sigma_1\sigma_2^{-a} &= \sigma_2^{-1}\sigma_1^{-1}\sigma_2\sigma_1\sigma_2\sigma_2^{-a} \\ &= (\sigma_2^{-1}\sigma_1^{-1}\sigma_2)\sigma_1\sigma_2^{-(a-1)} \\ &\dots \\ &= (\sigma_2^{-1}\sigma_1^{-1}\sigma_2)^a\sigma_1 \\ &= \sigma_2^{-1}\sigma_1^{-a}\sigma_2\sigma_1\end{aligned}$$

Additionally, we know  $\sigma_2\sigma_1 = \sigma_1^{-1}\sigma_2\sigma_1\sigma_2$ . We apply these manipulations to  $\beta$ :

$$\begin{aligned}\beta &= (\sigma_1\sigma_2)^{3d}(\sigma_1\sigma_2^{-a_1})(\sigma_1\sigma_2^{-a_2})\dots(\sigma_1\sigma_2^{-a_n}) \\ &= (\sigma_1\sigma_2)^{3d}(\sigma_2^{-1}\sigma_1^{-a_1}\sigma_2\sigma_1)(\sigma_2^{-1}\sigma_1^{-a_2}\sigma_2\sigma_1)\dots(\sigma_2^{-1}\sigma_1^{-a_n}\sigma_2\sigma_1) \\ &= (\sigma_1\sigma_2)^{3d}\sigma_2^{-1}\sigma_1^{-a_1}\sigma_1^{-1}\sigma_2\sigma_1\sigma_2\sigma_2^{-1}\sigma_1^{-a_2}\sigma_1^{-1}\sigma_2\sigma_1\sigma_2\dots\sigma_2^{-1}\sigma_1^{-a_n}\sigma_1^{-1}\sigma_2\sigma_1\sigma_2 \\ &= (\sigma_1\sigma_2)^{3d}\sigma_2^{-1}\sigma_1^{-(a_1+1)}\sigma_2\sigma_1^{-a_2}\sigma_2\sigma_1^{-a_3}\dots\sigma_2\sigma_1^{-a_n}\sigma_2\sigma_1\sigma_2 \\ &= \sigma_1\sigma_2(\sigma_1\sigma_2)^{3d}\sigma_2^{-1}\sigma_1^{-(a_1+1)}\sigma_2\sigma_1^{-a_2}\sigma_2\sigma_1^{-a_3}\dots\sigma_2\sigma_1^{-a_n}\sigma_2 \\ &= (\sigma_1\sigma_2)^{3d}\sigma_1\sigma_2\sigma_2^{-1}\sigma_1^{-(a_1+1)}\sigma_2\sigma_1^{-a_2}\sigma_2\sigma_1^{-a_3}\dots\sigma_2\sigma_1^{-a_n}\sigma_2 \\ &= (\sigma_1\sigma_2)^{3d}\sigma_1^{-a_1}\sigma_2\dots\sigma_1^{-a_{n-1}}\sigma_2\sigma_1^{-a_n}\sigma_2\end{aligned}$$

Then applying Erle's formula, we get the signature:

$$\sigma(\Lambda') = -4d + \sum_{i=1}^n (a_i - 1).$$

Thus,

$$\begin{aligned} -\frac{1}{2} &= d_3(\xi) \\ -\frac{1}{2} &= -\frac{3}{4}\sigma_\omega(K) - \frac{2-1}{2}sl(K) - \frac{1}{2}2 \\ -\frac{1}{2} &= -\frac{3}{4}(-4d + \sum_{i=1}^n (a_i - 1)) - \frac{1}{2}(6d + n - \sum_{i=1}^n a_i - 3) - 1 \\ -2 &= -3(-4d + \sum_{i=1}^n a_i - n) - 2(6d + n - \sum_{i=1}^n a_i - 3) - 4 \\ -4 &= -\sum_{i=1}^n a_i + n. \end{aligned} \quad \square$$

Another restriction of the braid word follows naturally:

**Corollary 3.3.6.** If  $\Lambda \neq U$  is a Legendrian knot which satisfies  $U \prec \Lambda \prec U$ , and if  $\Lambda'$ , the transverse pushoff of  $\Lambda$ , is the closure of a 3-braid of the form

$$\beta = (\sigma_1\sigma_2)^{3d}\sigma_1\sigma_2^{-a_1} \dots \sigma_1\sigma_2^{-a_n},$$

then  $d = 1$ .

*Proof.* Suppose we have such a  $\Lambda$  and  $\Lambda'$ . It follows that  $\Lambda'$  is slice, thus the signature of  $\Lambda'$  must vanish. Applying Theorem 3.3.5 to Erle's formula for signature, we get:

$$\begin{aligned} \sigma(\Lambda') &= -4d + \sum_{i=1}^n a_i - n \\ 0 &= -4d + (n + 4) - n \\ d &= 1. \end{aligned} \quad \square$$



**Corollary 3.3.7.** If  $\Lambda$  is a Legendrian knot which satisfies  $U \prec \Lambda \prec U$ , and  $\Lambda'$ , the transverse pushoff of  $\Lambda$ , is the closure of a 3-braid  $\beta$ , then the algebraic length of  $\beta$  is 2.

*Proof.* If  $\beta$  is of Murasugi type 1, then we have the restrictions coming from Theorem 3.3.2 and Corollary 3.3.6. Thus, the algebraic length of  $\beta$  is

$$\text{len}(\beta) = 6d + n - \sum_{i=1}^n a_i = 6 + n - (n + 4) = 2.$$

Otherwise,  $\beta$  is not of Murasugi type 1, then  $\Lambda = U$  and

$$\beta = (\sigma_1 \sigma_2)^3 \sigma_1^{-3} \sigma_2^{-1}$$

which has algebraic length  $6 - 4 = 2$ . □

## Chapter 4

# From open book decompositions to Weinstein diagrams

### 4.1 Open Book Decompositions and Lefschetz Fibrations

We begin this section by discussing open book decompositions and their relationship to Lefschetz fibrations. We begin with the definition of a Dehn twist, a well studied self-homeomorphism of a surface:

**Definition 4.1.1.** Let  $F$  be any surface. Let  $\alpha$  be a simple closed curve in  $F$ . Then a *right-handed Dehn twist*  $\tau_\alpha$  about  $\alpha$  acts on a neighbourhood of  $\alpha$ ,  $N = \alpha \times (0, 1) \subset F$ , by  $(\theta, t) \mapsto (\theta + 2\pi t, t)$  while fixing  $F \setminus N$ . A *left-handed Dehn twist* about  $\alpha$  is  $\tau_\alpha^{-1}$ , see Figure 4.1.

For notation, let

$$\tau_{\alpha_1\alpha_2} = \tau_{\alpha_1} \circ \tau_{\alpha_2} = \tau_{\alpha_1}\tau_{\alpha_2}$$

denote the composition of Dehn twists. If  $\alpha$  is a curve and  $f$  is an orientation preserving surface homeomorphism then  $\tau_{f(\alpha)} = f \circ \tau_\alpha \circ f^{-1}$ .

Open books provide a particularly useful perspective on contact manifolds. By work of Giroux [Gir02], and Thurston and Winkelnkemper [TW75], there is a correspondence between contact structures and open book decompositions. For details, see [Etn06].

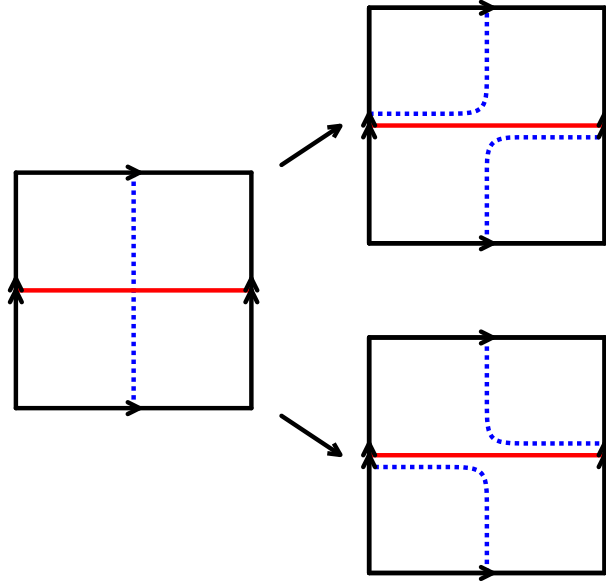


**Figure 4.1:** A right handed and left handed Dehn twist on the red curve in the torus.

**Definition 4.1.2.** An *open book decomposition* of a 3-manifold  $M$  is a pair  $(B, \pi)$  where

1.  $B$  is an oriented link in  $M$ , called the *binding* of the open book and
2.  $\pi : M \setminus B \rightarrow S^1$  is a fibration of the complement of  $B$  such that preimages  $\pi^{-1}(t)$  correspond to the interior of a compact surface  $F \subset M$  satisfying  $\partial F = B$ .  $F$  is called the *page* of the open book decomposition.

**Definition 4.1.3.** Alternatively, an *abstract open book* is a pair  $(F, \phi)$  where

1.  $F$  is a surface with non-empty boundary and
2.  $\phi$  is a diffeomorphism of  $F$  with  $\phi|_{\partial F} = \text{id}$ ,  $\phi$  is called the *monodromy* of the open book.

To obtain a manifold  $M$  from an abstract open book, we take the mapping torus  $F \times [0, 1] / \sim$ , where  $(x, 1) \sim (\phi(x), 0)$ , and for each boundary component of  $F$ , glue in a solid torus  $S^1 \times D^2$  via a diffeomorphism which identifies each circle of the form  $\{x\} \times [0, 1] / \sim$  for  $x \in \partial F$  with  $\{y\} \times \partial D^2$  for  $y \in S^1$ . The core of the solid tori form the binding  $B$ .

**Definition 4.1.4.** Given two open book decompositions,  $(F, \phi)$  and  $(F', \phi')$  we define the *Murasugi sum*  $(F, \phi) * (F', \phi')$  to be an open book decomposition constructed as follows: choose arcs  $\alpha$  and  $\alpha'$  in  $F$  and  $F'$  with product neighbourhoods  $R$  and  $R'$  respectively. Then let

$$F * F' := F \cup_{R=R'} F'$$

glued by  $\partial\alpha \times I \mapsto \alpha' \times \partial I$  and  $\alpha \times \partial I \mapsto \partial\alpha' \times I$ . And let

$$\phi * \phi' = \phi \circ \phi'.$$

If  $(F, \phi)$  supports a contact manifold  $(M, \xi)$  and  $(F', \phi')$  supports a contact manifold  $(M', \xi')$ , then  $(F, \phi) * (F', \phi')$  supports the contact connected sum  $(M \# M', \xi \# \xi')$ .

**Definition 4.1.5.** Let  $X$  be a compact, oriented symplectic 4-manifold, let  $\Sigma$  be a compact oriented manifold with dimension 2. A *Lefschetz fibration*  $\pi : X \rightarrow \Sigma$  is a smooth surjective map which is a locally trivial fibration except at finitely many isolated, nondegenerate critical points with distinct values on the interior of  $\Sigma$ . In local coordinates near a critical point, the fibration is modelled by  $\pi(z_1, z_2) = z_1^2 + z_2^2$ . The Lefschetz fibration is *symplectic* if the fibers are symplectic submanifolds.

Let  $x_0 \in \Sigma$  be a critical value. Let  $x \in \Sigma$  be a generic value. Take a path  $x \rightarrow x_0 \subset \Sigma$ . In a fiber  $\pi^{-1}(x)$  of a generic value  $x$ , there is a closed curve  $C$  called a *vanishing cycle* which collapses after parallel transport along this path.  $\pi^{-1}(x_0)$  can be identified with  $\pi^{-1}(x)$  by collapsing  $C$  to singular ordinary double point.

A Lefschetz fibration  $\pi : X \rightarrow \Sigma$  where  $X$  is a Weinstein domain is a *Weinstein Lefschetz fibration* if its generic fiber  $F$  is also a Weinstein domain and if  $X$  is obtained by attaching critical Weinstein handles along attaching Legendrians  $\Lambda_i \subset F \times S^1 \subset \partial(F \times D^2)$  obtained by lifting the vanishing cycles  $C_i \subset F$ .

**Remark 4.1.6.** Suppose we have an open book decomposition  $\pi : M \rightarrow S^1$  of a contact 3-manifold  $(M, \xi)$  with monodromy given by positive Dehn twists  $\tau_{\alpha_1}, \dots, \tau_{\alpha_k}$  about some curves  $\alpha_1, \dots, \alpha_k$  in  $F$ . Then we can build a Lefschetz fibration  $\pi : X \rightarrow D^2$  of the Stein filling  $X$  of  $M$  where total monodromy, given as the composition of the  $\tau_i$  Dehn twists about vanishing cycles  $C_i$  collapsing in the critical surfaces  $\pi^{-1}(x_i)$ , must agree with the monodromy of the open book. As long as the fiber  $F$  has a Weinstein structure,  $X$  also has a Weinstein structure corresponding to the attachment of critical Weinstein handles along the corresponding vanishing cycles.

## 4.2 Obtaining Weinstein Lefschetz fibrations

In this section, we find a way to draw a Weinstein diagram in Gompf standard form which represents a Weinstein manifold  $X_\Lambda$  whose boundary is  $\Sigma_2(\Lambda')$  where  $\Lambda'$  is the closure of a 3-braid with algebraic length 2. In particular, the Weinstein diagram will consist of a knot in  $S^1 \times S^2$ . We begin by expressing  $\Sigma_2(\Lambda)$  as a particular open book decomposition, for which we need the following lemma:

**Lemma 4.2.1.** Any quasipositive 3-braid of algebraic length 2 is conjugate to  $\sigma_1 B \sigma_1 B^{-1}$  for some braid  $B$ .

*Proof.* Suppose we have some quasipositive 3-braid of algebraic length 2, call it  $A$ . Then  $A$  is the product of two conjugates of positive generators of the braid group,

$$A = B_i \sigma_i B_i^{-1} B_j \sigma_j B_j^{-1}$$

for  $i, j \in \{1, 2\}$ . For  $k \in \{i, j\}$ , if  $k = 1$ , let  $B_k = B'_k$ , and if  $k = 2$ , since  $\sigma_2 = \sigma_1^{-1} \sigma_2^{-1} \sigma_1 \sigma_2 \sigma_1$ , let  $B'_k = B_k \sigma_1^{-1} \sigma_2^{-1}$ . Then

$$A = B'_1 \sigma_1 B'^{-1}_1 B'_2 \sigma_1 B'^{-1}_2$$

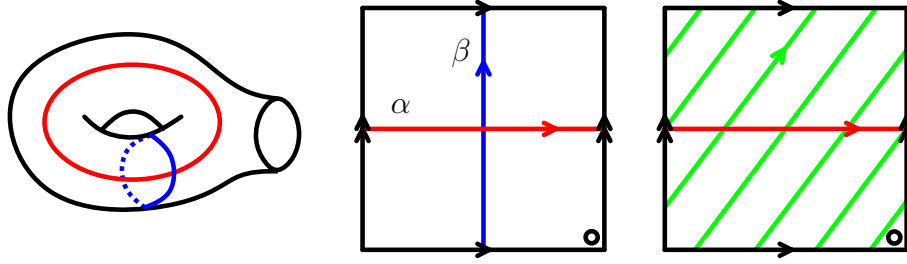


**Figure 4.2:** The curves  $\alpha$  (red),  $\beta$  (blue), and an example of a curve  $\gamma$  (green) on the torus with one boundary component. Here  $\gamma$  is the curve of slope  $(3, 4)$ .

Now we can conjugate by  $B_1'^{-1}$ :

$$\begin{aligned} A &= B_1'^{-1}(B_1'\sigma_1B_1'^{-1}B_2'\sigma_1B_2'^{-1})B_1' \\ &= \sigma_1B_1'^{-1}B_2'\sigma_1B_2'^{-1}B_1' \end{aligned}$$

So we take  $B = B_1'^{-1}B_2'$ . □

**Proposition 4.2.2.** Let  $\Lambda'$  be a transverse knot which is the closure of a quasipositive 3-braid of algebraic length 2. The double cover of  $S^3$  branched over  $\Lambda'$ ,  $(\Sigma_2(\Lambda'), \xi)$  has an open book decomposition  $(F, \phi)$  where  $F$  is a torus with one boundary component, and  $\phi = \tau_\alpha\tau_\gamma$ . Here,  $\alpha$  is the curve of slope  $(1, 0)$  and  $\gamma$  is some essential simple closed curve in  $F$ , see Figure 4.2.

*Proof.* To prove this, we will use the construction from Plamenevskaya [Pla06], described in more detail by Onaran [Ona14] and coming from a proof by Alexander [Ale20]. When a contact manifold  $(M, \xi)$  is the branched double cover of a transverse link  $L$  which is the closure of a  $(2k + 1)$ -stranded braid given by a braid word on  $2k$  generators and their inverses,  $\sigma_1, \sigma_1^{-1}, \dots, \sigma_{2k}, \sigma_{2k}^{-1}$ , we can think of  $L$  as a transverse link in the standard contact structure  $\xi_{std}$  on  $S^3$ .  $S^3$  has a planar open book decomposition with trivial monodromy and we arrange it so that the pages are transverse to the braid  $L$ . Then we may lift the contact structure on the double cover  $\Sigma_2(L)$  of  $S^3$  branched over  $L$ . The contact structure is compatible with the open book decomposition  $(F_{k,1}, \phi)$  where  $F_{k,1}$  is the genus  $k$ , 1 boundary component surface obtained by taking

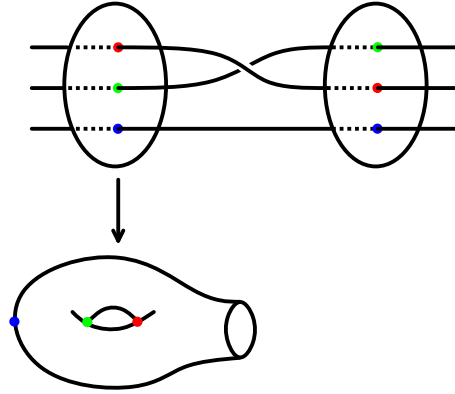


**Figure 4.3:** A torus with one boundary component is the double cover of a planar page branched over 3 points

each planar page branched over the three points where they intersect  $L$  (see Figure 4.3), and  $\phi$  is given by Dehn twists corresponding to the braid word which are the lifts of the half twists of  $L$  in  $S^3$ .

Thus the monodromy of the open book comes from the braid monodromy: each generator  $\sigma_i$  in the braid corresponds to a Dehn twist  $\tau_i$  along a curve in  $F_{k,1}$ .

Let  $\Lambda'$  be a transverse knot which is the closure of a quasipositive 3-braid of algebraic length 2. The double cover of  $S^3$  branched over  $\Lambda'$ ,  $(\Sigma_2(\Lambda'), \xi)$  has an open book decomposition  $(F, \phi)$ .

Since  $\Lambda'$  is a 3-braid,  $F := F_{1,1}$  is a torus with one boundary component with  $\sigma_1$  corresponding to a Dehn twist about  $\alpha$  and  $\sigma_2$  corresponding to a Dehn twist about  $\beta$  as seen in Figure 4.2.  $\phi$  is given by Dehn twisting along these curves corresponding to the braid monodromy of  $\Lambda'$ .

By Lemma 4.2.1,  $\Lambda'$  is the closure of of a braid of the form  $\sigma_1 B \sigma_1 B^{-1}$  for some braid  $B$  up to conjugation.

The first  $\sigma_1$  corresponds to a Dehn twist about  $\alpha$ ,  $\tau_\alpha$ .

The braid  $B \sigma_1 B^{-1}$  corresponds to a series of Dehn twists

$$\mu_1 \circ \cdots \circ \mu_m \circ \tau_\alpha \circ \mu_m^{-1} \circ \cdots \circ \mu_1^{-1}$$

where the  $\mu_i \in \{\tau_\alpha^{\pm 1}, \tau_\beta^{\pm 1}\}$  correspond to the braid generators in  $B$ . Then since

$$\begin{aligned} & (\mu_1 \circ \cdots \circ \mu_m) \circ \tau_\alpha \circ (\mu_m^{-1} \circ \cdots \circ \mu_1^{-1}) \\ &= (\mu_1 \cdots \mu_m) \circ \tau_\alpha \circ (\mu_1 \cdots \mu_m)^{-1} \\ &= \tau_{\mu_1 \cdots \mu_m(\alpha)}, \end{aligned}$$

we choose  $\gamma := \mu_1 \cdots \mu_m(\alpha)$ .

Thus the monodromy  $\phi$  of the open book decomposition is given by Dehn twists along  $\alpha$ , the curve of slope  $(1, 0)$ , and some essential simple closed curve  $\gamma$ .  $\square$

**Corollary 4.2.3.** Let  $\Lambda'$  be a transverse knot which is the closure of a quasi-positive 3-braid of algebraic length 2. The double cover of  $S^3$  branched over  $\Lambda'$ ,  $(\Sigma_2(\Lambda'), \xi)$  has Weinstein filling  $X_\Lambda$  with the following property.  $X_\Lambda$  has a Weinstein Lefschetz fibration  $\pi : X_\Lambda \rightarrow D^2$  with generic fiber  $F$ , a torus with one boundary component and monodromy given by vanishing cycles which are Dehn twists along the curves  $\alpha$  and  $\gamma$  where  $\alpha$  is the  $(1, 0)$  curve and  $\gamma$  is some essential simple closed curve in  $F$ , see Figure 4.2.

*Proof.* Let  $\Lambda'$  be a transverse knot which is the closure of a quasipositive algebraic length 2 3-braid. By Proposition 4.2.2, the double cover of  $S^3$  branched over  $\Lambda'$ ,  $(\Sigma_2(\Lambda'), \xi)$  has an open book decomposition  $(F, \phi)$  where  $F$  is a torus with one boundary component, and  $\phi$  is given by Dehn twisting along the curves  $\alpha$  and  $\gamma$  where  $\alpha$  is the  $(1, 0)$  curve and  $\gamma$  is some essential simple closed curve in  $F$ , see Figure 4.2. Then we may construct a Weinstein Lefschetz fibration by attaching handles along the lifts of vanishing cycles corresponding to  $\alpha$  and  $\gamma$  in a generic fiber  $F$ , as described in Remark 4.1.6.  $\square$

**Remark 4.2.4.** Repeated Dehn twists about  $\tau_\alpha$ ,  $\tau_\beta$ ,  $\tau_\alpha^{-1}$  and  $\tau_\beta^{-1}$  of the curve  $\alpha$  of slope  $(1, 0)$  and  $\beta$  of slope  $(0, 1)$  on the curve  $\alpha$  in Figure 4.2 results in a curve with some slope  $(p, q)$  in the torus with one boundary component  $F_{1,1}$ . Indeed, the mapping class group of the torus with one boundary component



is generated by the positive Dehn twists  $\tau_\alpha$  and  $\tau_\beta$  with presentation

$$\langle \tau_\alpha, \tau_\beta \mid \tau_\alpha \tau_\beta \tau_\alpha = \tau_\beta \tau_\alpha \tau_\beta \rangle,$$

see [FM11] for details. Any diffeomorphism of  $F_{1,1}$  generated by  $\tau_\alpha$  and  $\tau_\beta$  is equivalent to a Dehn twist along some non-separating curve with rational slope

$$\frac{p}{q} \in \mathbb{Q}\mathbb{P}^1 = \mathbb{Q} \cup \{\infty\}.$$

**Table 4.1:** Effect of a Dehn twist about  $\alpha$  or  $\beta$  on  $(p, q)$  in the torus with one boundary component.

Braid Generator	Dehn twist	Effect on $(p, q)$
$\sigma_1$	$\tau_\alpha$	$(p, q) \mapsto (p +  q , q)$
$\sigma_1^{-1}$	$\tau_\alpha^{-1}$	$(p, q) \mapsto (p -  q , q)$
$\sigma_2$	$\tau_\beta$	$(p, q) \mapsto (p, q -  p )$
$\sigma_2^{-1}$	$\tau_\beta^{-1}$	$(p, q) \mapsto (p, q +  p )$

Applying an additional Dehn twist about  $\alpha$  or  $\beta$  has the result on  $(p, q)$  as explained in Table 4.1. And given any  $(p, q)$  with  $p$  and  $q$  relatively prime, a  $(p, q)$  curve can be obtained by applying  $\tau_\alpha^{\pm 1}$  and  $\tau_\beta^{\pm 1}$  to  $(1, 0)$  according to the Euclidean algorithm. For instance if  $q > p > 0$ , the Euclidean algorithm gives:

$$q = n_k p + r_k$$

$$p = n_{k-1} r_k + r_{k-1}$$

$$r_k = n_{k-2} r_{k-1} + r_{k-2}$$

...

$$r_3 = n_3 r_2 + r_1$$

$$r_2 = n_2 r_1 + 1$$

$$r_1 = n_1.$$

So if  $\gamma$  is the curve of slope  $(p, q)$  in the torus with one boundary component,

$$\gamma = \tau_\beta^{-n_k} \circ \tau_\alpha^{n_{k-1}} \circ \tau_\beta^{-n_{k-2}} \circ \cdots \circ \tau_\beta^{-n_1}(\alpha).$$

**Lemma 4.2.5.** Let  $\Lambda'$  be a transverse knot which is the closure of a quasi-positive 3-braid of algebraic length 2,  $B$ , and  $\Lambda \neq U$ . Then we can always find a braid  $B'$  equivalent to  $B$  up to conjugation such that the procedure in Proposition 4.2.2 yields an open book decomposition with monodromy given by Dehn twists along the curves  $\alpha$  and  $\gamma$  of slopes  $(1, 0)$  and  $(p, q)$  respectively, where  $0 < p < q$ .

*Proof.* By Lemma 4.2.1, we know  $\Lambda$  is the closure of a braid of the form  $\sigma_1 B_0 \sigma_1 B_0^{-1}$ , and that after applying Proposition 4.2.2,  $(\Sigma_2(\Lambda'), \xi)$  corresponds to an open book decomposition  $(F, \phi)$  where  $\phi$  is given by a Dehn twist on  $\alpha$  and on  $\gamma$ , where

$$\gamma = (\mu_1 \cdots \mu_m)(\alpha) = \mu_1 \circ \cdots \circ \mu_m(\alpha),$$

where the  $\mu_i \in \{\tau_\alpha^{\pm 1}, \tau_\beta^{\pm 1}\}$  correspond to the braid generators in  $B_0$ .

By Remark 4.2.4,  $\gamma$  corresponds to a curve of slope  $\frac{p}{q} \in \mathbb{Q}\mathbb{P}^1$ . Without loss of generality, we may assume that  $q \geq 0$ .

We know  $q \neq 0$  since  $(p, q) = (1, 0)$  corresponds to

$$\Sigma_2(\Lambda') \cong (S^1 \times S^2) \# \mathbb{R}\mathbb{P}^3,$$

but  $\Sigma_2(\Lambda')$  must be a rational homology sphere so there is no such  $\Lambda'$ .

If  $p = 1$ , then if either  $q = 0$  or  $q = 1$ , then

$$\Sigma_2(\Lambda') \cong S^3,$$

and so  $\Lambda'$  is the unknot. Thus  $q \geq 2$ .

Notice the following equivalence of braids:

$$\begin{aligned}\sigma_1 B_0 \sigma_1 B_0^{-1} &= \sigma_1^k (\sigma_1 B_0 \sigma_1 B_0^{-1}) \sigma_1^{-k} \\ &= \sigma_1 (\sigma_1^k B_0) \sigma_1 (B_0^{-1} \sigma_1^{-k}).\end{aligned}$$

for any  $k \in \mathbb{Z}$ .

The braid  $\sigma_1^k B_0$  corresponds to the Dehn twists

$$\tau_\alpha^k \circ \mu_1 \circ \cdots \circ \mu_m$$

and the braid  $(\sigma_1^k B_0) \sigma_1 (B_0^{-1} \sigma_1^{-k})$  corresponds to the Dehn twists

$$(\tau_\alpha^k \circ \mu_1 \circ \cdots \circ \mu_m) \circ \tau_\alpha \circ (\mu_m^{-1} \circ \cdots \circ \mu_1^{-1} \circ \tau_\alpha^{-k}).$$

These Dehn twists correspond to the single Dehn twist about the curve

$$\tau_\alpha^k \mu_1 \cdots \mu_m(\alpha).$$

Since  $\gamma = \mu_1 \cdots \mu_m(\alpha)$  corresponds to a  $(p, q)$  curve, applying an additional  $k$  instances of  $\tau_\alpha$  to  $\mu_1 \cdots \mu_m(\alpha)$  corresponds to the curve of slope

$$(p + kq, q).$$

Thus, we can replace  $B_0$  with the braid  $B = \sigma_1^k B_0$  where  $k \in \mathbb{Z}$  satisfies  $0 < p - kq < q$ . We have an equivalence of braids up to conjugation:

$$\sigma_1 B_0 \sigma_1 B_0^{-1} = \sigma_1 B \sigma_1 B^{-1},$$

and  $B \sigma_1 B^{-1}$  corresponds to a curve  $\gamma$  with slope  $\frac{p'}{q}$  with

$$0 < p' = p - kq < q.$$

□

### 4.3 Drawing Weinstein diagrams

We now want to obtain a Weinstein diagram for  $X_\Lambda$  of the previous corollary. To obtain the attaching spheres the 2-handles we will use the recipe laid out by Casals and Murphy [CM19], which uses the following proposition to determine the attaching maps as simplified contact surgery curves on the boundary:

**Proposition 4.3.1.** [CM19] Let  $(Y, \xi)$  be a contact manifold with open book decomposition  $(F, \phi)$  and let  $\lambda$  denote the Liouville form on  $F$ . Let  $S, L \subset (F, \lambda)$  be two exact Lagrangian submanifolds such that  $S$  is diffeomorphic to a sphere. Suppose that the potential functions  $\psi_S$  and  $\psi_L$  where  $d\psi_S = \lambda|_S$  and  $d\psi_L = \lambda|_L$  are  $C^0$ -bounded by a small enough  $\epsilon > 0$ , and consider the contact manifold  $(Y', \xi')$  obtained by performing  $(+1)$ -surgery along  $\Lambda_S^\epsilon$ , an  $\epsilon$ -pushoff of  $\Lambda$  by  $\psi$ , and  $(-1)$ -surgery along  $\Lambda_S^{5\epsilon}$ . Then:

1. there exists a canonical contact identification  $(Y, \xi) = (Y', \xi')$  and
2. the Legendrian  $\Lambda_L^{3\epsilon} \subset (Y', \xi')$  is Legendrian isotopic to  $\Lambda_{\tau_S(L)}^0 \subset (Y, \xi)$ .

In an analogous manner, performing contact  $(-1)$  and  $(+1)$ -surgeries along  $\Lambda_S^\epsilon$  and  $\Lambda_S^{5\epsilon}$  in  $(Y, \xi)$  results in a contact manifold  $(Y, \xi)$  with a contact identification  $(Y, \xi) = (Y', \xi')$  under which  $\Lambda_L^{3\epsilon} \subset (Y, \xi)$  is Legendrian isotopic to  $\Lambda_{\tau_S^{-1}(L)} \subset (Y, \xi)$ .

The recipe of [CM19] is designed to find the attaching spheres in the Weinstein diagram by finding the lifts of corresponding vanishing cycles consisting of Dehn twists about some known spheres. In their paper, these vanishing cycles are obtained from a bifibration. For our Lefschetz fibrations, we already have the vanishing cycles in terms of Dehn twists, so we do not need all the steps of the recipe. We list the relevant steps here.

Let  $\pi : (X, \omega) \rightarrow D^2$  be a Weinstein Lefschetz fibration with generic fiber  $F$  and vanishing cycles  $C_1, \dots, C_k$ .

1. Choose a set of exact Lagrangian spheres  $\mathbb{L} = \{L_1, \dots, L_r\}$  in the generic fiber  $F$  for which we understand the Legendrian lifts in the front projection of the contact boundary  $\partial(F \times D^2)$ .

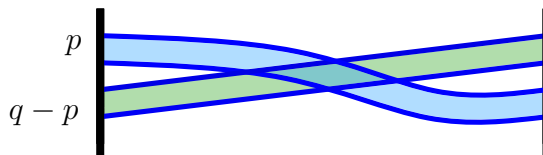


**Figure 4.4:** A Weinstein filling of  $\Sigma_2(\Lambda')$ . The shaded blue and shaded green represent  $p$  and  $q - p$  parallel strands respectively of a single Legendrian link in  $S^1 \times S^2$ .

2. Express each  $\tau_{C_i}$  as a word in Dehn twists about the Lagrangian spheres in the set  $\mathbb{L}$ .
3. For each vanishing cycle  $C_i$ , we apply Proposition 4.3.1 to draw the front projection of their Legendrian lifts  $\Lambda_i \subset \partial(F \times D^2)$ .
4. Then we consider the Legendrian link  $\bigcup_i \Lambda_i$  determined by the cyclic ordering of the indices  $i$ : we push the Legendrian component  $\Lambda_i$  in the Reeb direction by height equal to its index  $i$ , and this gives a well-defined link.
5. Simplify the Legendrian front projection of the link by applying Reidemeister moves, Gompf moves, handleslides, and handle cancellations. These moves are described in Section 2.3.

We apply this recipe to obtain the general form of the Weinstein diagram of a filling  $X_\Lambda$  of  $\Sigma_2(\Lambda')$ :

**Theorem 4.3.2.** Let  $\Lambda$  be a Legendrian knot which is the closure of a quasi-positive 3-braid of algebraic length 2. Let  $\Lambda'$  be a positive transverse push off of  $\Lambda$ . If Lemma 4.2.5 gives  $\gamma$  with slope  $(p, q)$ ,  $0 \leq p < q$ , then there is a filling of  $\Sigma_2(\Lambda')$ , the double cover of  $S^3$  branched over  $\Lambda'$ , given by the handle decomposition consisting of a single 1-handle and a single 2-handle pictured in Figure 4.4.

*Proof.* We apply the recipe of Casals and Murphy to the Weinstein Lefschetz fibration obtained via Corollary 4.2.3.

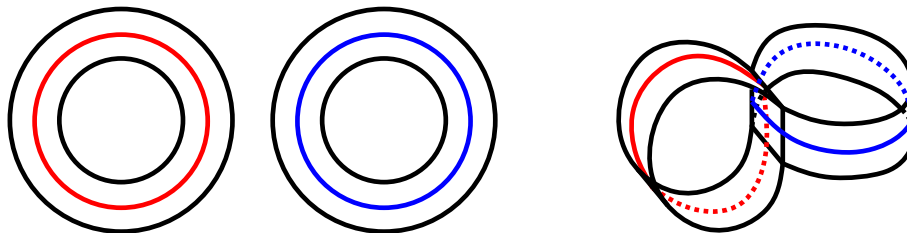


**Figure 4.5:** The annuli  $A_1$  and  $A_2$ , and the fiber of the open book decomposition  $(F_0, \phi_0)$  given by the Murasugi sum  $(A_1, \tau_\alpha) * (A_2, \tau_\beta)$ . The curve  $\alpha$  is in red and the curve  $\beta$  is in blue.

Let  $\Lambda'$  be a transverse knot which is the closure of a quasipositive 3-braid of algebraic length 2. Then by Corollary 4.2.3, the double cover of  $S^3$  branched over  $\Lambda'$ ,  $(\Sigma_2(\Lambda'), \xi)$  has Weinstein filling  $X_\Lambda$ .  $X_\Lambda$  has a Weinstein Lefschetz fibration  $\pi : X \rightarrow D^2$  with generic fiber  $F$  a torus with one boundary component, and monodromy given by vanishing cycles which are Dehn twists along the curves  $\alpha$  and  $\gamma$ .  $\alpha$  is the  $(1, 0)$  curve and  $\gamma$  is some  $(p, q)$  curve in  $F$ .

We apply Lemma 4.2.5 to ensure that the  $(p, q)$  curve satisfies  $0 < p < q$ .

We apply the recipe of Casals and Murphy. **Step 1:** First we need a set of Lagrangian spheres for which we understand the Legendrian lifts. We will choose the curves  $\alpha$  and  $\beta$  of slopes  $(1, 0)$  and  $(0, 1)$  respectively in  $F$ , see Figure 4.2. To find the Legendrian lifts  $\Lambda_\alpha$  and  $\Lambda_\beta$  of  $\alpha$  and  $\beta$ , we consider the following. Let  $(F_0, \phi_0)$  be the open book decomposition given by  $F_0 := F$  and  $\phi_0$  the monodromy given by Dehn twists  $\tau_\alpha$  and  $\tau_\beta$ . This open book decomposition is the Murasugi sum  $(A_1, \tau_\alpha) * (A_2, \tau_\beta)$  where  $A_1, A_2$  are annuli with monodromy given by Dehn twists about their cores,  $\alpha$  and  $\beta$ , see Figure 4.5. Thus,

$$(F_0, \phi_0) = (S^3 \# S^3, \xi_{std} \# \xi_{std}) = (S^3, \xi_{std})$$

and the Legendrian lifts  $\Lambda_\alpha$  and  $\Lambda_\beta$  of  $\alpha$  and  $\beta$  are the lifts of the cores of the annuli  $A_1$  and  $A_2$ .  $\Lambda_\alpha$  and  $\Lambda_\beta$  each correspond to the attaching sphere of a critical 2-handle cancelling a subcritical 1-handle attachment, as in Figure 4.6.

**Step 2** is to express  $\alpha$  and  $\gamma$  as the images of  $\alpha$  under words in Dehn twists along  $\alpha$  and  $\beta$ .  $\alpha$  is as given. For  $\gamma$  it suffices to find a series of Dehn

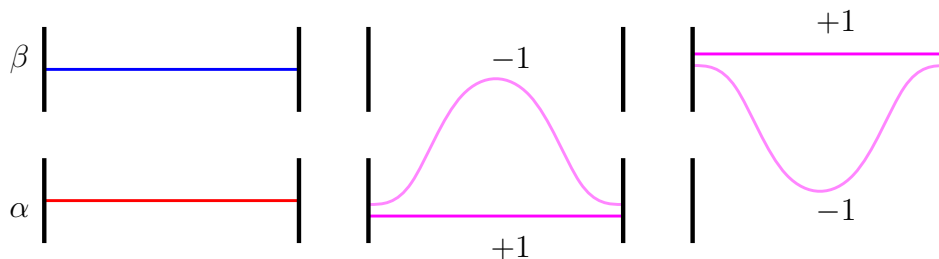


**Figure 4.6:** From left to right:

- (1.) the Legendrian lifts  $\Lambda_\alpha$  and  $\Lambda_\beta$  of  $\alpha$  and  $\beta$ ,
- (2.) The (+1) and (-1) surgery curves for a Dehn twist  $\tau_\alpha$ ,
- (3.) The (+1) and (-1) surgery curves for a Dehn twist  $\tau_\beta^{-1}$ .

twists about  $\alpha$  and  $\beta$  on the curve  $(1, 0)$  to obtain the curve with slope  $(p, q)$  in the torus with one boundary component. We obtain such a word using the Euclidean algorithm. Following Table 4.1,  $(p, q)$  is obtained by some sequence of the Dehn twists  $\tau_\alpha$  and  $\tau_\beta^{-1}$ . As in Remark 4.2.4, we perform the Euclidean algorithm to obtain successive coefficients  $n_i \in \mathbb{Z}^+$ :

$$\begin{aligned}
 q &= n_k p + r_k \\
 p &= n_{k-1} r_k + r_{k-1} \\
 r_k &= n_{k-2} r_{k-1} + r_{k-2} \\
 &\dots \\
 r_3 &= n_3 r_2 + r_1 \\
 r_2 &= n_2 r_1 + 1 \\
 r_1 &= n_1.
 \end{aligned}$$

Then,

$$\tau_\beta^{-n_k} \circ \tau_\alpha^{n_{k-1}} \circ \tau_\beta^{-n_{k-2}} \circ \dots \circ \tau_\beta^{-n_1}(\alpha) = \gamma.$$

**Step 3** is to use Proposition 4.3.1 repeatedly to obtain the Legendrian lifts  $\Lambda_\alpha$  and  $\Lambda_\gamma$ .  $\Lambda_\alpha$  is given and consists of an unknotted Legendrian knot which cancels the 1-handle labelled  $\alpha$  in Figure 4.6.

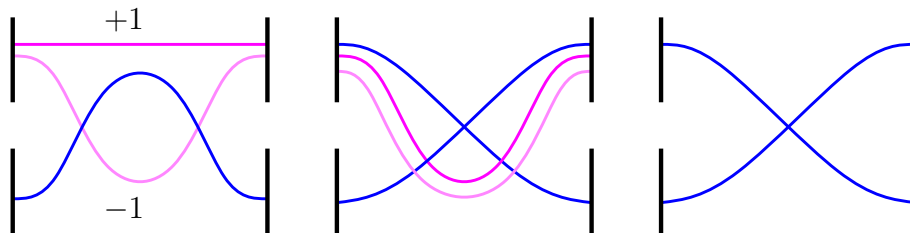


**Figure 4.7:** The Legendrian lift of  $\tau_\beta^{-1}(\alpha)$ . From left to right:  
 (1.) First the diagram given by Proposition 4.3.1,  
 (2.) we perform a handle slide of the blue curve over the (+1) curve,  
 (3.) and then we cancel out the parallel (+1) and (-1) surgery curves.

To find  $\Lambda_\gamma$ , we will draw the curve

$$\Lambda_{\tau_\beta^{-n_k} \circ \tau_\alpha^{n_{k-1}} \circ \tau_\beta^{-n_{k-2}} \circ \dots \circ \tau_\beta^{-n_1}(\alpha)}.$$

We apply Proposition 4.3.1 repeatedly to obtain the surgery diagram. This means repeatedly adding in a (+1) and a (-1) surgery curve along either  $\alpha$  or  $\beta$  with heights determined by the proposition, see Figure 4.6, and sliding over the current handle to cancel them out. We will see that applying an  $\tau_\beta^{-1}$  will increase the number of strands going through the topmost 1-handle labelled  $\beta$  in Figure 4.6, and applying  $\tau_\alpha$  will increase the number of strands going through the bottom 1-handle labelled  $\alpha$  in Figure 4.6.

To begin, the lift of  $\tau_\beta^{-1}(\alpha)$  is given by Figure 4.7.

Next, assuming  $n_1 > 1$ , applying more twists  $\tau_\beta^{-n_1-1}$  results in the series of diagrams in Figure 4.8. In  $\tau_\beta^{-n_1}(\alpha)$ , there are now  $n_1$  strands going through the 1-handle labelled  $\beta$  and 1 strand going through the 1-handle labelled  $\alpha$ .

We now apply  $\tau_\alpha$  to  $\tau_\beta^{-n_1}(\alpha)$ , resulting in the series of diagrams in Figure 4.9. In  $\tau_\alpha \tau_\beta^{-n_1}(\alpha)$ , there are now  $n_1$  strands going through the 1-handle labelled  $\beta$  and  $n_1 + 1$  strands going through the 1-handle labelled  $\alpha$ .

Now assuming  $n_2 > 1$ , we apply  $\tau_\alpha^{n_2-1}$  to  $\tau_\alpha \tau_\beta^{-n_1}(\alpha)$ . We obtain the diagrams in Figure 4.10. In the last diagram showing  $\tau_\alpha^{n_2} \tau_\beta^{-n_1}(\alpha)$ , we can count  $n_1$  strands going through the handle labelled  $\beta$  and  $n_1 n_2 + 1$  strands going through the handle labelled  $\alpha$ .



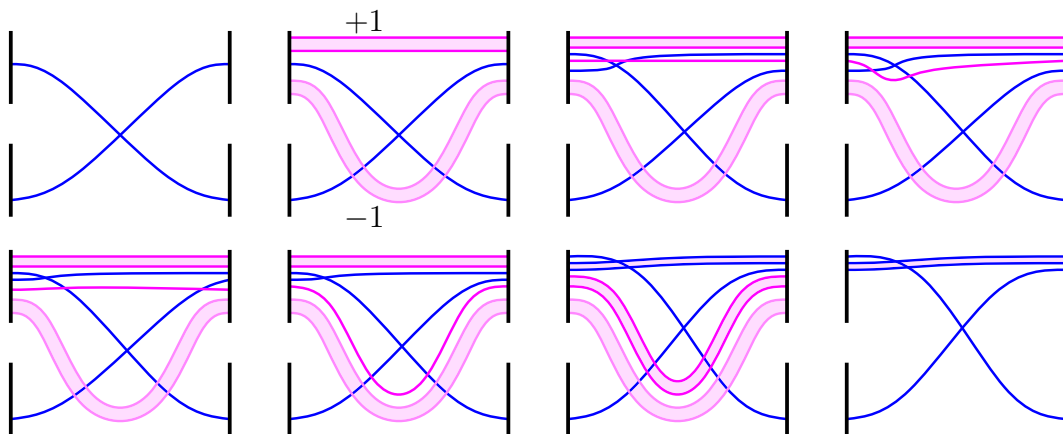


**Figure 4.8:** Shaded pink ribbons represent  $n_1 - 1$  parallel (+1) and (-1) curves given by Proposition 4.3.1. Describing these 8 diagrams in order:

- (1.)  $\tau_\beta^{-1}(\alpha)$ ,
- (2.) (+1) and (-1) curves added in,
- (3.) we slide the blue curve over the lowest of the parallel (+1) curves,
- (4.) Reidemeister 3,
- (5.) Gompf 5,
- (6.) Reidemeister 3,
- (7.) Repeat steps 3-6 with remaining (+1) curves, and
- (8.) we cancel the (+1) and (-1) curves to obtain  $\tau_\beta^{-n_1}(\alpha)$ .

We continue to apply successive  $\tau_\beta^{-n_i}$  and  $\tau_\alpha^{n_j}$  twists to the curve. In doing so, we obtain the diagrams of Figure 4.11. Applying  $\tau_\beta^{-n_i}$  results in the top row of diagrams, and applying  $\tau_\alpha^{n_j}$  results in the bottom row of diagrams. The count of strands passing through the 1-handles after each successive step correspond to the  $r_i$  in the Euclidean algorithm.

In the case that  $n_1 = 1$ , the diagrams in Figure 4.8 reflected horizontally give the  $\tau_\alpha^{n_2}\tau_\beta^{-1}(\alpha)$ , reflected versions of Figures 4.9 and 4.10 give  $\tau_\beta^{-1}\tau_\alpha^{n_2}\tau_\beta^{-1}(\alpha)$  and  $\tau_\beta^{-n_3}\tau_\alpha^{n_2}\tau_\beta^{-1}(\alpha)$  respectively. In general, we still end up with the diagrams of Figure 4.11, with  $\tau_\beta^{-n_i}$  resulting in the top row of diagrams, and  $\tau_\alpha^{n_j}$  resulting in the bottom row of diagrams.

Since  $p < q$ , the final Dehn twist applied will be a  $\tau_\beta^{-1}$ , so the final diagram will correspond to the bottom right of Figure 4.11, with  $q$  strands going through the top 1-handle and  $p$  strands going through the bottom 1-handle. We have found a Legendrian representative for  $\Lambda_\gamma$ .

We can proceed with **Step 4**. Since we are dealing with only 2 curves, we

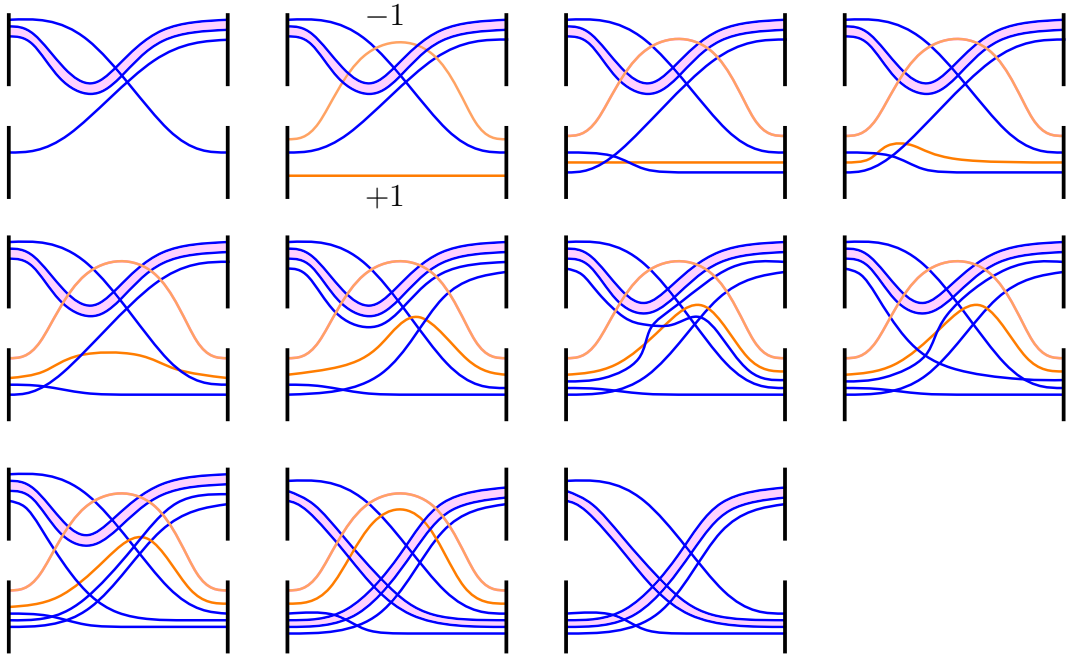


**Figure 4.9:** Shaded pink ribbons represent  $n_1 - 1$  parallel curves. Describing these 11 diagrams in order:

- (1.)  $\tau_\beta^{-n_1}(\alpha)$ ,
- (2.) (+1) and (-1) curves added in,
- (3.) we slide the blue curve over the orange (+1) curve,
- (4.) Reidemeister 3,
- (5.) Gompf 5,
- (6.) Reidemeister 3 and we separate the bottom most blue curve from the pink ribbon (which now represents  $n_1 - 2$  parallel strands),
- (7.) we slide the blue curve over the orange,
- (8.) Reidemeister 3,
- (9.) Reidemeister 3,
- (10.) repeat steps 7-9 with the remaining strands in the pink ribbon,
- (11.) we cancel the (+1) and (-1) orange curves to obtain  $\tau_\alpha \tau_\beta^{-n_1}(\alpha)$ .

can choose the cyclic ordering. We place  $\Lambda_\gamma$  above  $\Lambda_\alpha$ . The resulting Weinstein diagram is the top left diagram of Figure 4.12.

**Step 5** is to simplify the handle diagram. We do so following Figure 4.12 by some knot isotopies, a handle slide, and cancelling the bottom 1-handle with  $\Lambda_\alpha$ . The resulting diagram has one 2-handle winding about a single 1-handle  $q$  times. We can see this in the attaching curve in the bottom right of 4.12 which is colour coded: the blue shaded region represents  $p$  parallel curves and the green shaded region represents  $q - p$  parallel curves.  $\square$

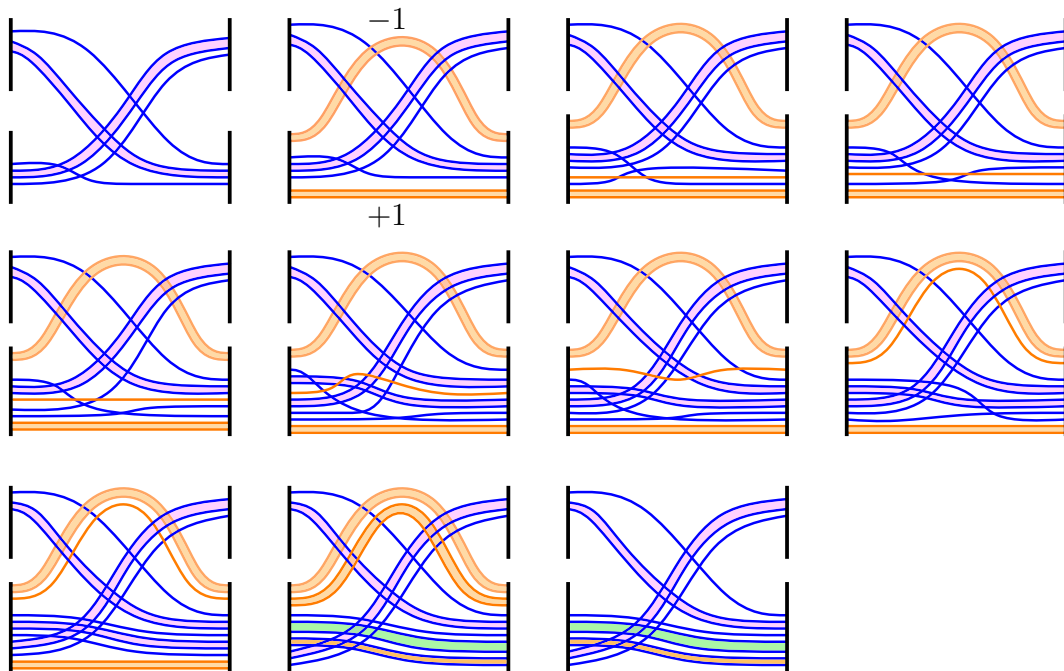


**Figure 4.10:** Shaded pink ribbons represent  $n_1 - 1$  parallel curves, shaded orange regions represent  $n_2 - 1$  parallel curves, shaded green region represents  $(n_1 - 1)(n_2 - 1)$  curves. Describing these 11 diagrams in order:

- (1.)  $\tau_\alpha \tau_\beta^{-n_1}(\alpha)$ ,
- (2.) (+1) and (-1) curves added in,
- (3.) slide the blue curve over the topmost of the parallel (+1) curves,
- (4.) Reidemeister 3,
- (5.) Gompf 5,
- (6.)  $n_1 - 1$  handleslides of the orange curve over the blue curves in the pink ribbon (see Appendix A),
- (7.) repeated applications of Reidemeister 3 followed by repeated applications of Gompf 5 (see Appendix A),
- (8.) repeated applications of Reidemeister 3,
- (9.) repeated applications of Gompf 5,
- (10.) repeat steps 3-9 with the remaining strands in the orange ribbon,
- (11.) we cancel the (+1) and (-1) curves to obtain  $\tau_\alpha^{n_2} \tau_\beta^{-n_1}(\alpha)$ .

In the next section, we will call the Weinstein diagram in Gompf standard form obtained in Theorem 4.3.2 method  $\mathcal{D}(\Lambda)$  for the knot  $\Lambda$ , where  $\mathcal{D}(\Lambda)$  depicts a filling of  $\Sigma_2(\Lambda')$ .

**Example 4.3.3.** We will apply this procedure to a particular knot.

The transverse  $m(8_{20})$  knot [BNMea] is the closure of the braid  $\sigma_1 \sigma_2^3 \sigma_1 \sigma_2^{-3}$  [CDGW]. We conjugate this braid word by  $\sigma_1 \sigma_2^{-3}$  and obtain an equivalent

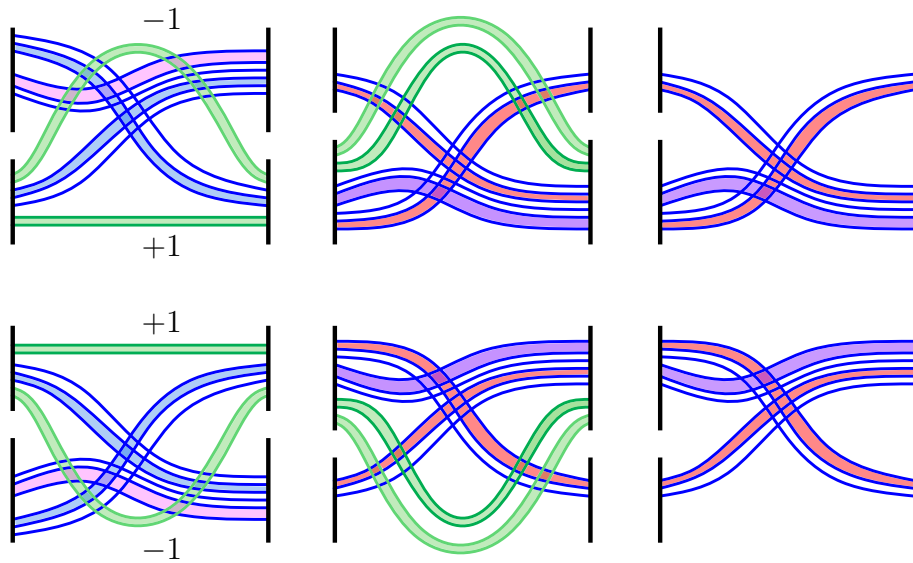


**Figure 4.11:** Coloured ribbons represent some number of parallel strands. In the top row, we apply Dehn twists  $\tau_\alpha^{n_j}$  and see the resulting diagram (the step by step procedure follows from Figure 4.10). In the bottom row, we apply Dehn twists  $\tau_\beta^{-n_i}$ , and see the resulting diagram (the step by step procedure consists of the same diagrams as the top row, reflected about a horizontal axis).

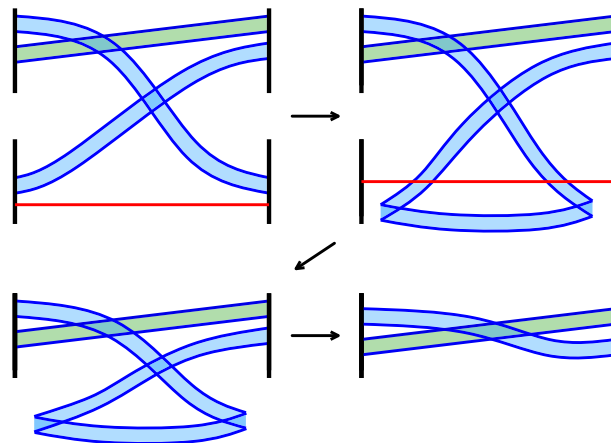


**Figure 4.12:** The blue shaded region represents  $p$  parallel curves and the green shaded region represents  $q - p$  parallel curves. 1. The Weinstein diagram obtained after Step 4 of the recipe, 2. handleslide the blue curves over the red curve, 3. cancel the bottom 1-handle with the red curve, 4. perform a series of Reidemeister moves on the parallel blue curves (see Appendix A).

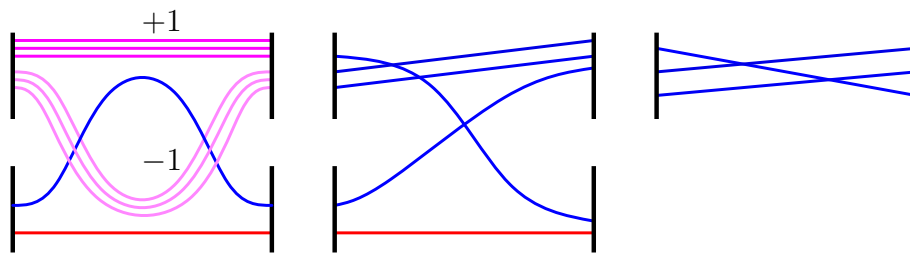


**Figure 4.13:**  $\mathcal{D}(m(8_{20}))$ , the Weinstein diagram for the filling of the double cover of the transverse  $m(8_{20})$  knot, following Theorem 4.3.2.

braid:

$$\sigma_1 \sigma_2^3 \sigma_1 \sigma_2^{-3} = \sigma_1 \sigma_2^{-3} (\sigma_1 \sigma_2^3 \sigma_1 \sigma_2^{-3}) \sigma_2^3 \sigma_1^{-1} = \sigma_1 \sigma_2^{-3} \sigma_1 \sigma_2^3.$$

By Corollary 4.2.3, the double cover of  $S^3$  branched over this knot has a Weinstein Lefschetz fibration  $\pi : X \rightarrow D^2$  with generic fibre  $F$ , a torus with one boundary component containing vanishing cycles given by  $\alpha$  and  $\tau_\beta^{-3}(\alpha)$  which are curves of slope  $(1, 0)$  and  $(1, 3)$  respectively.

Following the steps in the proof of Theorem 4.3.2, we obtain the lift of the  $(1, 3)$  curve and the surgery diagram  $\mathcal{D}(m(8_{20}))$ , as in Figure 4.13.

## Chapter 5

# Nonvanishing symplectic homology

## 5.1 The Chekanov-Eliashberg Differential Graded Algebra

In this section, we introduce the Chekanov-Eliashberg differential graded algebra and describe how to compute it for links in  $\#^m(S^1 \times S^2)$ . We will then compute the DGA of the knot in  $\mathcal{D}(\Lambda)$ , the Weinstein diagram built in the previous chapter, and use it to show that the symplectic homology of the Weinstein manifold obtained by attaching a 2-handle along the Legendrian attaching sphere in  $\mathcal{D}(\Lambda)$  is nonzero.

### 5.1.1 The DGA for Knots

We begin by describing how to compute the Chekanov-Eliashberg DGA for  $K$ , a Legendrian knot in  $\mathbb{R}^3$ . We consider  $K$  in the Lagrangian projection,  $\Pi(K)$ , which we obtain from the front projection via Theorem 2.2.4. We assume the strands of  $\Pi(K)$  meet orthogonally at crossings. We will fix a point  $*$  on  $\Pi(K)$  distinct from the double points, and label the crossings, which correspond to the Reeb chords of  $K$ , with letters  $a_1, \dots, a_n$ . We will define the classic Chekanov-Eliashberg DGA [Che02, ENS<sup>+</sup>02]  $(\mathcal{A}_K, \partial_K)$  in three steps: 1. algebra, 2. grading, 3. differentials.

The algebra  $\mathcal{A}_K$  is the associative, noncommutative, unital algebra over  $\mathbb{Z}$  generated by  $a_1, \dots, a_n, t, t^{-1}$  with the relation  $t \cdot t^{-1} = t^{-1} \cdot t = 1$ . We write this as

$$\mathcal{A}_K = \mathbb{Z}\langle a_1, \dots, a_n, t, t^{-1} \rangle.$$

This is generated as a  $\mathbb{Z}$ -module by words in the letters  $a_1, \dots, a_n, t, t^{-1}$  with multiplication given by concatenation. The empty word is the unit 1.

The grading associates a degree to each generator of  $\mathcal{A}_K$ , and the grading of a word in the generators is the sum of the gradings of the letters in the word. The grading of  $t$  is given by

$$|t| = 2\text{rot}(K),$$

and the grading of  $t^{-1}$  is

$$|t^{-1}| = -2\text{rot}(K).$$

For grading on the  $a_i$ , we consider the path  $\zeta_i$  running along  $\Pi(K)$  from the overcrossing at  $a_i$  to the undercrossing, avoiding the base point  $*$ . Let the number of counterclockwise rotations of the tangent vector of  $\zeta_i$  from beginning to end be denoted  $\text{rot}(\zeta_i)$ . The grading of  $a_i$  is defined to be:

$$|a_i| = 2\text{rot}(\zeta_i) - \frac{1}{2}.$$

Finally to define the differential of the algebra, we begin by placing additional labels at each crossing representing Reeb signs and orientation signs, as in Figure 5.1.

We now describe a set of immersed disks: Let  $D_n^2 = D^2 - \{x, y_1, \dots, y_n\}$ , where  $D^2$  is the closed unit disk in  $\mathbb{R}^2$  and  $x, y_1, \dots, y_n$  are points in  $\partial D^2$  appearing in counterclockwise order. If  $b_0, b_1, \dots, b_n$  take values in  $\{a_1, \dots, a_n\}$ , define the set

$$\Delta(b_0; b_1, \dots, b_n) = \{u : (D_n^2, \partial D_n^2) \rightarrow (\mathbb{R}_{xy}^2, \Pi(K)) : \text{satisfying (1. - 4.)}\} / \sim,$$

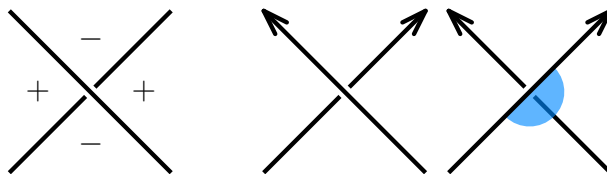


**Figure 5.1:** On the left, the Reeb signs of the quadrants near a crossing. On the right, the orientation signs, which are negative in the shaded quadrants and positive otherwise. The orientation signs are determined on whether we have a positive or negative crossing.

where  $\sim$  is reparametrization, and

1.  $u$  is an immersion,
2.  $u$  sends the boundary punctures to crossings in  $\Pi(K)$ ,
3.  $u$  sends  $x$  to  $b_0$ , and a neighbourhood of  $x$  is mapped to a quadrant of  $b_0$  labelled with a positive Reeb sign,
4. for  $i = 1, \dots, n$ ,  $u$  sends  $y_i$  to  $b_i$ , and a neighbourhood of  $y_i$  is mapped to a quadrant of  $b_i$  labelled with negative Reeb sign.

Let  $\gamma_i$  denote the path from  $b_i$  to  $b_{i+1}$ . Let  $t(\gamma_i)$  be  $t^k$  where  $k$  is the number of times  $\gamma_i$  crosses  $*$ , counted with sign according to the orientation of  $\Lambda$ . Let

$$w(u) := t(\gamma_0)b_1t(\gamma_1)b_2 \dots b_nt(\gamma_n),$$

and

$$\epsilon(u) = \prod_{i=0}^n \epsilon(b_i),$$

where  $\epsilon(c)$  for a corner  $c$  is the orientation sign of the quadrant that  $u$  covers at  $c$ . Let  $\partial_K : \mathcal{A}_K \rightarrow \mathcal{A}_K$  be defined as follows: for generators  $a \in \{a_1, \dots, a_n\}$ , let

$$\partial_K(a) = \sum_{\substack{n \geq 0, b_1, \dots, b_n \text{ double points,} \\ u \in \Delta(b_0; b_1, \dots, b_n)}} \epsilon(u)w(u).$$

See Figure 5.2 for an example of some disks counted by the differential.



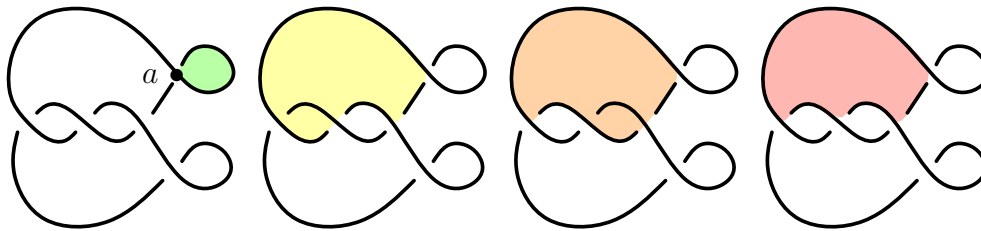


**Figure 5.2:** The immersed disks counted by the differential at the point  $a$  in a trefoil. The yellow and orange disks each have a single switch at a negative corner. The red disk has three.

Let  $\partial_K(t) = \partial_K(t^{-1}) = 0$ , and extend  $\partial_K$  by the signed Leibniz rule:

$$\partial_K(w w') = (\partial_K w) w' + (-1)^{|w|} w (\partial_K w').$$

For further details and examples, see [EN18].

Another way to choose a grading is to choose a *Maslov potential*: a locally constant map

$$m : L \setminus \{F^{-1}(\text{cusps}), \text{base points}\} \rightarrow \mathbb{Z}$$

which increases by 1 when we pass through a cusp of  $F(L)$  going upwards and decreases by 1 when going through a cusp downwards. Then the grading of a crossing  $a$  is given by  $m(a_-) - m(a_+)$  where  $a_-$  and  $a_+$  are the more negatively sloped and the more positively sloped strands at  $a$ , respectively.

This is particularly useful in the case of links, where the previous definition of grading is not well-defined for crossing between different components.

### 5.1.2 With 1-handles

Now we extend the DGA computations to Legendrian links in  $\#^m(S^1 \times S^2)$  following [EN15]. Let  $L$  be a knot in  $\#^m(S^1 \times S^2)$ .  $L$  is normally given in the front projection, with matching balls or walls to represent 1-handles (as in Gompf normal form). We begin by redrawing the front diagrams in the Lagrangian projection  $\Pi(L)$ . This means using a version of Ng's resolution from Theorem 2.2.4 [Ng03] along with the additional 1-handle half twist from Definition 2.3 of [EN15]. This half twist is depicted in Figure 5.3. For  $\Lambda$ , the

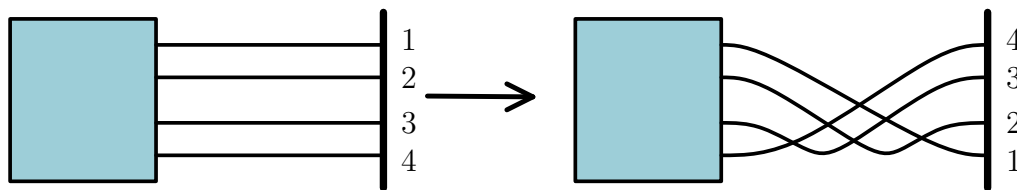


**Figure 5.3:** A half twist we add at a 1-handle to go from the front projection of a knot to its the Lagrangian resolution. At a crossing the more negatively sloped strands corresponds to the overcrossing strand.

closure of a 3-braid of algebraic length 2,  $\Lambda$ ,  $\mathcal{D}(\Lambda)$  has Lagrangian resolution as in Figure 5.5.

The DGA of  $L$  in  $\#^m(S^1 \times S^2)$  has a subalgebra called the internal DGA, generated from Reeb chords of  $L$  in each of the 1-handles. Let  $r$  denote the rotation number of  $L$ . We consider a 1-handle through which pass  $n$  strands. We label these strands from 1 to  $n$  from top to bottom on the left and from bottom to top on the right. Let  $m(1), \dots, m(n)$  denote the Maslov potentials for each of these strands, as defined on the previous page, such that this Maslov potential satisfies the following conditions on the front projection of  $L$ :

1. The same Maslov potential is assigned to the left and right sides of the same strand connected through a 1-handle, this potential is even if the strand is oriented left to right and odd otherwise.
2. At a cusp, the upper component has Maslov potential one more than the lower component.

Let  $(\mathcal{A}_n, \partial_n)$  denote the differential graded algebra with algebra over the coefficient ring  $\mathbb{Z}[t_1, t_1^{-1}]$  freely generated by  $\{c_{i,j}^0 | 1 \leq i < j \leq n\} \cup \{c_{i,j}^p | 1 \leq i, j \leq n, p \geq 1\}$ . Let  $c_{i,j}^0 = 0$  for  $i \geq j$ .

The gradings are given by  $|t_i| = -2r$ ,  $|t_i^{-1}| = 2r$ , and  $|c_{i,j}^p| = 2p - 1 + m(i) - m(j)$  for all  $i, j$ , and  $p$ . Then the differential is defined on the generators by:

$$\partial_n(c_{i,j}^0) = \sum_{m=1}^n \sigma_i \sigma_m c_{i,m}^0 c_{m,j}^0$$

$$\begin{aligned}\partial_n(c_{i,j}^1) &= \delta_{i,j} + \sum_{m=1}^n \sigma_i \sigma_m c_{i,m}^0 c_{m,j}^1 + \sum_{m=1}^n \sigma_i \sigma_m c_{i,m}^1 c_{m,j}^0 \\ \partial_n(c_{i,j}^p) &= \sum_{l=0}^p \sum_{m=1}^n \sigma_i \sigma_m c_{i,m}^l c_{m,j}^{p-l}\end{aligned}$$

where  $p \geq 2$ ,  $\sigma_i = (-1)^{m(i)}$  for all  $i$ , and  $\delta_{i,j}$  is the Kronecker delta. We extend  $\partial_n$  by the signed Leibniz rule as before. We do the same procedure for each 1-handle.

The full DGA is generated by the internal subalgebras  $(\mathcal{A}_n, \partial_n)$  (one for each 1-handle), as well as by the Reeb chords at crossings labelled  $a_1, \dots, a_n$  which we call the *external* generators. If  $a$  corresponds to a crossing in the front diagram,  $a$  has grading  $|a| = m(S_o) - m(S_u)$  where  $S_o$  is the overcrossing strand and  $S_u$  is the undercrossing strand.

The differential for these external generators is again a signed count of immersed disks. Disks are not allowed to pass through the 1-handle, but we allow negative corners on either side of the 1-handle. Such a corner on the Reeb chord between the  $i$ th and  $j$ th strands is denoted  $c_{i,j}^0$ ,  $i < j$ , see Figure 5.4. The sign associated to an immersed disk is determined by the product of the orientation signs at its corners. For a corner at  $c_{i,j}^0$ , the orientation sign is: +1 for a corner reaching the handle from the right, and  $(-1)^{m(i)-m(j)}$  for a corner reaching the handle from the left. For a corner at a crossing, we choose the convention that all orientation signs are +1, except if the crossing has even degree, the south and east corners have degree  $-1$ .

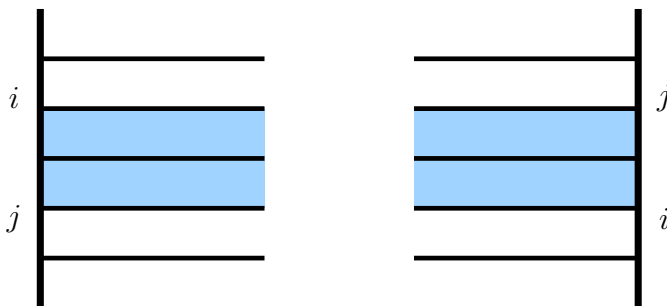


**Figure 5.4:** A negative corner at a 1-handle between the  $i$ th and  $j$ th strands, denoted  $c_{i,j}^0$  in the computation of the differential.

### 5.1.3 Cyclically composable Reeb chords

We want to compute invariants of a Weinstein manifold given its surgery presentation in terms of Legendrian links. From the perspective of Legendrian surgery, and in order to use results of [BEE12, Ekh19], we need to define the algebra over a ring with idempotents  $e_i$  in bijection with the connected components of the link  $L_i$  to ensure that Reeb chords will be cyclically composable. Since in our examples,  $L$  is always a knot, we take the DGA defined over the base ring  $\mathbb{Z}e_1$ .

In [EL19], such a version of the DGA is defined. Evgü and Lekili further show that this internal DGA is finitely generated up to quasi-isomorphism, by a subalgebra generated by only the elements  $c_{i,j}^k$  where  $k = 0$  or  $k = 1$ .

We will compute this version of the Chekanov-Eliashberg DGA in the next section, where we will call it  $(\mathcal{A}_L, \partial_L)$ .

## 5.2 Computing the Chekanov-Eliashberg DGA from $\mathcal{D}(\Lambda)$

In this section, we compute the Chekanov-Eliashberg DGA of the knots in the diagrams  $\mathcal{D}(\Lambda)$  of the previous chapter, drawn in  $S^1 \times S^2$ .

Let  $q$  denote the number of strands entering the 1-handle of  $\mathcal{D}(\Lambda)$ . Let  $p$  denote the number of negatively sloped overstrands in  $\mathcal{D}(\Lambda)$ . We begin by labelling the crossings, which correspond to generating Reeb chords of the DGA. We label crossings in the Lagrangian resolution of  $\mathcal{D}(\Lambda)$  which come from crossings in the front diagram (ie. any crossing on the left side of the diagram) with  $a_i$ , with the left most crossing labelled  $a$ . We label crossings which come from the 1-handle twist of the Lagrangian resolution with  $b_i$ , so that the indices increase from left to right from the bottom row upwards. We place a marked point at the minimum of the highest strand exiting the 1-handle on the left, and we label the marked point  $t$ . See for example the partially labelled Figure 5.5 when  $\Lambda$  is a closure of a 3-braid with an algebraic length 2. See also the fully labelled examples of the Lagrangian resolution of  $\mathcal{D}(\Lambda)$ ,

where  $\Lambda$  is the  $m(8_{20})$  knot, in Figure 5.7, and where  $\Lambda$  is the  $10_{155}$  knot, in Appendix B.

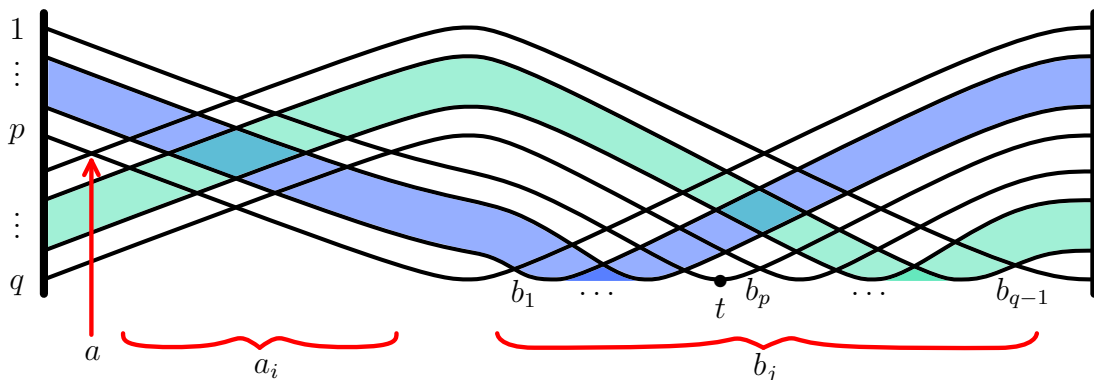


**Figure 5.5:**  $\mathcal{D}(\Lambda)$ . There are  $p - 2$  parallel curves in the blue band, and  $q - p - 2$  curves in the green band. The  $a$  and  $b_i$  generators of the DGA are labelled. The other crossings are labelled  $a_i$  if they are in the region on the left, and  $b_j$  if they are in the region on the right.

We can now compute the Chekanov-Eliashberg DGA  $(\mathcal{A}_K, \partial_K)$ . Since there are no cusps, we give each strand the Maslov number 0. The generators are  $t, a, a_1, \dots, a_k, b_1, \dots, b_l, c_{i,j}^0$  for  $1 \leq i < j \leq q$ , and  $c_{i,j}^1$  for  $1 \leq i, j \leq q$ . The gradings of the generators are as follows:

$$|t| = |a| = |a_i| = |b_i| = 0$$

$$|c_{i,j}^0| = 1$$

$$|c_{i,j}^1| = -1$$

The differentials of generators of the internal DGA are:

$$\begin{aligned} \partial(c_{i,j}^0) &= \sum_{m=1}^q c_{i,m}^0 c_{m,j}^0 \\ \partial(c_{i,j}^1) &= \delta_{i,j} + \sum_{m=1}^q c_{i,m}^0 c_{m,j}^1 + \sum_{m=1}^q c_{i,m}^1 c_{m,j}^0 \end{aligned}$$

where  $\delta_{i,j} = e_1$  if  $i = j$  and is 0 otherwise.

The differentials of the external DGA are given by the count of immersed disks. Notably,  $\partial a$ , from the leftmost crossing of Figure 5.5, has one contribu-

ting disk to its left labelled  $c_p^0$  in the differential. Each of the differentials  $\partial b_i$  for  $i = \{1, \dots, q-1\}$  count two disks, one to the right of  $b_i$  and one to the left, except  $\partial b_p = c_{q-p}^0$  which only counts one disk to the right. For  $a_i$  and  $b_j$  where  $j > q-1$ , the differential counts at least 2 disks, including at least one which contributes a term of the form  $\mu c_{i' j'}^0$  or  $c_{i' j'}^0 \mu$  where  $\mu$  is  $a$ , or some  $a_i$  or  $b_j$ . We extend  $\partial_L$  by the signed Leibniz rule as before.

**Lemma 5.2.1.** Let  $K$  be the Legendrian knot of a diagram  $\mathcal{D}(\Lambda)$ . Let  $q$  be the number of strands passing through the 1-handle. Then the terms  $a, b_1, \dots, b_{q-1}$  do not appear in any differentials of the Chekanov-Eliashberg DGA  $\mathcal{A}_K/\mathbb{Z}\langle e_1 \rangle$  as degree 1 monomials.

*Proof.* Suppose  $a$  appears in the differential of some generator  $\mu$ . Then there is an immersed disk with a negative corner at  $a$ . The boundary of this immersed disk must follow one of the strands from  $a$  to the left. Suppose it's the overcrossing strand. Then the strand immediately enters the 1-handle, so  $a$  appears in the differential in a word of the form  $\mu_1 a c_{i p}^0 \mu_2$  or  $\mu_1 c_{i p}^0 a \mu_2$ , where  $i < p$  and  $\mu_i$  is some other string of generators, possibly none. Likewise if it's the undercrossing strand, we immediately reach the 1-handle to the left of the crossing, so  $a$  appears in the differential in a word of the form  $\mu_1 a c_{i p+1}^0 \mu_2$  or  $\mu_1 c_{i p+1}^0 a \mu_2$ ,  $i < p+1$ .

We can make an equivalent argument for any of the  $b_i$  following their overcrossing and undercrossing strands to the left or right, as we see that we do not meet any negative corners until we reach the 1-handle.

Since we have quotiented out the constant terms (any monomials of the form  $e_1$ ) and the differential on products is generated by the Leibniz rule: the only way to obtain a monomial of smaller degree is if there is a constant term in one of the differentials, but no such term exists. Thus  $a, b_1, \dots, b_{q-1}$  cannot appear as a degree 1 monomial in the differential of some product of generators. □

**Example 5.2.2.** In this example, we fully compute the internal and external DGA of  $D(\Lambda)$  for a particular knot  $\Lambda$ . Consider the case where  $\Lambda$  is the  $m(8_{20})$

knot. We saw in Example 4.3.3 that  $\mathcal{D}(\Lambda)$  is the diagram on the left in Figure 5.6. The Lagrangian resolution of  $\mathcal{D}(\Lambda)$  is the diagram on the right of Figure 5.6.

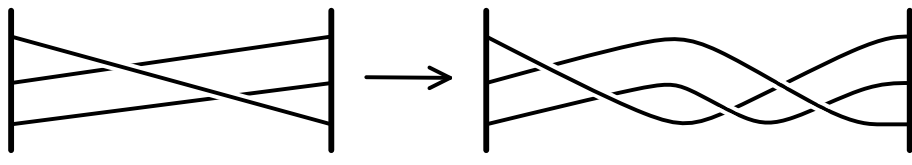


**Figure 5.6:** The Lagrangian resolution for  $\mathcal{D}(\Lambda)$ , where  $\Lambda$  is the  $m(8_{20})$  knot.

We can then label the crossings which generate the DGA as in Figure 5.7.

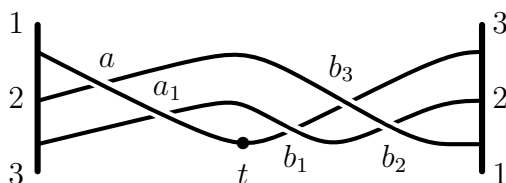


**Figure 5.7:** The external Reeb chords generating the DGA of  $L$  in  $\mathcal{D}(m(8_{20}))$  labelled.

The generators are  $t, a, a_1, b_1, b_2, b_3, c_{i_j}^0$  for  $1 \leq i < j \leq 3$ , and  $c_{i_j}^1$  for  $1 \leq i, j \leq 3$ .

Then the gradings of the generators are:

$$|t| = |a| = |a_1| = |b_1| = |b_2| = |b_3| = 0$$

$$|c_{i_j}^0| = 1$$

$$|c_{i_j}^1| = -1$$

We get following differentials for the labelled Reeb chord generators:

$$\partial a = c_{1_2}^0$$

$$\partial a_1 = c_{1_3}^0 + a c_{2_3}^0$$

$$\partial b_1 = c_{2_3}^0$$

$$\partial b_2 = c_{1_2}^0 + c_{2_3}^0$$

$$\partial b_3 = c_{13}^0 + b_2 c_{23}^0 + c_{23}^0 b_1,$$

along with differentials for the internal generators as follows:

$$\partial c_{12}^0 = 0$$

$$\partial c_{13}^0 = c_{12}^0 c_{23}^0$$

$$\partial c_{23}^0 = 0$$

$$\partial c_{11}^1 = e_1 + c_{12}^0 c_{21}^1 + c_{13}^0 c_{31}^1$$

$$\partial c_{12}^1 = c_{12}^0 c_{22}^1 + c_{13}^0 c_{32}^1 + c_{11}^1 c_{12}^0$$

$$\partial c_{13}^1 = c_{12}^0 c_{23}^1 + c_{13}^0 c_{33}^1 + c_{11}^1 c_{13}^0 + c_{12}^1 c_{23}^0$$

$$\partial c_{21}^1 = c_{23}^0$$

$$\partial c_{22}^1 = e_1 + c_{23}^0 c_{32}^1 + c_{21}^1 c_{12}^0$$

$$\partial c_{23}^1 = c_{23}^0$$

$$\partial c_{31}^1 = 0$$

$$\partial c_{32}^1 = c_{31}^1 c_{12}^0$$

$$\partial c_{33}^1 = e_1 + c_{31}^1 c_{13}^0 + c_{32}^1 c_{23}^0.$$

Another fully computed example of a DGA can be found in Appendix B for a slightly more complicated  $\Lambda$ .

We can now use the Chekanov-Eliashberg DGA to compute symplectic invariants of the Weinstein manifold given by handle attachments along  $\mathcal{D}(\Lambda)$ .

### 5.3 Nonvanishing symplectic homology

Symplectic homology (and cohomology) are very useful invariants of exact symplectic manifolds with contact type boundary, introduced by Viterbo in [Vit99]. It can be used to prove the existence of closed Hamiltonian orbits and Reeb chords, and the wrapped Fukaya category [FSS08] is built using the wrapped Floer cohomology, which are modules over the symplectic cohomology.



logy ring for non-compact symplectic manifolds. See [Sei06] for a survey on symplectic homology. Work of Bourgeois and Oancea first related symplectic homology to linearized contact homology [BO09] and a way to compute symplectic homology via the Chekanov-Eliashberg DGA was established by Bourgeois, Ekholm, and Eliashberg in [BEE12, Ekh19]. In this section, we will summarize the results of [BEE12]. We begin with Corollary 5.7 of [BEE12] which states:

**Theorem 5.3.1.** [BEE12]

$$S\mathbb{H}(X) = LH^{Ho}(L)$$

where  $LH^{Ho}(L)$  is the homology of the Hochschild complex associated to the Chekanov-Eliashberg differential graded algebra of  $L$  over  $\mathbb{Q}$ .

Thus, in order to compute the symplectic homology  $S\mathbb{H}(X)$ , we first compute

$$LH^{Ho+}(L) := \widetilde{LHO}^+(L) \oplus \widehat{LHO}^+(L),$$

defined as follows. We consider the DGA  $\mathcal{A}_L$  defined in the previous section and generated by cyclically composable monomials of Reeb chords. Let  $LHO(L) = \mathcal{A}_L$ . Let

$$LHO^+(L) := LHO(L)/\mathbb{Z}\langle e_1 \rangle$$

be the subalgebra of  $LHO(L)$  generated by non-trivial cyclically composable monomials of Reeb chords. Let

$$\widetilde{LHO}^+(L) := LHO^+(L)$$

and let

$$\widehat{LHO}^+(L) := LHO^+(L)[1],$$

that is  $LHO^+(L)$  with grading shifted up by 1. Now, given a monomial  $w = c_1 \dots c_l \in LHO^+(L)$ , we denote the corresponding elements in  $\widetilde{LHO}^+(L)$  and

$\widehat{LHO}^+(L)$  as  $\check{w} = \check{c}_1 \dots c_l$  and  $\hat{w} = \hat{c}_1 \dots c_l$ , respectively. The hat or check may mark a variable in the monomial which is not the first one, in which case the monomial is the word obtained by the graded cyclic permutation which puts the marked letter in the first position. Let  $S : LHO^+ \rightarrow \widehat{LHO}^+$  denote the linear operator defined by the formula:

$$S(c_1 \dots c_l) := \hat{c}_1 c_2 \dots c_l + (-1)^{|c_1|} c_1 \hat{c}_2 \dots c_l + \dots + (-1)^{|c_1 \dots c_{l-1}|} c_1 c_2 \dots \hat{c}_l.$$

Then the differential  $d_{Ho+} : LH^{Ho+} \rightarrow LH^{Ho+}$  is given by

$$d_{Ho+} = \begin{pmatrix} \check{d}_{LHO^+} & d_{M Ho+} \\ 0 & \hat{d}_{LHO^+} \end{pmatrix}.$$

The maps in the matrix on generators are as follows:

1. If  $w \in LHO^+(L)$  is a monomial, then

$$\check{d}_{LHO^+}(\check{w}) := \sum_{j=1}^r \check{v}_j,$$

where  $d_{LHO^+}(w) := \partial_{\mathcal{A}L}(w) = \sum_{j=1}^r v_j$  for monomials  $v_j$ .

2. If  $c$  is a chord and  $w$  is a monomial such that  $cw \in LHO^+(L)$ , then

$$\hat{d}_{LHO^+}(\hat{c}w) = S(d_{LHO^+}(c))w + (-1)^{|c|+1} \hat{c}(d_{LHO^+}(w)).$$

3. If  $w = c_1 \dots c_l \in LHO^+(\Lambda)$ , then

$$d_{M Ho+}(\hat{w}) := \check{c}_1 \dots c_l - c_1 \dots \check{c}_l.$$

**Remark 5.3.2.** Note that  $d_{M Ho+}$  is zero on linear monomials.

Now we can define  $LH^{Ho}(L) := LH^{Ho+}(L) \oplus C(L)$  where  $C(L)$  is the vector space generated by a single element  $\tau_1$  of grading 0.

Then the differential  $d_{Ho} : LH^{Ho}(L) \rightarrow LH^{Ho}(L)$  is defined as:

$$d_{Ho} = \begin{pmatrix} d_{Ho+} & 0 \\ \delta_{Ho} & 0 \end{pmatrix}.$$

For any chord  $c$ , we define  $\delta_{Ho}(\check{c}) := n_c \tau_1$  where  $n_c$  is the count of the zero-dimensional moduli space of holomorphic disks asymptotic to  $\infty$  at  $c$ . If  $w$  is a nonlinear monomial, then  $\delta_{Ho}(\check{w}) = 0$ .

Then we have the following:

**Proposition 5.3.3.** [BEE12]  $d_{Ho}^2 = 0$  and the homology

$$L\mathbb{H}^{Ho}(L) = H_*(LH^{Ho}(L), d_{Ho})$$

is independent of choices and is a Legendrian isotopy invariant of  $L$ .

We apply Theorem 5.3.1 to the diagrams  $\mathcal{D}(\Lambda)$  obtained in Section 4.3 to obtain the following theorem:

**Theorem 5.3.4.** Let  $\Lambda \neq U$  be a Legendrian knot which is the closure of a quasipositive 3-braid of algebraic length 2. Let  $\Lambda'$  be a positive transverse push off of  $\Lambda$ . Then there is a filling of  $\Sigma_2(\Lambda')$ , the double cover of  $S^3$  branched over  $\Lambda'$ , which has nonvanishing symplectic homology.

*Proof.* Let  $X_\Lambda$  be the filling of  $\Sigma_2(\Lambda)$  given by the Weinstein handle decomposition depicted in  $\mathcal{D}(\Lambda)$ . We will show that

$$S\mathbb{H}(X_\Lambda) = L\mathbb{H}^{Ho}(L)$$

is nonzero by finding a  $(\check{w}, \hat{v}, a_i \tau_i) \in \widetilde{LHO}^+(L) \oplus \widehat{LHO}^+(L) \oplus C(L) = LH^{Ho}(\Lambda)$  such that  $d_{Ho}((\check{w}, \hat{v}, a_i \tau_i)) = 0$  but  $(\check{w}, \hat{v}, a_i \tau_i) \notin \text{Im}(d_{Ho})$ .

First, we consider the Chekanov-Eliashberg DGA  $\mathcal{A}_L = LHO(L)$  of the link  $L$  in the Weinstein diagram  $\mathcal{D}(\Lambda)$ . Recall that  $\mathcal{D}(\Lambda)$  is constructed via surgery on a  $(p, q)$  and a  $(1, 0)$  curve in the torus with one boundary component,

and consists of the attaching curves of a single 2-handle and a single 1-handle. Since  $\Lambda \neq U$ , by Lemma 4.2.5, we choose  $p$  and  $q$  satisfying  $0 < p < q$ .

The attaching sphere of the 2-handle winds around the 1-handle  $q$  times.

As in section 5.2, we will write  $a_i$  (or  $a$ ) to denote generators coming from crossings present in the front diagram,  $b_j$  to denote generators coming from crossings formed by the Lagrangian resolution, and  $c_{i,j}^0, c_{i,j}^1$  to denote generators coming from the internal Reeb chords within the 1-handle. In particular, consider the generators  $a$  and  $b_j$ 's as labelled in Figure 5.5. The differential for  $a$  and the  $b_j$ 's are as follows:

$$\begin{aligned}
\partial a &= c_{p,p+1}^0 \\
\partial b_1 &= c_{q-1,q}^0 + c_{p-1,p}^0 \\
\partial b_2 &= c_{q-2,q-1}^0 + c_{p-2,p-1}^0 \\
&\dots \\
\partial b_{p-1} &= t c_{q-p+1,q-p+2}^0 + c_{1,2}^0 \\
\partial b_p &= c_{q-p,q-p+1}^0 \\
\partial b_{p+1} &= c_{q-p-1,q-p}^0 + c_{q-1,q}^0 \\
&\dots \\
\partial b_{q-1} &= c_{1,2}^0 + c_{p+1,p+2}^0
\end{aligned}$$

Note that every  $c_{i,j}^0$  appears in these differentials twice, with the marked point giving an extra  $t$  coefficient only to the term  $c_{q-p+1,q-p+2}^0$  in  $\partial b_{p-1}$  when  $p > 1$ .

Note also that for any  $i \neq j$ ,  $\partial b_i \neq \partial b_j$ . This is because otherwise, we would have  $q - p - 1 = p - 1$ , so  $q = 2p$ . We know  $q$  and  $p$  are necessarily relatively prime, so we must have  $q = 2$  and  $p = 1$ . Then the diagram  $\mathcal{D}(\Lambda)$  consists of a Legendrian winding around the 1-handle twice with one crossing in  $\mathcal{D}(\Lambda)$  and one additional crossing in the Lagrangian resolution. Thus, there is only one crossing labelled with a  $b$ , so  $i = j$ , a contradiction.

Let

$$c := ta + \sum_{i=1}^{q-1} \epsilon_i t^{s_i} b_i$$

where we choose  $s_i \in \{0, 1\}$  and  $\epsilon_i \in \{-1, 1\}$  using the following procedure:

1. Let  $c_0 := a + \sum_{i=1}^{q-1} b_i$ . Rearrange the terms in sum  $c_0 = a + \sum_{i=1}^{q-1} b_i$  in terms of the differentials of the generators so that matching terms are adjacent and relabel with the index  $i_j$ :

$$\begin{aligned} \partial(c_0) &= (c_{p \ p+1}^0) + (c_{p \ p+1}^0 + c_{i_0 \ j_0}^0) + (c_{i_0 \ j_0}^0 + c_{i_1 \ j_1}^0) + \dots \\ &\quad + (tc_{q-p+1 \ q-p+2}^0 + c_{1 \ 2}^0) + (c_{1 \ 2}^0 + c_{p+1 \ p+2}^0) + \dots + (c_{q-p \ q-p+1}^0) \\ &= \partial a + \partial b_{i_1} + \dots + \partial b_{i_{q-1}} \\ &= \partial a + \sum_{j=1}^{q-1} \partial b_{i_j} \end{aligned}$$

2. Let  $j'$  satisfy  $b_{p-1} = b_{i_{j'}}$ . Then for  $j < j'$  let  $s_i = 1$ , and for  $j \geq j'$ , let  $s_i = 0$ . If  $p = 1$ ,  $s_i = 0$  for all  $i$ .
3. Let  $\epsilon_i = (-1)^j$ .

Then  $\partial_{\mathcal{A}}(c) = 0$ .

Consider the element  $(\check{c}, \hat{c}, \tau_1) \in LH^{Ho}(L)$ . Then  $\partial_{\mathcal{A}}(c) = d_{LHO}(c) = 0$ , so  $d_{LHO^+}(c) = 0$ . Thus we obtain the following:

$$\check{d}_{LHO^+}(\check{c}) = 0,$$

$$\hat{d}_{LHO^+}(\hat{c}) = 0,$$

$$d_{M \ Ho^+}(\hat{c}) = 0$$

by Remark 5.3.2. Finally,  $\delta_{Ho}$  counts the zero-dimensional moduli space of holomorphic disks asymptotic to Reeb chords at  $\infty$ . These are disks with boundary consisting of a smooth curve along the front diagram that does not pass through a negative corner. Since the curves in  $\mathcal{D}(\Lambda)$  pass monotonically

left to right, any such boundary would necessarily have a negative corner at the 1-handle. Thus,

$$\delta_{Ho}(c) = 0.$$

Thus we conclude that  $d_{Ho}(\check{c}, \hat{c}, \tau_1) = 0$ .

To see that  $(\check{c}, \hat{c}, \tau_1) \notin \text{Im}(d_{Ho})$ , note that in the image of  $d_{LHO+}$  is generated by the differentials of the generators of  $\mathcal{A}_L/\mathbb{Z}\langle e_1 \rangle$ . Thus we can apply Lemma 5.2.1, and we know that the terms  $a, b_1, \dots, b_{q-1}$  do not appear in any differentials of the Chekanov-Eliashberg DGA  $\mathcal{A}_L/\mathbb{Z}\langle e_1 \rangle$  as degree 1 monomials. Thus  $c \notin \text{Im}(d_{LHO+})$ .  $\square$

**Example 5.3.5.** Following the above proof, for the  $m(8_{20})$  knot with differential algebra given by 5.2.2, the cycle  $c$  is given by  $a - b_2 + b_1$ .

For an example in which the coefficient  $t$  appears in the differential of  $c$ , see the case of the  $10_{155}$  knot in Appendix B.

## 5.4 The Main Theorem

We will use the filling with nonzero symplectic homology of the previous section along with a result of McLean [McL09] to prove the main theorem.

McLean's result is based on the work of Viterbo in [Vit99]. Specifically, from *Viterbo functoriality* which says that a codimension 0 exact embedding of a symplectic manifold with boundary into another induces a *transfer map* on the symplectic homologies between them. More precisely,

**Theorem 5.4.1.** [Vit99] Suppose  $(W, d\lambda)$  is an exact symplectic manifold with a Liouville vector field which is transverse at the boundary. Suppose  $W_0 \hookrightarrow W$  is an embedding of a compact codimension 0 submanifold. Then there exists a natural homomorphism

$$SH_*(W, d\lambda) \rightarrow SH_*(W_0, d\lambda).$$

Moreover, this map, along with the natural map on relative singular homology

$H_*(W, \partial W) \rightarrow H_*(W_0, \partial W_0)$  forms the following commutative diagram:

$$\begin{array}{ccc} H_{*+n}(W, \partial W) & \longrightarrow & H_{*+n}(W_0, \partial W_0) \\ \downarrow & & \downarrow \\ S\mathbb{H}_*(W, d\lambda) & \longrightarrow & S\mathbb{H}_*(W_0, d\lambda) \end{array}$$

McLean checked that this transfer map was in fact a unital ring map and proved the following theorem (Cor 10.5 in [McL09]) which we will use in the proof of the main theorem:

**Theorem 5.4.2.** [McL09] Let  $X$  and  $W$  be compact convex symplectic manifolds. Suppose  $W$  is subcritical. Suppose  $S\mathbb{H}(X) \neq 0$ . Then  $X$  cannot be embedded in  $W$  as an exact codimension 0 submanifold. In particular, if  $H_1(X) = 0$ , then  $X$  cannot be symplectically embedded into  $W$ .

We are ready to conclude the main theorem:

**Theorem 5.4.3.** Let  $U$  be the standard  $tb = -1$  unknot. Let  $\Lambda$  be a Legendrian knot satisfying  $U \prec \Lambda \prec U$ , and  $\Lambda \neq U$ . Then  $\Lambda$  cannot be smoothly the closure of a 3-braid.

*Proof.* We proceed by contradiction. Suppose  $\Lambda \neq U$  is smoothly the closure of a 3-braid which satisfies  $U \prec \Lambda \prec U$ .  $\Lambda$  must be quasipositive.  $\Lambda$  has a positive transverse push off  $\Lambda'$  of the same topological knot type. By Remark 1.0.12,  $\Lambda'$  is transversely isotopic to a quasipositive 3-braid. By Corollary 3.3.7,  $\Lambda$  must have algebraic length 2. By Theorem 4.3.2,  $\mathcal{D}(\Lambda)$  is the Weinstein diagram of a filling of  $\Sigma_2(\Lambda')$ , call it  $X_\Lambda$ . By Theorem 5.3.4,  $X_\Lambda$  has nonzero symplectic homology.

Next, we'll show that  $X_\Lambda$  embeds in  $B^4$  as a codimension 0 exact submanifold. Recall the construction from the proof of Theorem 3.1.6. In particular, we will need the submanifold  $V$  of  $\Sigma_p(C')$ , where  $C'$  is the symplectic approximation of the Lagrangian concordance cylinder of  $U \prec \Lambda \prec U$ . Here we fix  $p = 2$ . Then we have  $\partial V = \Sigma_2(\Lambda') \cup S^3$ . In the proof of Theorem 3.1.6, we

showed that any 4-manifold constructed by gluing a filling of  $\Sigma_2(\Lambda')$  to  $V$  must embed in a blow-up of  $B^4$ .

Let  $X$  be the branched double cover of  $B^4$  branched over the symplectic disk bounding  $\Lambda'$ . Then the manifold we get by gluing  $X$  to  $V$  along  $\Sigma_2(\Lambda')$  is  $B^4$ . Then we obtain the following Mayer-Vietoris sequence:

$$H_3(B^4) \longrightarrow H_2(\Sigma_2(\Lambda')) \longrightarrow H_2(X) \oplus H_2(V) \longrightarrow H_2(B^4)$$

$\Sigma_2(\Lambda')$  is a rational homology sphere, thus  $H_2(\Sigma_2(\Lambda'), \mathbb{Q}) = 0$ . Then since  $H_3(B^4, \mathbb{Q}) = H_2(X, \mathbb{Q}) = H_2(B^4) = 0$ , we have that

$$H_2(V, \mathbb{Q}) = 0.$$

Now instead take  $W = X_\Lambda \cup V$  to be the manifold obtained by gluing  $X_\Lambda$  to  $V$ . We obtain the following Mayer-Vietoris sequence:

$$H_2(\Sigma_p(\Lambda')) \longrightarrow H_2(X_\Lambda) \oplus H_2(V) \longrightarrow H_2(W) \longrightarrow H_1(\Sigma_p(\Lambda'))$$

From  $\mathcal{D}(\Lambda)$ , we see that  $X_\Lambda$  is constructed via attaching a single 1-handle and a single 2-handle to a 0-handle. The 2-handle is attached along a curve which runs along the 1-handle nontrivially. Thus  $H_2(X_\Lambda, \mathbb{Q}) = 0$ . And since  $H_2(\Sigma_p(\Lambda'), \mathbb{Q}) = H_2(V, \mathbb{Q}) = H_1(\Sigma_p(\Lambda'), \mathbb{Q}) = 0$ ,

$$H_2(W, \mathbb{Q}) = 0.$$

Thus  $W$  must be minimal, so  $W$  is  $B^4$ , which is subcritical. Since  $X_\Lambda$  has a Weinstein structure, it is exact and convex.

This contradicts Theorem 5.4.2. Thus if  $\Lambda$  satisfies  $U \prec \Lambda \prec U$ ,  $\Lambda \neq U$ , then  $\Lambda$  is not smoothly the closure of a 3-braid.  $\square$

In other words, we have shown:

**Corollary 5.4.4.** Let  $U$  be the standard  $tb = -1$  unknot. The only Le-



gendrian knot  $\Lambda$  which satisfies  $U \prec \Lambda \prec U$  and is smoothly the closure of a 3-braid is  $U$ .

*Proof.*  $\prec$  is reflexive and Theorem 5.4.3 eliminates all other 3-braid closures.  $\square$

Additionally the following result about contact embeddings follows from the proof of Theorem 5.4.3. The double covers of  $S^3$  branched over a quasipositive transverse knot  $\Lambda'$  which is the closure of a 3-braid of algebraic length 2 form an infinite family of contact manifolds which are rational homology spheres but do not embed in  $\mathbb{R}^4$  as contact type hypersurfaces, motivated by the work of Mark and Tosun [MT20].

**Corollary 5.4.5.** Let  $\Sigma_2(\Lambda')$  be the double cover of  $S^3$  branched over a quasipositive transverse knot which is the closure of a 3-braid of algebraic length 2. Suppose  $\Lambda'$  is not the unknot. Then  $\Sigma_2(\Lambda')$  does not embed as a contact type hypersurface in  $\mathbb{R}^4$ .

*Proof.* Suppose  $\Sigma_2(\Lambda')$  be the double cover of  $S^3$  branched over a quasipositive transverse knot  $\Lambda'$  which is the closure of a 3-braid of algebraic length 2. Suppose  $\Lambda'$  is not the unknot. Suppose  $\Sigma_2(\Lambda')$  embeds as a contact type hypersurface in  $\mathbb{R}^4$ . Then it bounds a codimension-0 symplectic submanifold of  $\mathbb{R}^4$ , call it  $X$ .

We now follow the same arguments as in the proof of Theorem 5.4.3, to reach a contradiction. We have a Mayer-Vietoris sequence:

$$H_3(\mathbb{R}^4) \longrightarrow H_2(\Sigma_2(\Lambda')) \longrightarrow H_2(X) \oplus H_2(\mathbb{R}^4 \setminus X) \longrightarrow H_2(\mathbb{R}^4)$$

So  $H_2(X) = 0$ . Consider  $(\mathbb{R}^4 \setminus X)$  which has boundary  $\Sigma_2(\Lambda')$ . We can glue in the filling  $X_\Lambda$  of  $\Sigma_2(\Lambda')$  corresponding to the diagram  $\mathcal{D}(\Lambda)$  of Theorem 4.3.2 along the boundary  $\Sigma_2(\Lambda')$ . Let  $W := (\mathbb{R}^4 \setminus X) \cup X_\Lambda$ . By p. 311 of [Gro85],  $W = \mathbb{R}^4 \# m \overline{\mathbb{C}\mathbb{P}^2}$  for some  $m \geq 0$ . We have another Mayer-Vietoris sequence:

$$H_2(\Sigma_p(\Lambda')) \longrightarrow H_2(X_\Lambda) \oplus H_2(B^4 \setminus X) \longrightarrow H_2(W) \longrightarrow H_1(\Sigma_p(\Lambda')).$$

Thus,  $H_2(W) = 0$  and we know that  $W$  is  $\mathbb{R}^4$ . Thus  $X_\Lambda$  embeds as an exact codimension 0 submanifold of  $W = \mathbb{R}^4$ .

By Theorem 5.3.4,  $X_\Lambda$  has nonzero symplectic homology. Thus by Theorem 5.4.2,  $X_\Lambda$  cannot embed in  $\mathbb{R}^4$ , a contradiction.  $\square$

To see that these  $\Sigma_2(\Lambda')$  are indeed an infinite family, we distinguish infinitely many of them by their first homology, which we can compute from their Weinstein diagrams.

**Proposition 5.4.6.** There are infinitely many non homeomorphic manifolds which are double covers of  $S^3$  branched over quasipositive transverse knots which are the closures of 3-braids of algebraic length 2.

*Proof.* Consider the 3-braids  $\beta_k := \sigma_1 \sigma_2^{-k} \sigma_1 \sigma_2^k$  for  $k \in \mathbb{Z}, k \geq 2$ . Let  $\Lambda'_k$  be a transverse knot which is the closure of  $\beta_k$ . By Proposition 4.2.2, there is an open book decomposition of the double cover of  $S^3$  branched over  $\Lambda'_k$ ,  $\Sigma_2(\Lambda'_k)$ , with pages consisting of tori with one boundary component and monodromy  $\phi = \tau_\alpha \tau_\gamma$  where  $\alpha$  is a  $(1, 0)$  curve and  $\gamma$  is a curve with slope  $(1, k)$ .

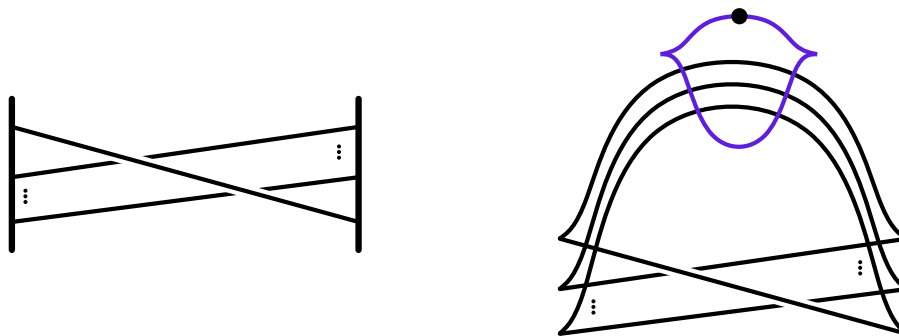


**Figure 5.8:** The Weinstein diagram of  $X_{\Lambda'_k}$  with  $k$  strands entering the 1-handle (left) and the corresponding surgery diagram of  $\Sigma_2(\Lambda'_k)$  (right).

Then by Theorem 4.3.2,  $\Sigma_2(\Lambda'_k)$  has a filling  $X_{\Lambda'_k}$  with surgery diagram as in Figure 5.8. We can replace the 1-handle in this diagram with a 0-framed surgery on an unknot to obtain a surgery diagram of  $\Sigma_2(\Lambda'_k)$ , as in Figure 5.8. We call the unknot  $U$  and the other knot  $L$ . We see that  $U$  has linking number

$k$  with  $L$ , so their linking matrix is

$$\begin{bmatrix} 0 & k \\ k & tb(L) - 1 \end{bmatrix}$$

which has determinant  $-k^2$ , thus

$$|H_1(\Sigma_2(\Lambda'_k))| = k^2.$$

Thus,  $\Sigma_2(\Lambda'_k)$  is not homeomorphic to  $\Sigma_2(\Lambda'_j)$  for  $j \neq k$ . □

## Chapter 6

# Weinstein Complements of Smoothed Toric Divisors

In this chapter, we outline the results obtained in collaboration with Bahar Acu, Orsola Capovilla-Searle, Agnes Gadbled, Aleksandra Marinković, Emmy Murphy, and Laura Starkston. These results were introduced in [ACSG<sup>+</sup>20a] and their full proofs can be found in [ACSG<sup>+</sup>20b].

### 6.1 Existence of a Weinstein structure

Our work in [ACSG<sup>+</sup>20a, ACSG<sup>+</sup>20b] provides a connection between the study of toric geometry and Weinstein handlebody theory. In particular our main result is an algorithm which produces the Weinstein handlebody diagram in Gompf standard form for a large class of 4-dimensional manifolds. These are the complements of *centered* toric divisors smoothed at some of their normal crossing singularities.

Symplectic divisors are co-dimension 2 symplectic submanifolds that may have controlled singularities. Donaldson proved that every closed integral symplectic manifold  $(M, \omega)$  has a smooth symplectic divisor Poincaré dual to  $k[\omega]$  [Don96], and Giroux proved such a divisor can be chosen so that the complement has a Weinstein structure [Gir02, Gir17].

A *toric manifold* is a symplectic manifold with an effective Hamiltonian action of the torus of the maximal dimension [Sym03]. The Hamiltonian action

induces a moment map whose image is a Delzant polytope,  $\Delta$ . The preimage under the moment map of the facets of the Delzant polytope is a *toric divisor*, a divisor fixed by the Hamiltonian action. In 4 dimensions, these toric divisors consist of some number of transversally intersecting embeddings of  $\mathbb{C}\mathbb{P}^1$  and initially have normal crossing singularities, which are nodes mapped to vertices of the Delzant polytope in a one to one correspondence. Any of the nodes can be smoothed so the divisor has fewer singularities. We call a toric divisor which has been smoothed at some subset of nodes a *smoothed toric divisor*, see Figure 6.1.

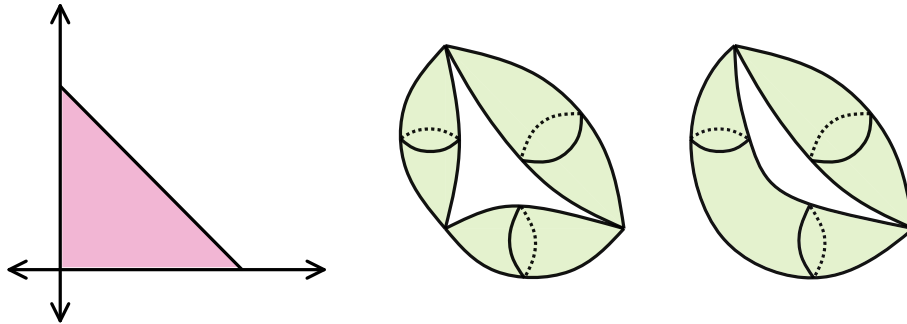


**Figure 6.1:** From left to right: the Delzant polytope for  $\mathbb{C}\mathbb{P}^2$ , the preimage of the facets of  $\mathbb{C}\mathbb{P}^2$  consisting of 3 transversally intersecting copies of  $\mathbb{C}\mathbb{P}^1$ , and the toric divisor in  $\mathbb{C}\mathbb{P}^2$  smoothed at one node.

We define a special class of smoothed toric manifolds as follows:

**Definition 6.1.1.** [ACSG<sup>+</sup>20a] For each vertex  $V$  of the Delzant polytope of a toric manifold, we associate a ray  $R$  generated by the sum of the unit edge vectors of  $\Delta$  adjacent to  $V$  and beginning at  $V$ . A toric manifold with a chosen subset  $\{V_1, \dots, V_k\}$  of the vertices is called  $\{V_1, \dots, V_k\}$ -centered if the corresponding rays  $R_1, \dots, R_k$  all intersect at a common single point in the interior of the Delzant polytope.

Figure 6.2 illustrates some examples of centered toric manifolds. With this definition in mind, the first main results of the paper are as follows. We show that if we have a  $\{V_1, \dots, V_k\}$ -centered toric manifold, then the complement of the toric divisor smoothed precisely at the nodes  $V_1, \dots, V_k$  admits a Weinstein

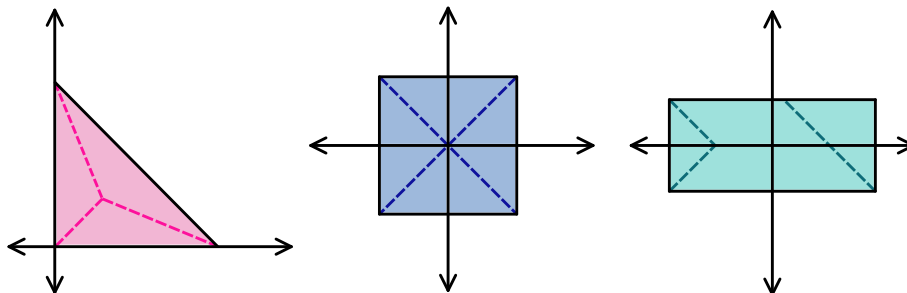


**Figure 6.2:** From left to right: the Delzant polytope for  $\mathbb{C}\mathbb{P}^2$  showing that it's centered with respect to all of its nodes, the Delzant polytope for  $(\mathbb{C}\mathbb{P}^1 \times \mathbb{C}\mathbb{P}^1, \omega_{a,a})$  showing that it's centered with respect to all of its nodes, and the preimage of the facets of  $\mathbb{C}\mathbb{P}^2$ , and the Delzant polytope for  $(\mathbb{C}\mathbb{P}^1 \times \mathbb{C}\mathbb{P}^1, \omega_{a,b}), a > b$  showing that it's centered with respect to two but not three of its nodes.

structure. We describe how to obtain the attaching spheres of the Weinstein handles of such a complement:

**Theorem 6.1.2.** [ACSG<sup>+</sup>20b] Let  $(M, \omega)$  be a toric 4-manifold corresponding to Delzant polytope  $\Delta$  which is  $\{V_1, \dots, V_k\}$ -centered. Let  $D$  denote the divisor obtained by smoothing the toric divisor at the nodes  $V_1, \dots, V_k$ . Then there exist arbitrarily small neighborhoods  $N$  of  $D$  such that  $M \setminus N$  admits the structure of a Weinstein domain.

Furthermore,  $M \setminus N$  is Weinstein homotopic to the Weinstein domain obtained by attaching Weinstein 2-handles to the unit disk cotangent bundle of the torus  $D^*T^2$ , along the Legendrian co-normal lifts of co-oriented curves of slope  $s(V_1), \dots, s(V_k)$ . Here  $s(V_i)$  is equal to the difference of the inward normal vectors of the edges adjacent to  $V_i$  in  $\Delta$ .

We outline the proof of this theorem: The first main step is to embed the model Weinstein structure on a 2-handle into a model neighborhood of the node. Then we can apply the symplectomorphism coming from the appropriate  $SL(2, \mathbb{Z})$  transformation to send this model to a node  $V_i$ . Let  $U$  denote the complement of a neighborhood of the nodal divisor in the local model. The second main step is to show how to glue the Weinstein structure on the handle to the Weinstein structure of  $U$  in a neighborhood of the attaching region,

in a way that avoids creating any additional critical points. The gluing we perform will occur in a local neighborhood of the node  $V_i$ , and the Weinstein structure outside of this neighborhood will agree with the canonical structure on  $U$ . Therefore we will be able to repeat this gluing at each of the nodes  $V_1, \dots, V_n$  independently to obtain the global Weinstein structure. We will use the centeredness condition to ensure that the Legendrian attaching spheres of the 2-handles can be simultaneously Legendrian with respect to the contact structure induced on  $\partial(D^*T)$ .

## 6.2 The Centeredness Condition

We then ask: *how restrictive is the centeredness condition?* If  $\{V_1, \dots, V_k\}$  is the set of all vertices of the polytope  $\Delta$ , then we show that the polytope is  $\{V_1, \dots, V_k\}$ -centered if and only if it is monotone. This is very restrictive:  $\Delta$  must correspond to one of the 5 monotone toric 4-manifolds (up to rescale of a symplectic form).

However, our examples come primarily from partially smoothed toric divisor complements, where not all but some nodes are smoothed. This way, we can realize many different manifolds. In fact, we show an explicit construction of a family of  $\{V_1, \dots, V_k\}$ -centered toric 4-manifolds, for any  $k \in \mathbb{N}$ :

**Theorem 6.2.1.** [ACSG<sup>+</sup>20b] There are infinitely many non-diffeomorphic Weinstein manifolds obtained by taking the completion of the complement of a neighborhood of a partially smoothed toric divisor in a toric 4-manifold.

This does not give a complete list of such toric manifolds, but shows the existence an infinite family of examples. On the other hand, we also give an infinite family of distinct slopes that cannot be realised as a subset of the slopes of the vertices of any partially centered Delzant polytope.

**Theorem 6.2.2.** [ACSG<sup>+</sup>20b] For any  $K \geq 2$ , there is no  $\{V_1, V_2, V_3, V_4\}$ -centered Delzant polytope where

$$s(V_1) = (1, 1), s(V_2) = (1, 2), s(V_3) = (-K, -1), s(V_4) = (0, -1).$$

By contrast, if one removes the partially centered requirement, any collection of slopes can be realized by a Delzant polytope. We prove:

**Proposition 6.2.3.** [ACSG<sup>+</sup>20b] For any choice of primitive vectors  $\{(a_1, b_1), \dots, (a_k, b_k)\}$  there is a Delzant polytope with at least  $k$  edges such that there are  $k$  vertices whose slopes are precisely  $\{(a_1, b_1), \dots, (a_k, b_k)\}$ .

Thus, the centeredness criterion is a non-trivial constraint for toric manifolds on their combinatorial slope data. In the non-centered case, the complement of a neighborhood of the divisor does not in general support a Weinstein structure. In fact, for many non-centered cases we can prove that the complement is not even exact.

**Proposition 6.2.4.** [ACSG<sup>+</sup>20b] Let  $(M, \omega)$  be a symplectic toric manifold and  $\Delta$  its Delzant polytope. Let  $V_1, \dots, V_k$  be a subset of the vertices of  $\Delta$ . Assume that  $M$  fails to be  $\{V_1, \dots, V_k\}$ -centered because either

- (i) Two rays associated to two of the vertices  $\{V_1, \dots, V_k\}$  are parallel, or;
- (ii) There exists three vertices,  $\{V_{i_1}, V_{i_2}, V_{i_3}\}$  such that for the associated rays  $R_{i_1}, R_{i_2}, R_{i_3}$ ,  $R_{i_1}$  intersects  $R_{i_2}$  at a point  $c_1 \in \text{int}(\Delta)$  in the interior of the polytope  $\Delta$  that does not belong to  $R_{i_3}$ .

Then the complement of its toric divisor smoothed at  $\{V_1, \dots, V_k\}$  is not an exact symplectic manifold (and in particular cannot support a Weinstein handlebody structure).

There are other situations where a toric manifold may fail to be  $\{V_1, \dots, V_k\}$ -centered which do not fall the cases listed in Proposition 6.2.4. For example, the rays may all intersect at points outside the interior of the polytope, or the directed rays may fail to intersect at all because of the placement of the vertices and the directions of the rays. In certain examples, we prove that even though the complement of the  $\{V_1, \dots, V_k\}$ -smoothing is exact, it still does not admit a Weinstein structure.



### 6.3 Drawing handlebody diagrams

As part of the proof of Theorem 6.3.2 we establish the Gompf standard handle diagram for  $D^*F$  with no additional 2-handles attached. In [Gom98], Gompf produced Weinstein handle diagrams which are *diffeomorphic* to  $D^*F$ , see Figure 6.5. Although it was expected that these structures were Weinstein homotopic to the canonical (Morse-Bott) Weinstein structure on the cotangent bundle, the proof was lacking in the literature. When  $F = T^2$ , Weinstein homotopy follows from a result of Wendl [Wen10]. Additionally, the case for the contact boundary is proved by Ozbagci [Ozb19b, Ozb19a]. Because we build off of this Weinstein homotopy in establishing our procedure, we first fill this gap.

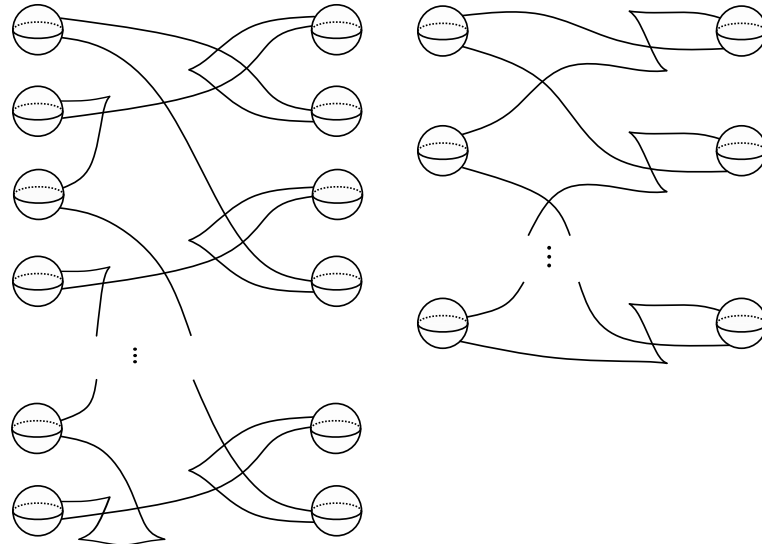


**Figure 6.3:** Weinstein handle diagrams which are Weinstein homotopic to the canonical Weinstein structure on the cotangent bundles of an orientable surface (left), of a non-orientable surface (right).

**Theorem 6.3.1.** [ACSG<sup>+</sup>20b] The Gompf handlebody diagram for  $D^*F$  corresponds to a Weinstein structure which is Weinstein homotopic to the canonical Weinstein structure on the cotangent bundle of  $F$ .

This allows us to develop a systematic procedure to take the Weinstein manifolds produced by Theorem 6.1.2 and convert them into Weinstein handlebody diagrams in Gompf standard form. Let  $F$  be a surface, and  $c$  a finite set

of co-oriented curves in  $F$ . Then, we let  $\mathcal{W}_{F,c}$  denote the Weinstein 4-manifold obtained by attaching 2-handles to  $D^*F$  along the Legendrian co-normal lifts of the set of curves  $c$ . In the case that we have a smoothed toric divisor, the curves  $c$  are given by the slopes as shown in Theorem 6.1.2. In either case, we have the following theorem:

**Theorem 6.3.2.** [ACSG<sup>+</sup>20b] Let  $F$  be any surface and  $\{\gamma_i\}_{i=1}^n$  a finite collection of co-oriented curves in  $F$ . Then there is a procedure which produces a Weinstein handle diagram in standard form representing a Weinstein manifold  $\mathcal{W}$  which is Weinstein homotopic to  $\mathcal{W}_{F,c}$ .

The steps of the procedure are carefully outlined in Section 8 of [ACSG<sup>+</sup>20b] but we summarize them here:

1. If starting with a  $\{V_1, \dots, V_k\}$ -centered toric manifold, for each vertex  $V_i$  for  $i$  from 1 to  $k$  compute  $s(V_i)$  given by the difference of the inward normals of the edges meeting at  $V_i$ .
2. Draw on the square diagram of a torus an oriented curve of slope  $s(V_i)$  for each  $i$ . For general surface  $F$ , draw the curve on the appropriate polytope.
3. Isotope all these curves in a consistent normal direction in the torus so that they are as far as possible from the center of the square.
4. Cut the square along a line from the bottom left corner of the square to the center and unfold it into a rectangle, representing  $J^1(S^1)$ .
5. Satellite the curves which are parallel positive Reeb pushoffs of the 0-section in the  $J^1(S^1)$  picture so that they are parallel positive Reeb pushoffs of the attaching sphere of the 2-handle in the  $T^*T^2$  handlebody diagram.
6. The Weinstein handlebody diagram can now be simplified using Reidemeister moves, Legendrian handle slides and cancellations.

We can say some things in general about the Weinstein manifolds constructed this way. In fact, using the Weinstein handle description our procedure produces, we show that the symplectic invariants of the Weinstein manifolds appearing in Theorem 6.3.2 are non-trivial. In particular, we prove:

**Proposition 6.3.3.** [ACSG<sup>+</sup>20b] Any Weinstein 4-manifold  $X$  constructed by attaching 1- or 2-handles to  $T^*F$  for  $i = 1, \dots, k$  for any orientable surface  $F$ , has nonvanishing symplectic homology.

**Corollary 6.3.4.** [ACSG<sup>+</sup>20b] Any Weinstein 4-manifold  $X$  constructed by attaching 1- or 2-handles to  $T^*F$  for  $i = 1, \dots, k$  for any orientable surface  $F$ , is not a flexible Weinstein manifold.

Finally, we apply the procedure to produce previously unknown Weinstein handlebody diagrams of the complements of certain smoothed toric divisors. Some examples of such diagrams include the following:

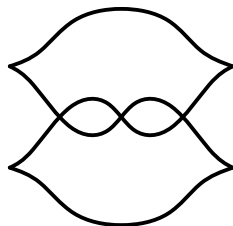


**Figure 6.4:** The Legendrian trefoil with  $tb = 1$ , also the Weinstein diagram of the complement of any toric divisor smoothed in adjacent nodes of a blow up.

**Theorem 6.3.5.** [ACSG<sup>+</sup>20b] The Weinstein handlebody diagram of the complement of any toric divisor smoothed in adjacent nodes of a blow up is a Legendrian trefoil with maximum Thurston Bennequin number, as in Figure 6.4.

**Theorem 6.3.6.** [ACSG<sup>+</sup>20b] The complement of a toric divisor in  $(\mathbb{C}\mathbb{P}^1 \times \mathbb{C}\mathbb{P}^1, \omega_{a,a})$  smoothed in opposite nodes is Weinstein homotopic to the cyclic plumbing of two disk cotangent bundles of spheres, see Figure 6.5.

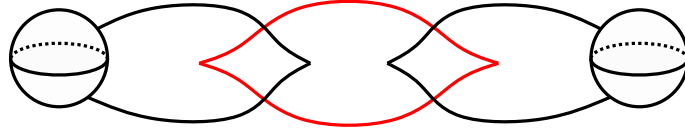


**Figure 6.5:** The Weinstein handlebody diagram of the complement of the toric divisor of  $\mathbb{C}\mathbb{P}^1 \times \mathbb{C}\mathbb{P}^1$  smoothed in two opposite nodes.

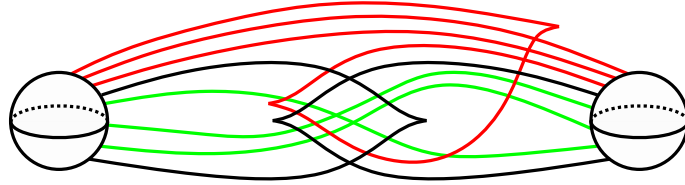


**Figure 6.6:** The Weinstein diagram of the complement the smooth cubic in  $\mathbb{C}\mathbb{P}^2$ .

**Theorem 6.3.7.** [ACSG<sup>+</sup>20b] The Weinstein handlebody diagram of the complement of a smooth cubic in  $\mathbb{C}\mathbb{P}^2$  is Figure 6.6.

## Appendix A

# Handle moves on parallel strands

In section 4, some computations involving Weinstein diagrams involve sliding a single strand over multiple parallel strands or repeated Reidemeister or Gompf moves. These moves were not included in the section so we construct them here from elementary moves and demonstrate their intermediate steps.

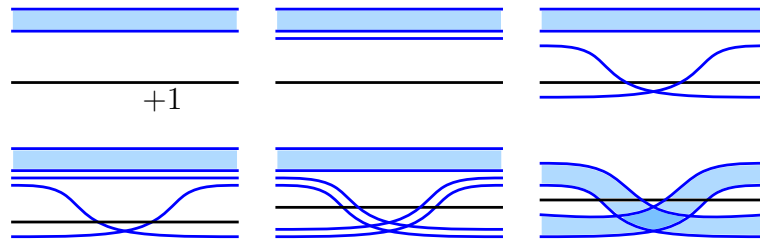


**Figure A.1:** Sliding parallel strands over a (+1) curve, the blue shaded region representing some number of parallel strands. In order, we have

- (1.) the set up,
- (2.) separating out the bottom most blue strand,
- (3.) sliding this strand over the (+1) surgery curve,
- (4.) separating the next strand,
- (5.) sliding over a second strand,
- (6.) sliding over all strands.

Firstly, Figure A.1 demonstrates sliding a parallel set of strands over a (+1) surgery curve. A similar move holds for sliding over a (-1) surgery curve though this was not used in our computations in Chapter 4.

Figure A.2 demonstrates performing Gompf move 5 repeatedly on a set

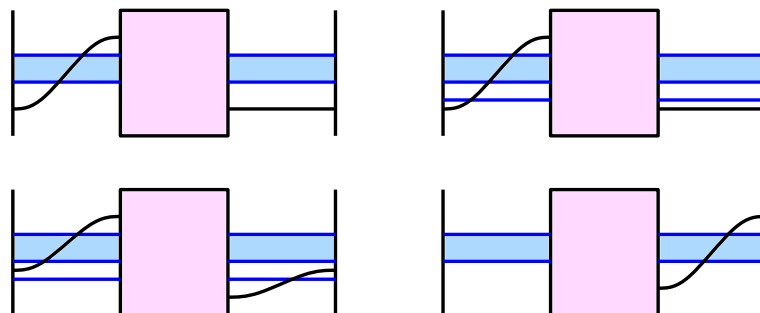


**Figure A.2:** Performing Gompf move 5 with parallel strands, the blue shaded region representing some number of parallel strands. In order, we have

- (1.) the set up,
- (2.) separating out the bottom most blue strand,
- (3.) pushing the bottom crossing through the 1-handle (Gompf 5),
- (4.) repeating step 3. with all other strands.

of parallel strands. For our computations in Chapter 4, we did not use Gompf 4 or 6, though a parallel version of these moves also works.

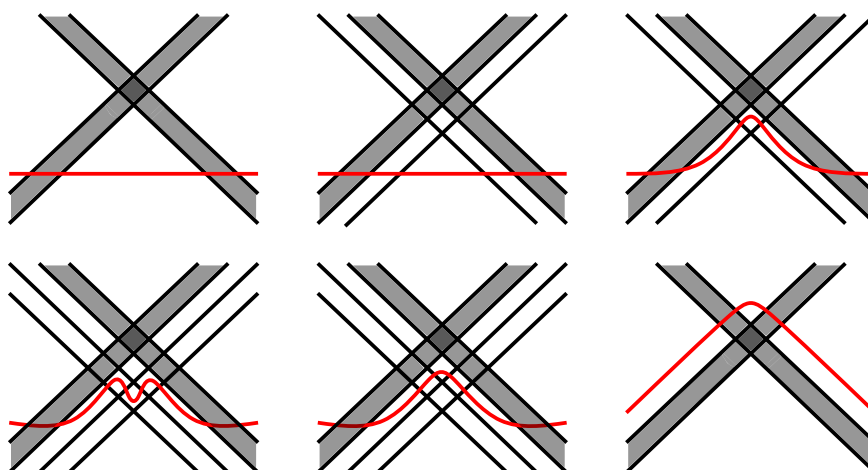


**Figure A.3:** Performing Reidemeister 3 with parallel strands, the grey shaded region representing some number of parallel strands. In order, we have

- (1.) the set up,
- (2.) separating out the bottom most strands,
- (3.) Reidemeister 3,
- (4.) Reidemeister 3 twice,
- (5.) Reidemeister 3,
- (6.) repeating these steps with all other strands.

Now we observe the three Reidemeister moves on parallel strands. Figure A.3 demonstrates performing repeated Reidemeister 3 moves with parallel

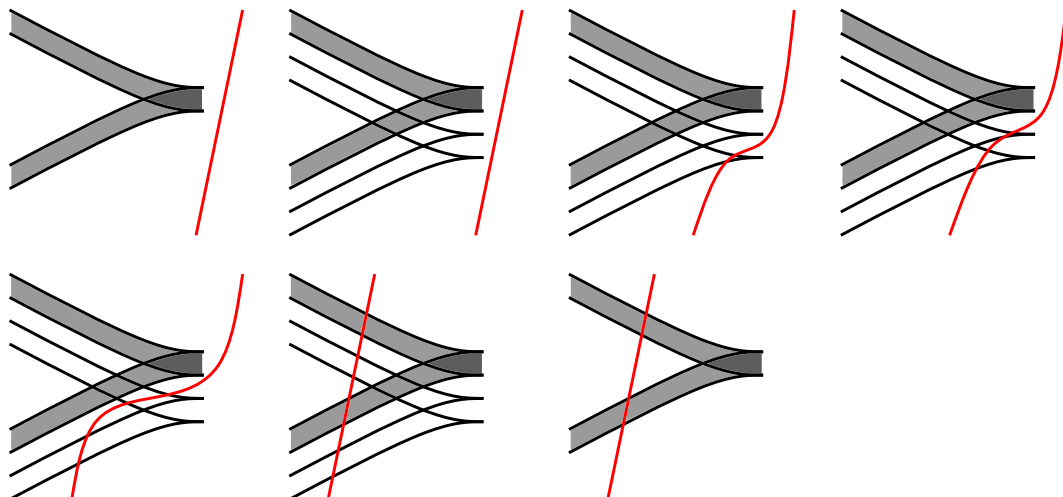


**Figure A.4:** Performing Reidemeister 2 with parallel strands, the grey shaded region representing some number of parallel strands. In order, we have

- (1.) the set up,
- (2.) separating out the bottom most strands,
- (3.) Reidemeister 2,
- (4.) Reidemeister 2,
- (5.) Reidemeister 3,
- (6.) repeating these steps with all other strands,
- (7.) the final result.

strands.

We use parallel stranded Reidemeister 3 moves in Figure A.4, which demonstrates performing repeated Reidemeister 2 moves with parallel cusping strands.

Finally, Figure A.5 demonstrates performing repeated Reidemeister 1 moves with parallel strands. We use both parallel stranded Reidemeister 2 and 3 moves in the figure.

Note that the Reidemeister moves for parallel strands also follow from Proposition 5.9 of [NT04] where Ng and Traynor show that Legendrian satellites are well-defined, meaning that if  $L$  and  $L'$  are related by Legendrian isotopy, then so too are their satellites  $S(L)$  and  $S(L')$ . Thus if a single stranded version of the Legendrian Reidemeister moves preserves Legendrian isotopy, so too must the parallel stranded version.

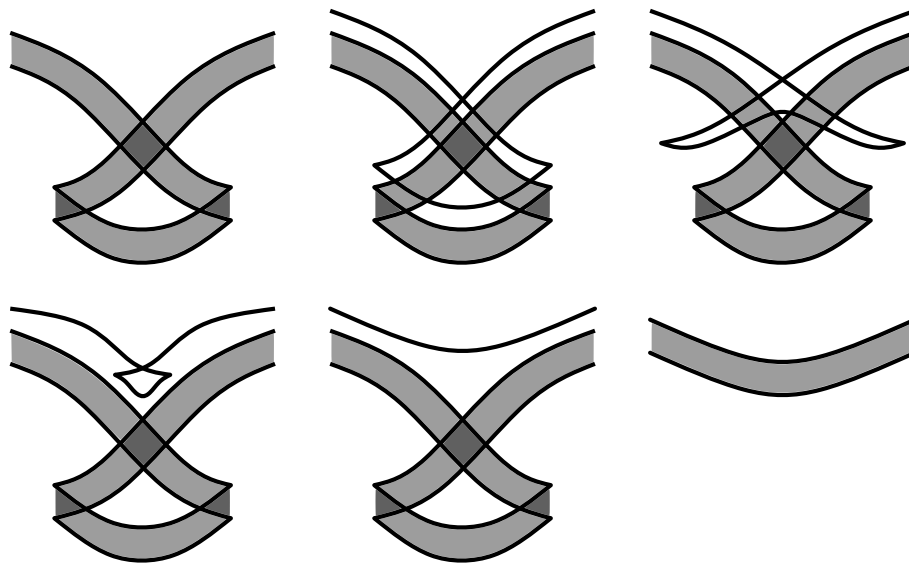


**Figure A.5:** Performing Reidemeister 1 with parallel strands, the grey shaded region representing some number of parallel strands. In order, we have

- (1.) the set up,
- (2.) separating out the top most strand,
- (3.) Reidemeister 3 on parallel strands,
- (4.) Reidemeister 2 on parallel strands twice,
- (5.) Reidemeister 1,
- (6.) repeating these steps 2-5 with all other strands.



## Appendix B

# The Chekanov-Eliashberg DGA for another example

The  $10_{155}$  knot [BNMea] is doubly slice, meaning that it appears as a cross section of an unknotted  $S^2$  in  $S^4$  [LM15]. We can conclude from the main theorem that it cannot be Lagrangian doubly slice. We will now demonstrate the constructions of Section 4. and 5. explicitly for this example.

The transverse  $10_{155}$  is the closure of the braid  $\sigma_1\sigma_2^{-2}\sigma_1\sigma_2^{-1}\sigma_1\sigma_2\sigma_1^{-1}\sigma_2^2$  [CDGW].

By Corollary 4.2.3, its double cover has a Weinstein Lefschetz fibration  $\pi : X \rightarrow D^2$  with generic fibre  $F$  a punctured torus, and vanishing cycles given by  $\alpha$  and  $\tau_{\beta-2\alpha}(\alpha)$  which are curves of slope  $(1, 0)$  and  $(2, 5)$  respectively.

Following the steps in the proof of Theorem 4.3.2, we obtain the surgery diagram  $\mathcal{D}(10_{155})$ , as in Figure B.1.

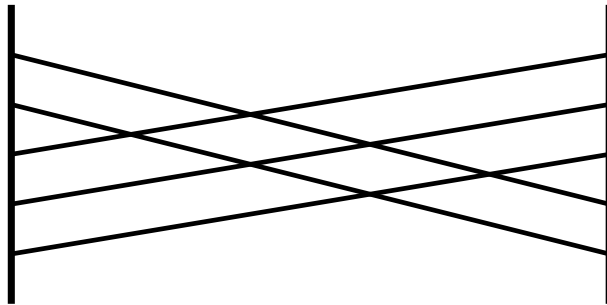


**Figure B.1:** A front diagram of  $\mathcal{D}(\Lambda)$  where  $\Lambda$  is the knot  $10_{155}$ .

The Lagrangian resolution of  $\mathcal{D}(\Lambda)$  is given by Figure B.2. We label the crossings of this diagram with the conventions described in Section 5.2.

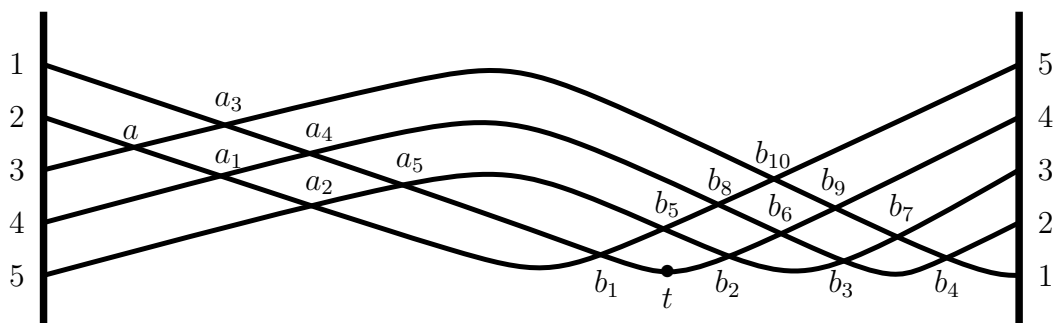


**Figure B.2:** The Lagrangian resolution of  $\mathcal{D}(\Lambda)$  where  $\Lambda$  is the knot  $10_{155}$ . The Reeb chords generating the external DGA and the strands entering the 1-handles are labelled.

The generators are  $t, a, a_1, \dots, a_5, b_1, \dots, b_{10}, c_{i,j}^0$  for  $1 \leq i < j \leq 5$ , and  $c_{i,j}^1$  for  $1 \leq i, j \leq 5$ . The gradings are:

$$|t| = |a| = |a_i| = |b_i| = 0$$

$$|c_{i,j}^0| = 1$$

$$|c_{i,j}^1| = -1$$

The differentials of generators of the internal DGA are:

$$\begin{aligned} \partial(c_{i,j}^0) &= \sum_{m=1}^5 c_{i,m}^0 c_{m,j}^0 \\ \partial(c_{i,j}^1) &= \delta_{i,j} + \sum_{m=1}^5 c_{i,m}^0 c_{m,j}^1 + \sum_{m=1}^n c_{i,m}^1 c_{m,j}^0 \end{aligned}$$

where  $\delta_{i,j} = e_i = e_j$  if  $i = j$  and is 0 otherwise.

The differentials of the generators of the external DGA are:

$$\partial a = c_{2,3}^0$$

$$\partial a_1 = c_{2\ 4}^0 + ac_{3\ 4}^0$$

$$\partial a_2 = c_{2\ 5}^0 + ac_{3\ 5}^0 + a_1c_{4\ 5}^0$$

$$\partial a_3 = c_{1\ 2}^0a + c_{1\ 3}^0$$

$$\partial a_4 = c_{1\ 2}^0a_1 + c_{1\ 4}^0 + a_3c_{3\ 4}^0$$

$$\partial a_5 = c_{1\ 2}^0a_2 + c_{1\ 5}^0 + a_3c_{3\ 5}^0 + a_4c_{4\ 5}^0$$

$$\partial b_1 = c_{1\ 2}^0 + tc_{4\ 5}^0$$

$$\partial b_2 = c_{3\ 4}^0$$

$$\partial b_3 = c_{2\ 3}^0 + c_{4\ 5}^0$$

$$\partial b_4 = c_{1\ 2}^0 + c_{3\ 4}^0$$

$$\partial b_5 = b_2c_{4\ 5}^0 + c_{3\ 5}^0$$

$$\partial b_6 = b_3c_{3\ 4}^0 + c_{2\ 4}^0 + c_{4\ 5}^0b_2$$

$$\partial b_7 = b_4c_{2\ 3}^0 + c_{1\ 3}^0 + c_{3\ 5}^0 + c_{3\ 4}^0b_3$$

$$\partial b_8 = b_6c_{4\ 5}^0 + b_3c_{3\ 5}^0 + c_{2\ 5}^0 + c_{4\ 5}^0b_5$$

$$\partial b_9 = b_7c_{3\ 4}^0 + b_4c_{2\ 4}^0 + c_{1\ 4}^0 + c_{3\ 4}^0b_6 + c_{3\ 5}^0b_2$$

$$\partial b_{10} = b_9c_{4\ 5}^0 + b_7c_{3\ 5}^0 + b_4c_{2\ 5}^0 + c_{1\ 5}^0 + c_{3\ 4}^0b_8 + c_{3\ 5}^0b_5$$

Then the cycle in the symplectic homology of the filling depicted in  $\mathcal{D}(\Lambda)$  as described in the proof of Theorem 5.3.4 is given by  $(\check{c}, \hat{c}, \tau_1)$ , where

$$c = ta_1 - tb_3 + b_1 - b_4 + b_2.$$

We see that  $\partial c = 0$ .

# Bibliography

- [ACSG<sup>+</sup>20a] B. Acu, O. Capovilla-Searle, A. Gable, A. Marinković, E. Murphy, L. Starkston, and A. Wu. An introduction to Weinstein handlebodies for complements of smoothed toric divisors. *arXiv:002.07983*, 2020.
- [ACSG<sup>+</sup>20b] B. Acu, O. Capovilla-Searle, A. Gable, A. Marinković, E. Murphy, L. Starkston, and A. Wu. Weinstein handlebodies for complements of smoothed toric divisors. *arXiv:2012.08666*, 2020.
- [Ale20] James W Alexander. Note on Riemann spaces. *Bulletin of the American Mathematical Society*, 26(8):370–372, 1920.
- [Ale23] James W Alexander. A lemma on systems of knotted curves. *Proc Natl Acad Sci U S A*, 332(3):93–95, 1923.
- [BEE12] Frédéric Bourgeois, Tobias Ekholm, and Yasha Eliashberg. Effect of Legendrian surgery. *Geom. Topol.*, 16(1):301–389, 2012. With an appendix by Sheel Ganatra and Maksim Maydanskiy.
- [Ben83] Daniel Bennequin. Entrelacements et équations de Pfaff. In *IIIe rencontre de géométrie du Schnepfenried (Volume 1) - 10 - 15 mai 1982*, number 107-108 in Astérisque, pages 87–161. Société mathématique de France, 1983.
- [BLL<sup>+</sup>20] Sarah Blackwell, Noémie Legout, Caitlin Levenson, Maÿlis Limouzineau, Ziva Myer, Yu Pan, Samantha Pezzimenti, Lara Si-

- mone Suárez, and Lisa Traynor. Constructions of Lagrangian cobordisms, 2020.
- [BNMea] Dror Bar-Natan, Scott Morrison, and et al. The Knot Atlas.
- [BO01] Michel Boileau and Stepan Orevkov. Quasi-positivité d'une courbe analytique dans une boule pseudo-convexe. *Comptes Rendus de l'Académie des Sciences - Series I - Mathematics*, 332(9):825–830, 2001.
- [BO09] Frédéric Bourgeois and Alexandru Oancea. An exact sequence for contact-and symplectic homology. *Inventiones mathematicae*, 175(3):611–680, 2009.
- [CDGW] Marc Culler, Nathan M. Dunfield, Matthias Goerner, and Jeffrey R. Weeks. SnapPy, a computer program for studying the geometry and topology of 3-manifolds. Available at <http://snappy.computop.org> (26/04/2021).
- [CE12] Kai Cieliebak and Yakov Eliashberg. *From Stein to Weinstein and back*, volume 59 of *American Mathematical Society Colloquium Publications*. American Mathematical Society, Providence, RI, 2012. Symplectic geometry of affine complex manifolds.
- [CE19] Roger Casals and John B Etnyre. Transverse universal links. *Breadth in contemporary topology*, 102:43–55, 2019.
- [CGHS13] Chang Cao, Nathaniel Gallup, Kyle Hayden, and Joshua M Sabloff. Topologically distinct Lagrangian and symplectic fillings. *arXiv:1307.7998*, 2013.
- [Cha10] Baptiste Chaintraine. Lagrangian concordance of Legendrian knots. *Algebr. Geom. Topology*, 10(1):63–85, 2010.

- [Cha13] Baptiste Chantraine. Lagrangian concordance is not a symmetric relation. *Quantum Topology*, 6, 01 2013.
- [Che02] Yuri Chekanov. Differential algebra of Legendrian links. *Invent. Math.*, 150(3):441–483, 2002.
- [CM19] Roger Casals and Emmy Murphy. Legendrian fronts for affine varieties. *Duke Math. J.*, 168(2):225–323, 2019.
- [CNS16] Christopher Cornwell, Lenhard Ng, and Steven Sivek. Obstructions to Lagrangian concordance. *Algebr. Geom. Topology*, 16:797–824, 2016.
- [Con19] Anthony Conway. The Levine-Tristram signature: a survey. *arXiv:1903.04477*, 2019.
- [DG09] Fan Ding and Hansjörg Geiges. Handle moves in contact surgery diagrams. *J. Topol.*, 2:105–122, 2009.
- [DGS04] Fan Ding, Hansjörg Geiges, and András I Stipsicz. Surgery diagrams for contact 3-manifolds. *Turkish Journal of Mathematics*, 28(1):41–74, 2004.
- [Don96] S. K. Donaldson. Symplectic submanifolds and almost-complex geometry. *J. Differential Geom.*, 44(4):666–705, 1996.
- [EH02] John B. Etnyre and Ko Honda. Tight contact structures with no symplectic fillings. *Invent. Math.*, 148:609–626, 2002.
- [Ekh19] Tobias Ekholm. Holomorphic curves for Legendrian surgery. *arXiv:1906.07228*, 2019.
- [EL17] Tobias Ekholm and Yankı Lekili. Duality between Lagrangian and Legendrian invariants. *arXiv:1701.01284*, 2017.

- [EL19] Tolga Etgü and Yankı Lekili. Fukaya categories of plumbings and multiplicative preprojective algebras. *Quantum Topol.*, 10(4):777–813, 2019.
- [Eli92] Yakov Eliashberg. Contact 3-manifolds twenty years since J. Martinet’s work. *Ann. Inst. Fourier*, 42(1–2):165–192, 1992.
- [Eli95] Yakov Eliashberg. Topology of 2-knots in  $\mathbb{R}^4$  and symplectic geometry. In *The Floer memorial volume*, pages 335–353. Springer, 1995.
- [Eli98] Yakov Eliashberg. Invariants in contact topology. *Documenta Mathematica*, pages 327–338, 1998.
- [EN15] Tobias Ekholm and Lenhard Ng. Legendrian contact homology in the boundary of a subcritical Weinstein 4-manifold. *J. Differential Geom.*, 101(1):67–157, 2015.
- [EN18] John B Etnyre and Lenhard L Ng. Legendrian contact homology in  $\mathbb{R}^3$ . *arXiv:1811.10966*, 2018.
- [ENS<sup>+</sup>02] John B Etnyre, Lenhard L Ng, Joshua M Sabloff, et al. Invariants of Legendrian knots and coherent orientations. *Journal of Symplectic Geometry*, 1(2):321–367, 2002.
- [EP96] Yakov Eliashberg and Leonid Polterovich. Local Lagrangian 2-knots are trivial. *Ann. of Math.*, 144(1):61–76, 1996.
- [Erl99] Dieter Erle. Calculation of the signature of a 3-braid link. *Kobe journal of mathematics*, 16(2):161–175, 1999.
- [Etn03] John B. Etnyre. Legendrian and transversal knots, 2003.
- [Etn06] John B Etnyre. Lectures on open book decompositions and contact structures. In *Floer Homology, Gauge Theory, and Low-Dimensional Topology: Proceedings of the Clay Mathematics In-*

- stitute 2004 Summer School, Alfréd Rényi Institute of Mathematics, Budapest, Hungary, June 5-26, 2004*, volume 5, page 103. American Mathematical Soc., 2006.
- [EY00] Hofer H. Eliashberg Y., Givental A. Introduction to symplectic field theory. *Visions in Mathematics*, pages 560–673, 2000.
- [FM66] Ralph H. Fox and John W. Milnor. Singularities of 2-spheres in 4-space and cobordism of knots. *Osaka Journal of Mathematics*, 3(2):257 – 267, 1966.
- [FM11] Benson Farb and Dan Margalit. *A primer on mapping class groups (pms-49)*. Princeton University Press, 2011.
- [FSS08] Kenji Fukaya, Paul Seidel, and Ivan Smith. Exact Lagrangian submanifolds in simply-connected cotangent bundles. *Inventiones mathematicae*, 172(1):1–27, 2008.
- [Gir02] Emmanuel Giroux. Géométrie de contact: de la dimension trois vers les dimensions supérieures. In *Proceedings of the International Congress of Mathematicians, Vol. II (Beijing, 2002)*, pages 405–414. Higher Ed. Press, Beijing, 2002.
- [Gir17] Emmanuel Giroux. Remarks on Donaldson’s symplectic submanifolds. *Pure Appl. Math. Q.*, 13(3):369–388, 2017.
- [Gom98] Robert E. Gompf. Handlebody construction of Stein surfaces. *Ann. of Math. (2)*, 148(2):619–693, 1998.
- [Gro85] Misha Gromov. Pseudo holomorphic curves in symplectic manifolds. *Invent. Math.*, 82:307–347, 1985.
- [GSI+99] R.E. Gompf, A.I. Stipsicz, S.A. I, A. Stipsicz, and American Mathematical Society. *4-Manifolds and Kirby Calculus*. Graduate studies in mathematics. American Mathematical Society, 1999.



- [Hay18] Kyle Hayden. Minimal braid representatives of quasipositive links. *Pacific Journal of Mathematics*, 295(2):421–427, 4 2018.
- [HKP08] Shelly Harvey, Keiko Kawamuro, and Olga Plamenevskaya. On transverse knots and branched covers. *International Mathematics Research Notices*, 2009(3):512–546, 12 2008.
- [Ito17] Tetsuya Ito. On the 3-dimensional invariant for cyclic contact branched coverings. *Topology and its Applications*, 216:1–7, 2017.
- [KM93] Peter B Kronheimer and Tomasz S Mrowka. Gauge theory for embedded surfaces, i. *Topology*, 32(4):773–826, 1993.
- [LM15] Charles Livingston and Jeffrey Meier. Doubly slice knots with low crossing number. *arXiv:1504.03368*, 2015.
- [McD90] Dusa McDuff. The structure of rational and ruled symplectic 4-manifolds. *Journal of the American Mathematical Society*, 3(3):679–712, 1990.
- [McL09] Mark McLean. Lefschetz fibrations and symplectic homology. *Geometry & Topology*, 13(4):1877–1944, 2009.
- [Msr09] Msr657. Standard contact structure, 2009. [Online; accessed Oct 9, 2020].
- [MT20] Thomas E. Mark and Bülent Tosun. On contact type hypersurfaces in 4-space, 2020.
- [Mur74] Kunio Murasugi. *On Closed 3-braids*. Number 151 in Memoirs of the American Mathematical Society. American Mathematical Society, 1974.
- [Ng03] Lenhard L. Ng. Computable Legendrian invariants. *Topology*, 42(1):55–82, 2003.

- [NT04] Lenhard Ng and Lisa Traynor. Legendrian solid-torus links. *Journal of Symplectic Geometry*, 2(3):411–443, 2004.
- [Ona14] Sinem Onaran. Planar open book decompositions of 3-manifolds. *The Rocky Mountain Journal of Mathematics*, 44(5):1621–1630, 2014.
- [OS03] S. Y. Orevkov and V. V. Shevchishin. Markov theorem for transversal links. *Journal of Knot Theory and Its Ramifications*, 12(07):905–913, 2003.
- [Ozb19a] Burak Ozbagci. Correction to: Stein and Weinstein structures on disk cotangent bundles of surfaces. *Arch. Math. (Basel)*, 113(6):671–672, 2019.
- [Ozb19b] Burak Ozbagci. Stein and Weinstein structures on disk cotangent bundles of surfaces. *Arch. Math. (Basel)*, 113(6):661–670, 2019.
- [Pla06] Olga Plamenevskaya. Transverse knots, branched double covers and Heegaard Floer contact invariants. *J. Symplectic Geom.*, 4(2):149–170, 06 2006.
- [Rud93] Lee Rudolph. Quasipositivity as an obstruction to sliceness. *Bulletin of the American Mathematical Society*, 29(1):51–59, 1993.
- [Sei06] Paul Seidel. A biased view of symplectic cohomology. *Current developments in mathematics*, 2006(1):211–254, 2006.
- [Sym03] Margaret Symington. Four dimensions from two in symplectic topology. In *Topology and geometry of manifolds (Athens, GA, 2001)*, volume 71 of *Proc. Sympos. Pure Math.*, pages 153–208. Amer. Math. Soc., Providence, RI, 2003.
- [TW75] William P Thurston and Horst E Winkelnkemper. On the existence of contact forms. *Proceedings of the American Mathematical Society*, pages 345–347, 1975.

- [Vit99] Claude Viterbo. Functors and computations in floer homology with applications, i. *Geometric & Functional Analysis GAFA*, 9(5):985–1033, 1999.
- [Wei91] Alan Weinstein. Contact surgery and symplectic handlebodies. *Hokkaido Math.*, 20(2):241–251, 1991.
- [Wen10] Chris Wendl. Strongly fillable contact manifolds and  $J$ -holomorphic foliations. *Duke Math. J.*, 151(3):337–384, 2010.
- [Wri02] Nancy C. Wrinkle. The Markov theorem for transverse knots. *arXiv:0202055*, 2002.